A chaotic lattice field theory in one dimension

H Liang and P Cvitanović

School of Physics, Georgia Institute of Technology, Atlanta, GA 30332-0430, USA

E-mail: predrag.cvitanovic@physics.gatech.edu

27 December 2021

Abstract.

We use lattice-discretized scalar field theories, in particular spatiotemporal cat, Hénon ϕ^3 and ϕ^4 theories to explain how to reformulate dynamics of spatiotemporally 'chaotic' or 'turbulent' PDEs in

Motivated by a Gutzwiller's ideas of periodic orbits of deterministic dynamics serving as WKB 'skeleton' for chaotic quantum mechanics, in this paper we focus on deterministic chaotic field theory.

We abandon initial state evolution, local in time, and seek instead to determine global solutions compatible with system's defining equations.

The reformulation aligns 'chaos theory' with the standard solid state, field theory and statistical mechanics partition functions, related to the well-known forward-in-time Gutzwiller trace formulas by Hill's formulas.

In spatiotemporal, crystallographer formulation, time-periodic orbits of dynamical systems theory are replaced by periodic d-dimensional Bravais cell tilings (d-tori) of spacetime. In contrast to conventional solid state calculations, due to hyperbolic shadowing of large cells by smaller ones, the predictions of the theory are dominated by the smallest Bravais cells.

In the field-theoretical formulation, there is no evolution in time, and there is no 'Lyapunov horizon'; every contributing *lattice state* is a robust global solution of a spatiotemporal fixed point condition.

The form of the partition function of a given field theory is determined by the group of its spatiotemporal symmetries, i.e., by the space group of its lattice discretization, and its reciprocal lattice.

In particular, from a spatiotemporal field theory perspective, 'time'-reversal is a purely crystallographic notion, a reflection point group, leading to a perhaps unfamiliar symmetry quotienting of time-reversible theories.

The theory is compactly summarized by its topological zeta function that counts Bravais lattices.

On the level of counting lattice-states, their topological zeta functions are purely group-theoretic Lind zeta functions.

PACS numbers: 02.20.-a, 05.45.-a, 05.45.Jn, 47.27.ed

Submitted to: *J. Phys. A: Math. Theor.*

Dedicated to Fritz Haake 1941–2019 [113]

The year was 1988. Roberto Artuso, Erik Aurell and P.C. had just worked out the cycle expansions formulation of the deterministic and semiclassical chaotic systems [12, 13], and a Niels Bohr Institute "Quantum Chaos Symposium" was organized to introduce the new-fangled theory to unbelievers (for a history, see ChaosBook Append. A.4 *Periodic orbit theory*). In the first row of the famed auditorium, where long ago Niels Bohr and his colleagues used to nod off, sat a man with an impressive butterfly and a big smile. At the end of our presentation, Fritz –for that was Fritz Haake– stood up and exclaimed

"Amazing! I did not understand a single word!"

And indeed, there is a problem of understanding what is 'chaos' as encountered in different disciplines, so we start this offering to Fritz Haake's memory by 'a fair coin toss' theory of chaos, section 2, as was presented in the 1988 symposium, but in a modern, field theorist's vision. In those days 'chaos' was a phenomenon exhibited by low-dimensional systems. In this and companion papers [65, 121] we explain how to think of 'chaotic' or 'turbulent' ∞-dimensional deterministic field theories. Deterministic chaotic field theory is of interest on its merits, as a method of describing turbulence in strongly nonlinear deterministic field theories, such as Navier-Stokes or Kuramoto-Sivashinsky [120, 121], or as a Gutzwiller WKB 'skeleton' for a chaotic quantum field theory [59, 126] or a stochastic field theory [66–69, 181]. The lattice reformulation aligns 'chaos' with standard solid state, field theory and statistical mechanics, but the claims are radical: we've been doing 'turbulence' all wrong. In "explaining" chaos we talk the talk as though we have never moved beyond Newton; here is an initial state of a system, at an instant in time, and here are the differential equations that evolve it forward in time. But when we -all of us- walk the walk, we do something altogether different (see the references preceding eq. (75)), much closer to the 20th century spacetime physics. Our papers realign the theory to what we actually *do* when solving 'chaos equations', using not much more than linear algebra. In the field-theoretical formulation, there is no evolution in time, and there is no 'Lyapunov horizon'; every contributing *lattice state* is a robust global solution of a spatiotemporal fixed point condition, there is no dynamicist's exponential blowup of initial state perturbations.

To a field theorist, the fundamental object is *global*, the partition function sum over probabilities of all possible spacetime field configurations. To a dynamicist, the fundamental notion is *local*, an ordinary or partial differential time-evolution equation. From the field-theoretic perspective, the spacetime formulation is fundamental, elegant and computationally powerful, while moving in step-lock with time is only one of the methods, a 'transfer matrix' method for construction of the partition sum, at times awkward and computationally unstable.

We start our introduction to chaotic field theory (section 1) by rewriting the two most elementary examples of deterministic chaos, the forward-in-time first order difference equation for the Bernoulli map (section 2), and the forward-in-time second order difference equation for a 1-dimensional lattice of coupled rotors (section 3) as,

respectively, the 'temporal Bernoulli' two-term discrete lattice recurrence relation, and the 'temporal cat' three-term discrete lattice recurrence relation. We then apply the approach to the simplest nonlinear field theories, the 1-dimensional discretized scalar ϕ^3 and ϕ^4 theories (sections 4 and 5).

Their spacetime generalization, the simplest of all chaotic field theories, is the 'spatiotemporal cat' [65, 123, 124], a discretization of the Klein-Gordon equation, a deterministic scalar field theory on a d-dimensional hyper-cubic lattice, with an unstable "anti-harmonic" rotor ϕ_z at each lattice site z, a rotor that gives, rather than pushes back, coupled to its nearest neighbors. In contrast to its elliptic sister, the Helmholtz equation and its oscillatory solutions, spatiotemporal cat's lattice states are hyperbolic and 'turbulent', just as in contrast to oscillations of a harmonic oscillator, Bernoulli coin flips are unstable and chaotic.

The key to constructing partition sums for deterministic field theories (section 1) are Hill determinants, determinants of the 'orbit Jacobian matrices' (section 7) that describe the global stability of the linearized deterministic equations. How is this global, high-dimensional orbit stability related to the stability of the conventional low-dimensional, forward-in-time evolution? The two notions of stability are related by Hill's formulas (section 8), relations that rely on higher-order derivative equations being rewritten as sets of first order ODEs, relations equally applicable to the mechanical, energy conserving systems, as to the viscous, dissipative systems.

The lattice discretization of the theory enables us to apply the solid state computational methods, such as reciprocal lattice and space group crystallography to what are convenitonally dynamical system problems (section 8.6). In section 9 we show that the partition function of a given field theory is determined by the group of its symmetries, i.e., by the space group of its lattice discretization, and its reciprocal lattice. In particular, from a spatiotemporal field theory perspective, 'time'-reversal is a purely crystallographic notion, leading to a perhaps unfamiliar symmetry quotienting of 'time-reversible' theories.

On the level of counting lattice-states, their topological zeta functions are purely group-theoretic Lind zeta functions, see section 12.

Our results are summarized and open problems discussed in the section 13.

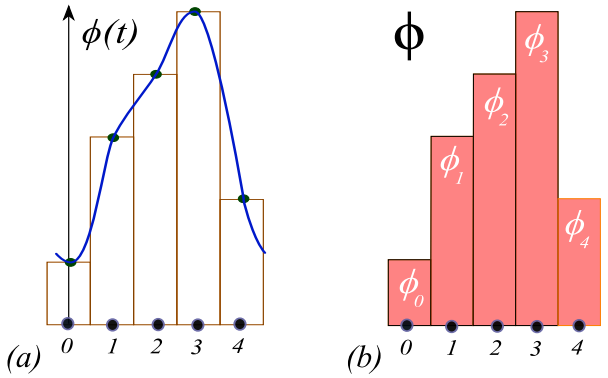

Figure 1. (Color online) Discretization of a 1-dimensional field theory. Horizontal: t coordinate, with lattice sites marked by dots and labelled by $t \in \mathbb{Z}$. (a) A periodic field $\phi(t)$, plotted as a function of continuous coordinate t. (b) A corresponding discretized period-5 lattice state $\Phi = \overline{\phi_0\phi_1\phi_2\phi_3\phi_4}$, with discretized field ϕ_t plotted as a bar centred at lattice site t. In what follows we use 'lattice units' $a = 1$.

1. Deterministic lattice field theory

A scalar field $\phi(x)$ over d Euclidean coordinates can be discretized by replacing the continuous space by a d-dimensional hypercubic integer lattice $\mathcal{L}$, with lattice spacing a, and evaluating the field only on the lattice points [200, 204]

$$\phi_z = \phi(x)\,, \qquad x = az = \text{lattice point}\,, \quad z \in \mathbb{Z}^d\,, \tag{1}$$

see figure 1. A given *field configuration* (here in one spatiotemporal dimension)

$$\Phi = \cdots \phi_{-3}\phi_{-2}\,\phi_{-1}\,\phi_0\,\phi_1\phi_2\phi_3\phi_4\cdots\,, \tag{2}$$

taking any value in system's ∞-dimensional *state space* $\phi_z \in \mathbb{R}$, occurs with probability

$$p(\Phi) \;=\; \frac{1}{Z}\,\mathrm{e}^{-S[\Phi]}\,, \qquad Z = Z[0]\,. \tag{3}$$

Here Z is a normalization factor, given by the *partition function*, the integral over probabilities of all configurations,

$$Z[\mathsf{M}] \;=\; \int d\Phi\, e^{-S[\Phi]+\Phi\cdot\mathsf{M}}\,, \qquad d\Phi = \prod_z^{\mathcal{L}} d\phi_z\,, \tag{4}$$

where $\mathsf{M} = \{m_z\}$ is an external 'source' that one can vary at will, site-by-site, and $S[\Phi]$ is the action that defines the theory. The dimension of the partition function integral is the number of lattice sites $N_{\mathcal{L}}$.

Motivated by WKB 'semi-classical' or saddle-point approximations [126] to the partition function (4), in this paper we describe their deterministic underpinning, the corresponding *deterministic* field theory, with partition function built from solutions to the variational saddle-point condition

$$F[\Phi_c]_z = -S[\Phi_c]_z + m_z = 0\,, \qquad S[\Phi]_z = \frac{\delta S[\Phi]}{\delta\phi_z}\,, \tag{5}$$

with a global deterministic solution Φ_c satisfying this local extremal condition on every lattice site. In order to distinguish a *solution* to the Euler–Lagrange equations (5) from an arbitrary *field configuration* (2), we refer to the solutions as *lattice states*, each a set of lattice site field values

$$\Phi_c = \{\phi_z\}\,, \tag{6}$$

that satisfies the local condition (5) globally, over all lattice sites. For a finite lattice segment Φ, one needs to specify the boundary conditions (bc's). The companion article [124] tackles the Dirichlet bc's, a difficult, time-translation symmetry breaking, and from the periodic orbit theory perspective, a wholly unnecessary, self-inflicted pain. All that one needs to solve the temporal cat are the T-periodic, time-translation enforced bc's that we shall use here.

> [2020-02-08 Predrag] Complain about that stupidity clearly both in the intro and in conclusions.

An example is the 1 spatiotemporal dimension block of fields of period $n = 5$ sketched in figure 1 (b),

$$\Phi_c = \overline{\phi_0\phi_1\phi_2\phi_3\cdots\phi_{n-1}}\,, \tag{7}$$

with its infinite repetition –for a sketch, see figure 11 (1)– denoted by an overbar. The first field value ϕ_0 in the block is evaluated on the lattice site 0, the second ϕ_1 on the lattice site 1, the nth $\phi_n = \phi_0$ on the lattice site n, with kth lattice site field value $\phi_k = \phi_\ell$, where $\ell = k \pmod n$.

What we call here a chaotic 'field' at a discretized spacetime lattice site z, a solid state physicist would call the state of a 'particle' at crystal site z, coupled to its nearest neighbors. A solid state physicist endeavours to understand N-particle chaotic systems in many-body or 'large N' settings, where in practice any N larger than 2 is 'large'. Chaotic field theory is *ab initio* formulated for infinite time and infinite space lattice, but its periodic theory description is -thanks to hyperbolicity– computationally powerful already for $N = 2, 3, \cdots$, where N is the number of sites in Bravais cells that tile the spacetime.

Each lattice state is a distinct deterministic solution Φ_c to the discretized Euler–Lagrange equations (5), so its probability is a $N_{\mathcal{L}}$-dimensional Dirac delta function (that's what we mean by the system being *deterministic*)

$$p_c(\Phi) \;=\; \frac{1}{Z}\,\delta(F[\Phi_c - \Phi])\,. \tag{8}$$

In section 8.1 we verify that this definition agrees with the customary forward-in-time Perron-Frobenius probability evolution [70] (see ChaosBook sect. 19.2). The new, field-theoretical formulation is vastly preferable to the forward-in-time formulation when it comes to higher spatiotemporal dimensions [65].

As is case for a WKB approximation [126], the deterministic field theory partition sum has support only on lattice field values that are solutions to the variational saddle-point condition (5), and the partition function (3) is now a sum over configuration state

space (2) *points*,

$$\begin{aligned} Z_c[\mathsf{M}] &= \sum_c e^{N_{\mathcal{L}} W_c[\mathsf{M}]} \\ e^{N_{\mathcal{L}} W_c[\mathsf{M}]} &= \int_{\mathcal{M}_c} d\Phi\, \delta(F[\Phi]) \;=\; \frac{1}{|\mathrm{Det}\, \mathcal{J}_c|}\,, \end{aligned} \tag{9}$$

where $\mathcal{M}_c$ is a small neighborhood of Φ_c, and we refer to the $[N_c \times N_c]$ matrix of second derivatives

$$(\mathcal{J}_c)_{z'z} = \frac{\delta F[\Phi_c]_{z'}}{\delta \phi_z} = S[\Phi_c]_{z'z} \tag{10}$$

as the *orbit Jacobian matrix*.

In what follows, we shall almost exclusively deal only with deterministic field theory and omit the subscript 'c' in Φ_c througout.

1.1. Lattice Laplacian

Let's have a look at the lattice free field theory action

$$S_0[\Phi] = \frac{1}{2} \Phi^\top \left(-\Box + \mu^2 1 \right) \Phi\,, \tag{11}$$

where the 'discrete Laplace operator', 'central difference operator', or the 'graph Laplacian' [52, 114, 203, 217, 222, 223]

$$\Box\, \phi_z = \sum_{||z'-z||=1} (\phi_{z'} - \phi_z) \quad \text{for all } z, z' \in \mathcal{L} \tag{12}$$

is the average of the lattice field variation $\phi_{z'} - \phi_z$ over the sites nearest to the site z. For example, for a hypercubic lattice in one and two dimensions this discretized Laplacian is given by

$$\Box\, \phi_t \;= \phi_{t+1} - 2\,\phi_t + \phi_{t-1} \tag{13}$$

$$\Box\, \phi_{jt} = \phi_{j,t+1} + \phi_{j+1,t} - 4\,\phi_{jt} + \phi_{j,t-1} + \phi_{j-1,t}\,. \tag{14}$$

For action (11) this is the discretized screened Poisson equation [98], also known as the Yukawa or Klein–Gordon equation, where $\mu^2 > 0$ is the Klein–Gordon mass-squared. An example is the Gutkin and Osipov [123] spatiotemporal cat in $d = 2$ dimensions [65], an Arnold cat map-inspired scalar field theory of form (11) for which the Euler–Lagrange equation (5) is a 5-term recurrence relation

$$-\phi_{j,t+1} - \phi_{j,t-1} + 2s\,\phi_{jt} - \phi_{j+1,t} - \phi_{j-1,t} = m_{jt}\,, \tag{15}$$

where we refer to parameter s, related to the Klein-Gordon mass in (11) by $\mu^2 = d(s-2)$, as the 'stretching parameter'.

1.2. 1-dimensional lattice field theories

Discrete time evolution is frequently recast into a 1-dimensional temporal lattice field theory form, essentially by anyone who rewrites a dynamical systems discrete time evolution problem as a k-point recurrence, for example in [67–69, 97]. As already in one spatiotemporal dimension there is much to be learned about the role symmetries play in solving lattice field theories, that is what we will focus on in this paper (time-reversal sections 9 and 12), with the 2-dimensional spatiotemporal field theories discussed in the sequel [65].

We shall consider scalar field theories of polynomial type, with a local potential [5–7, 89, 104, 172]

$$V(\phi_t) = \frac{g}{k}\phi_t^k - m_t\phi_t \tag{16}$$

on each 1-dimensional lattice site t added to the free field theory action (11). The discrete Euler–Lagrange equations (5) now take form of 3-term recurrence, second-order difference equations

$$-\phi_{t+1} + V'(\phi_t) - \phi_{t-1} = 0\,. \tag{17}$$

We start with the first order difference equation that we call 'temporal Bernoulli' (section 2),

$$-\phi_{t+1} + s\,\phi_t \qquad\qquad = m_t \tag{18}$$

in order to motivate the second-order difference Euler–Lagrange equations (17) that we call, in the cases considered here, the 'temporal cat' (section 3), 'temporal Hénon' (section 4), and 'temporal ϕ^4 theory' (section 5), respectively:

$$-\phi_{t+1} + s\,\phi_t - \phi_{t-1} = m_t \tag{19}$$

$$-\phi_{t+1} + a\,\phi_t^2 - \phi_{t-1} = m_t \tag{20}$$

$$-\phi_{t+1} + g\,\phi_t^3 - \phi_{t-1} = m_t \tag{21}$$

Qualifier 'temporal' is used here to emphasize that we view 1-dimensional examples as special cases of 'spatiotemporal' field theories; much of our methodology for d-dimensional deterministic field theories can be profitably explained by working out 1-dimensional field theories. Lurking here is the totality of the map-iteration dynamical systems theory, but the reader will find it more profitable, and less confusing, to think of these simply as lattice problems, and forget that the index t often stands for 'time'.

So, what is a 'chaotic', or 'turbulent' field theory? As we shall see, all of the above, as well as their higher-dimensional spatiotemporal siblings are 'chaotic' for sufficiently strong 'stretching parameters' or 'coupling constants' s, a or g. Our goal here is to make this 'spatiotemporal chaos' tangible and precise, by acquainting the reader what we believe are some of the simplest, most elegant examples chaotic field theories.

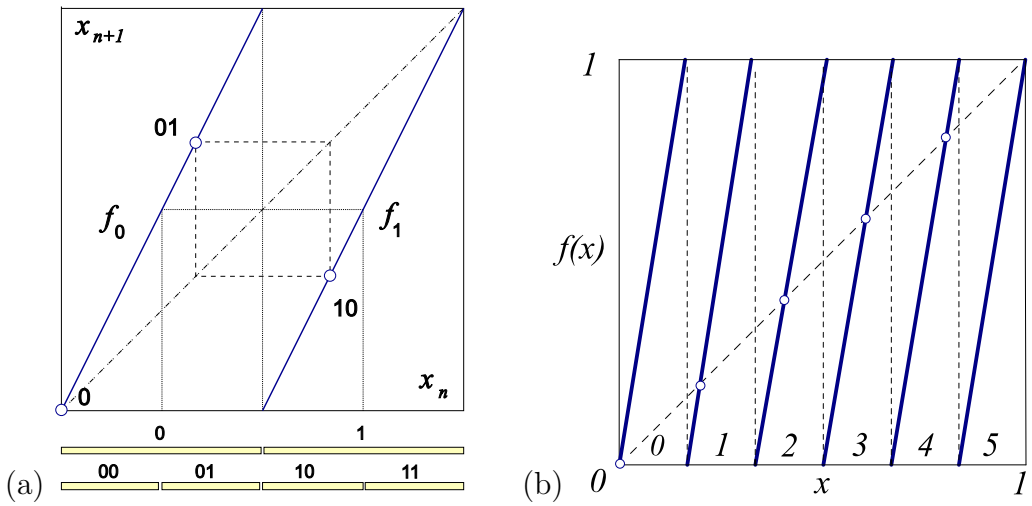

Figure 2. (Color online) (a) The 'coin toss' map (22), together with the $\overline{0}$ fixed point, and the $\overline{01}$ 2-cycle. Preimages of the critical point $x_c = 1/2$ partition the unit interval into $\{\mathcal{M}_0, \mathcal{M}_1\}$, $\{\mathcal{M}_{00}, \mathcal{M}_{01}, \mathcal{M}_{10}, \mathcal{M}_{11}\}$, ..., subintervals. (b) The base-s Bernoulli map, here with the 'dice throw' stretching parameter $s = 6$, partitions the unit interval into 6 subintervals $\{\mathcal{M}_m\}$, labeled by the 6-letter alphabet (26). As the map is a circle map, $x_5 = 1 = 0 = x_0 \pmod 1$.

2. A fair coin toss

The very simplest example of a deterministic law of evolution that gives rise to 'chaos' is the *Bernoulli* map, figure 2 (a), which models a coin toss. Starting with a random initial state, the map generates, deterministically, a sequence of tails and heads with the 50-50% probability.

We introduce the model in its conventional, time-evolution dynamical formulation, than reformulate it as a lattice field theory, solved by enumeration of all admissible *lattice states*, field configurations that satisfy a global fixed point condition, and use this simple setting to motivate (1) the *fundamental fact*: for a given lattice period, the *Hill determinant* of stabilities of global solutions counts their number (section 8.5), and (2) the topological zeta function counts their translational symmetry group orbits (section 11).

2.1. Bernoulli map

The base-2 *Bernoulli* shift map,

$$x_{t+1} = \begin{cases} f_0(x_t) = 2x_t\,, & x_t \in \mathcal{M}_0 = [0, 1/2) \\ f_1(x_t) = 2x_t \pmod 1\,, & x_t \in \mathcal{M}_1 = [1/2, 1) \end{cases}\,, \tag{22}$$

is shown in figure 2 (a). If the linear part of such map has an integer-valued slope, or 'stretching' parameter $s \geq 2$,

$$x_{t+1} \;=\; s x_t \tag{23}$$

that maps state x_t into a state in the 'extended state space', outside the unit interval, the (mod 1) operation results in the base-s Bernoulli circle map,

$$\phi_{t+1} = s\phi_t \pmod 1 \,, \tag{24}$$

sketched as a dice throw in figure 2 (b). The (mod 1) operation subtracts $m_t = \lfloor s\phi_t \rfloor$, the integer part of $s\phi_t$, or the circle map *winding number*, to keep ϕ_{t+1} in the unit interval $[0, 1)$, and partitions the unit interval into s subintervals $\{\mathcal{M}_m\}$,

$$\phi_{t+1} = s\phi_t - m_t \,, \qquad \phi_t \in \mathcal{M}_{m_t} \,, \tag{25}$$

where m_t takes values in the s-letter alphabet

$$m \in \mathcal{A} = \{0, 1, 2, \cdots, s-1\} \,. \tag{26}$$

The Bernoulli map is a highly instructive example of a hyperbolic dynamical system. Its symbolic dynamics is simple: the base-s expansion of the initial point ϕ_0 is also its temporal itinerary, with symbols from alphabet (26) indicating that at time t the orbit visits the subinterval $\mathcal{M}_{m_t}$. The map is a 'shift': a multiplication by s acts on the base-s representation of $\phi_0 = .m_1 m_2 m_3 \cdots$ (for example, binary, if $s = 2$) by shifting its digits,

$$\phi_1 = f(\phi_0) = .m_2 m_3 \cdots \,. \tag{27}$$

Periodic points can be counted by observing that the preimages of critical points $\{\phi_{c1}, \phi_{c2}, \cdots \phi_{c,s-1}\} = \{1/s, 2/s, \cdots, (s-1)/s\}$ partition the unit interval into $\{\mathcal{M}_0, \mathcal{M}_1, \cdots, \mathcal{M}_{s-1}\}$, $\{\mathcal{M}_{m_1 m_2}\}$, ..., s^n subintervals, each containing *one* unstable period-n periodic point $\phi_{m_1 m_2 \cdots m_n}$, with stability multiplier s^n, see figure 2. The Bernoulli map is a full shift, in the sense that every itinerary is admissible, with one exception: on the circle, the rightmost fixed point is the same as the fixed point at the origin, $\phi_{s-1} = \phi_0 \pmod 1$, so these fixed points are identified and counted as one, see figure 2. The total number of periodic points of period n is thus

$$N_n = s^n - 1 \,. \tag{28}$$

2.2. Temporal Bernoulli

To motivate our formulation of a spatiotemporal chaotic field theory to be developed below, we now recast the local initial value, time-evolution Bernoulli map problem as a *temporal lattice* fixed point condition, the problem of enumerating and determining all global solutions.

'Temporal' here refers to the lattice site field ϕ_t and the source (winding number) m_t taking their values on the lattice sites of a 1-dimensional *temporal* integer lattice $t \in \mathbb{Z}$. Over a finite lattice segment, these can be written compactly as a *lattice state* and the corresponding *symbol block*

$$\boldsymbol{\Phi}^\top = (\phi_{t+1}, \cdots, \phi_{t+n}) \,, \quad \mathsf{M}^\top = (m_{t+1}, \cdots, m_{t+n}) \,, \tag{29}$$

where $(\cdots)^\top$ denotes a transpose. The Bernoulli equation (25), rewritten as a first-order difference equation

$$-\phi_{t+1} + s\phi_t - m_t = 0 \,, \qquad \phi_t \in [0, 1) \,, \tag{30}$$

takes the matrix form

$$\mathcal{J}\,\Phi - \mathsf{M} = 0\,, \qquad \mathcal{J} = -r + s\,\mathbb{1}, \tag{31}$$

where the $[n\times n]$ matrix

$$r_{jk} = \delta_{j+1,k}\,, \qquad r = \begin{pmatrix} 0 & 1 & & & \\ & 0 & 1 & & \\ & & & \ddots & \\ & & & 0 & 1 \\ 1 & & & & 0 \end{pmatrix}, \tag{32}$$

implements the shift operation (27), a cyclic permutation that translates forward-in-time lattice state Φ by one site, $(r\Phi)^\top = (\phi_2, \phi_3, \cdots, \phi_n, \phi_1)$. The time evolution law (25) must be of the same form for all times, so the shift operator r has to be time-translation invariant, with $r_{n+1,n} = r_{1n} = 1$ matrix element enforcing the periodicity. After n shifts, a lattice state returns to the initial state,

$$r^n = \mathbb{1}. \tag{33}$$

As the temporal Bernoulli condition (31) is a linear relation, a given block M, or 'code' in terms of alphabet (26), corresponds to a unique temporal lattice state Φ. That is why Percival and Vivaldi [217] refer to such symbol block M as a *linear code*.

2.3. Bernoulli as a continuous time dynamical system

The discrete time derivative of a lattice configuration Φ evaluated at the lattice site t is given by the difference operator [91]

$$\dot{\phi}_t = \left[\frac{\partial\Phi}{\partial t}\right]_t = \frac{\phi_{t+1} - \phi_t}{\Delta t}\,. \tag{34}$$

The temporal Bernoulli condition (31) can be thus viewed as a time-discretized, first-order ODE dynamical system

$$\dot{\Phi} \;=\; v(\Phi)\,, \tag{35}$$

where the 'velocity' vector field v is given by

$$v(\Phi) \;=\; (s-1)\,\Phi - \mathsf{M}\,,$$

with the time increment set to $\Delta t = 1$, and perturbations that grow (or decay) with rate $(s-1)$. By inspection of figure 2 (a), it is clear that for *shrinking*, $s < 1$ parameter values the orbit is stable forward-in-time, with a single linear branch, 1-letter alphabet $\mathcal{A} = \{0\}$, and the only lattice states being the single fixed point $\phi_0 = 0$, and its repeats $\Phi = (0, 0, \cdots, 0)$. However, for *stretching*, $s > 1$ parameter values, the Bernoulli system (more generally, Rényi's beta transformations [226]) that we study here, every lattice state Φ_M is unstable, and there is a lattice state for each admissible symbol block M.

[2021-08-23 Predrag] Should we include "Quotienting the temporal Bernoulli system" (**??**)?

A fair coin toss, summarized. We refer to the *global* temporal lattice condition (31) as the '*temporal* Bernoulli', in order to distinguish it from the one-time step Bernoulli evolution *map* (24), in preparation for the study of *spatiotemporal* systems to be undertaken in [65]. In the lattice formulation, a *global* temporal lattice state Φ_{M} is determined by the requirement that the *local* temporal lattice condition (30) is satisfied at every lattice site. In spatiotemporal formulation there is no need for forward-in-time, close recurrence searches for the returning periodic points. Instead, one determines each global temporal lattice state Φ_{M} at one go, by solving the fixed point condition (77). The most importantly for what follows, the spatiotemporal field theory of [65], this calculation requires no recourse to any *explicit coordinatization and partitioning of system's state space*, and *no explicit symbolic dynamics*.

[2020-12-17 Predrag] Link to the ChaosBook. Maybe refer to Adler-Weiss.

3. A kicked rotor

Temporal Bernoulli is the simplest example of a chaotic lattice field theory. Our next task is to formulate a deterministic spatiotemporally chaotic field theory, Hamiltonian and energy conserving, because (a) that is physics, and (b) one cannot do quantum theory without it. We need a system as simple as the Bernoulli map, but mechanical. So, we move on from running in circles, to a mechanical rotor to kick.

The 1-degree of freedom maps that describe kicked rotors subject to discrete time sequences of angle-dependent force pulses $P(q_t)$, $t \in \mathbb{Z}$,

$$q_{t+1} = q_t + p_{t+1} \qquad (\mathrm{mod}\ 1), \tag{36}$$

$$p_{t+1} = p_t + P(q_t)\,, \tag{37}$$

with $2\pi q$ the angle of the rotor, p the momentum conjugate to the angular coordinate q, and the angular pulse $P(q_t) = P(q_{t+1}) = -V'(q_t)$ lattice periodic with period 1, play a key role in the theory of deterministic and quantum chaos in atomic physics, from the Taylor, Chirikov and Greene standard map [48, 175], to the cat maps that we turn to now. The equations are of the Hamiltonian form: eq. (36) is $\dot{q} = p/m$ in terms of discrete time derivative (34), i.e., the configuration trajectory starting at q_t reaches $q_{t+1} = q_t + p_{t+1}\Delta t/m$ in one time step Δt. Eq. (37) is the time-discretized $\dot{p} = -\partial V(q)/\partial q$: at each kick the angular momentum p_t is accelerated to p_{t+1} by the force pulse $P(q_t)\Delta t$, with the time step and the rotor mass set to $\Delta t = 1$, $m = 1$.

3.1. Cat map

The simplest kicked rotor is subject to force pulses $P(q) = \kappa q$ proportional to the angular displacement q: in that case, the map (36,37) is of form

$$\begin{pmatrix} q_{t+1} \\ p_{t+1} \end{pmatrix} = \mathbb{J} \begin{pmatrix} q_t \\ p_t \end{pmatrix} \quad (\mathrm{mod}\ 1)\,, \qquad \mathbb{J} = \begin{pmatrix} \kappa+1 & 1 \\ \kappa & 1 \end{pmatrix}. \tag{38}$$

The (mod 1) makes the map a discontinuous 'sawtooth,' unless κ is a positive integer. The map is then a Continuous Automorphism of the Torus known as the Thom-Anosov-Arnol'd-Sinai *'cat map'* [9, 76, 244], extensively studied as the simplest example of a chaotic Hamiltonian system.

The determinant of the one-time-step Jacobian is $\det \mathbb{J} = 1$, i.e., the mapping is area-preserving. Let $s = \mathrm{tr}\, \mathbb{J} = \kappa + 2$ be the trace of the Jacobian. For $|s| > 2$ the $\mathbb{J}$ characteristic equation

$$\Lambda^2 - s\Lambda + 1 = 0\,, \tag{39}$$

has real roots $(\Lambda\,,\ \Lambda^{-1})$ and a positive Lyapunov exponent $\lambda > 0$,

$$\Lambda = e^{\lambda} = \frac{1}{2}(s + \sqrt{(s-2)(s+2)})\,, \qquad s = \mathrm{tr}\, \mathbb{J} = \Lambda + \Lambda^{-1}\,. \tag{40}$$

The eigenvalues are functions of the stretching parameter s, and for $|s| > 2$ the cat map (38) is a fully chaotic Hamiltonian dynamical system.

3.2. Temporal cat

In order to motivate our formulation of higher-dimensional spatiotemporal chaotic field theories, to be developed in [65], we now recast the *local* initial value, Hamiltonian time-evolution as a *global* solution to the Euler–Lagrange equations.

The 2-component field at the temporal lattice site t, $\phi_t = (q_t, p_t) \in (0,1] \times (0,1]$ is kicked rotor's the angular position and momentum. Hamilton's equations (36,37) induce forward-in-time evolution on a 2-torus (q_t, p_t) *phase space*. Eliminating the momentum by Hamilton's discrete time velocity eq. (36),

$$(q_t, p_t) = \left(q_t, \frac{q_t - q_{t-1}}{\Delta t}\right)\,, \tag{41}$$

setting the time step to $\Delta t = 1$, and forgetting for a moment the (mod 1) condition, the forward-in-time Hamilton's first order difference equations are brought to the second order difference, 3-term recurrence Euler–Lagrange equations for scalar field $\phi_t = q_t$,

$$\phi_{t+1} - 2\,\phi_t + \phi_{t-1} = P(\phi_t)\,. \tag{42}$$

But that is Newton's Second Law: "acceleration equals force," so Percival and Vivaldi [217] refer to this formulation as 'Newtonian'. Here we follow Allroth [2], Mackay, Meiss, Percival, Kook & Dullin [88, 164, 187, 188, 192], and Li and Tomsovic [171] in referring to it as 'Lagrangian'.

For the cat map (38), the Lagrangian passage (41) to the scalar field ϕ_t leads to the Percival-Vivaldi 'two-configuration representation' [217]

$$\begin{pmatrix} \phi_t \\ \phi_{t+1} \end{pmatrix} = \mathbb{J}_{PV} \begin{pmatrix} \phi_{t-1} \\ \phi_t \end{pmatrix} - \begin{pmatrix} 0 \\ m_t \end{pmatrix}\,, \qquad \mathbb{J}_{PV} = \begin{pmatrix} 0 & 1 \\ -1 & s \end{pmatrix}\,, \tag{43}$$

with matrix $\mathbb{J}_{PV}$ acting on the 2-dimensional space of successive configuration points $(\phi_{t-1}, \phi_t)^\top$. As was case for the Bernoulli map (30), the cat map (mod 1) condition (38)

is enforced by integers $m_t \in \mathcal{A}$, where for a given integer stretching parameter s the alphabet $\mathcal{A}$ ranges over $|\mathcal{A}| = s+1$ possible values for m_t,

$$\mathcal{A} = \{\underline{1}, 0, \dots s-1\}\,, \tag{44}$$

necessary to keep ϕ_t for all times t within the unit interval $[0, 1)$. (We find it convenient to have symbol $\underline{m_t}$ denote m_t with the negative sign, i.e., '$\underline{1}$' stands for symbol '-1'.)

Written out as a second-order difference equation, the Percival-Vivaldi map (43) takes a particularly elegant form, that we shall refer to as the *temporal cat* (19),

$$-\phi_{t+1} + s\,\phi_t - \phi_{t-1} = m_t\,, \tag{45}$$

or, in terms of a lattice state Φ, the corresponding symbol block M (29), and the $[n\times n]$ shift operator r (32),

$$(-r + s\,\mathbb{1} - r^{-1})\,\Phi = \mathsf{M}\,, \tag{46}$$

very much like the temporal Bernoulli condition (31), and the winding numbers (sources) M taking their values on the lattice sites of a 1-dimensional *temporal* lattice $t \in \mathbb{Z}$.

As was the case for temporal Bernoulli (31), the condition (43) is a linear relation: a given 'code' $\{m_t\}$ in terms of alphabet (44) corresponds to a unique temporal sequence $\{\phi_t\}$. That is why Percival and Vivaldi [217] refer to such symbol block M as a *linear code*. As for the Bernoulli system, m_t can also be interpreted as 'winding numbers' [160], or, as they shepherd stray points back into the unit torus, as 'stabilising impulses' [217]. Here we use the field-theoretical parlance, and refer to them as 'sources'. 2CB

3.3. Temporal cat as a continuous time dynamical system

Recall that the Bernoulli first-order difference equation could be viewed as a time-discretization of the first-order linear ODE (35). The second-order difference equation (45) can be interpreted as the second order discrete time derivative d^2/dt^2, or the temporal lattice Laplacian (13),

$$\Box\,\phi_t \equiv \phi_{t+1} - 2\phi_t + \phi_{t-1} = (s-2)\phi_t - m_t\,, \tag{47}$$

with the time step set to $\Delta t = 1$. In other words, if we include the cat map forcing pulse (37) $P(\phi_t) = -V'(\phi_t) = -(s-2)\,\phi + m_t$ into the definition of the on-site potential (17),

$$V(\Phi, \mathsf{M}) = \sum_{t\in\mathcal{L}} \left(\frac{1}{2}\mu^2\phi_t^2 - m_t\,\phi_t\right)\,, \tag{48}$$

the force is linear in the angular displacement ϕ, so the temporal cat Euler-Lagrange equation takes form (see free action (11))

$$(-\Box + \mu^2\,\mathbb{1})\,\Phi = \mathsf{M}\,, \tag{49}$$

where the Klein-Gordon mass μ is related to the cat-map stretching parameter s by $\mu^2 = s - 2$.

For small stretching parameter values, $s < 2$, this discretized Euler–Lagrange equation (5) describes a set of coupled penduli, with oscillatory solutions, known as the

discrete Helmholtz equation in applied math [78, 98, 176], as the tight-binding model, the Harper's or Azbel-Hofstadter model in solid state physics [56, 57, 90, 199, 216], and the critical almost Mathieu operator in mathematical physics [234], with quadratic action (11) written as Hamiltonian

$$H = \sum_{\ell} |\ell\rangle \epsilon_0 \langle \ell| + \sum_{\ell m} |\ell\rangle V_{\ell m} \langle m| \,, \quad V_{\ell m} = \begin{cases} V & \text{if } \ell, m \text{ nearest neighbors} \\ 0 & \text{otherwise} \end{cases}$$

with the stretching factor $s = -\epsilon_0/V$ in (47).

Here we study the strong stretching, $s > 2$ case, known as the discrete screened Poisson equation [82, 98, 116, 140, 141, 223], whose solutions are hyperbolic. We refer to the Euler–Lagrange equation (49) as the '*temporal cat*', both to distinguish it from the forward-in-time Hamiltonian cat *map* (38), and in the anticipation of the *spatiotemporal cat* to be discussed in the sequel [65]. Spatiotemporal cat differs from all of the above models because the field ϕ_t compactification to unit circle makes it a strongly nonlinear deterministic field theory, with nontrivial symbolic dynamics.

Temporal cat, summarized. In the spatiotemporal formulation a *global* temporal lattice state

$$\mathbf{\Phi}^\top = (\phi_t, \phi_{t+1}, \cdots, \phi_{t+k}) \tag{50}$$

is not determined by a forward-in-time 'cat map' evolution (38), but rather by the fixed point condition (5) that the *local*, 3-term discrete temporal lattice Euler–Lagrange equations (45) are satisfied at every lattice point. This temporal 1-dimensional lattice reformulation is the bridge that takes us from the single cat map (38) to the higher–dimensional coupled "multi-cat" spatiotemporal lattices[65, 123, 124].

And, did you know that the cute Arnold cat is but the screened Poisson equation in disguise? And that the lattice form (45) of the theory is so much more elegant than the cat-map form (38)? A cat is Hooke's wild, 'anti-harmonic' sister. For $s < 2$ Hooke rules: restoring oscillations around the sleepy resting state. For $s > 2$ cats rule: exponential runaway, wrapped globally around a state space torus. Cat is to chaos what harmonic oscillator is to order. There is no more fundamental example of chaos in mechanics.

4. A ϕ^3 field theory

The 'mod 1' in the definition of the 'linear' kicked rotor, the cat map (38), makes cat map a highly nonlinear, discontinuous map. In contrast, field theory action $S[\mathbf{\Phi}]$ is typically polynomial and smooth. The simplest such nonlinear action turns out to correspond to the paradigmatic dynamicist's model of a 2-dimensional nonlinear dynamical system, the Hénon map [130]

$$\begin{aligned} x_{t+1} &= 1 - a\, x_t^2 + b\, y_t \\ y_{t+1} &= x_t \,. \end{aligned} \tag{51}$$

For the contraction parameter value $b = -1$ this is a Hamiltonian map.

The *temporal evolution* Jacobian matrix for the nth iterate of the Hamiltonian Hénon map is the product of consecutive one time-step Jacobian matrices

$$J^n(x_0, y_0) = \prod_{m=n-1}^{0} \begin{pmatrix} -2a\, x_m & -1 \\ 1 & 0 \end{pmatrix} , \qquad x_m = f_1^m(x_0, y_0) , \tag{52}$$

where the successive 1-time step Jacobian matrices are multiplied in the order they are applied, as $J^n(x_0) = J(x_{n-1}) \cdots J(x_0)$. So, once we have a Hénon map periodic orbit, we also have its Floquet matrix (monodromy matrix). When J^n is hyperbolic, only the expanding eigenvalue $\Lambda_1 = 1/\Lambda_2$ needs to be determined, as the determinant of the Hénon 1-time step Jacobian matrix is unity,

$$\det J = \Lambda_1 \Lambda_2 = 1 . \tag{53}$$

The map is Hamiltonian in the sense that it preserves areas in the $[x, y]$ plane.

The Hénon map is the simplest map that captures chaos that arises from the smooth stretch & fold dynamics of nonlinear return maps of flows such as Rössler [228]. Written as a 2nd-order inhomogeneous difference equation [89], (51) takes the *temporal Hénon* 3-term recurrence form, explicitly time-translation and time-reversal invariant Euler–Lagrange equation

$$-\phi_{t+1} + a\, \phi_t^2 - \phi_{t-1} = 1 . \tag{54}$$

Just as the kicked rotor (36,37), the map can be interpreted as a kicked driven anaharmonic oscillator [129], with the nonlinear, cubic Biham-Wenzel [28] lattice site potential (16)

$$V(\Phi, \mathsf{M}) = \sum_{t \in \mathcal{L}} \left(\frac{a}{3} \phi_t^3 - m_t\, \phi_t \right) , \qquad m_t = -1 , \tag{55}$$

giving rise to kicking pulse (37).

> [2021-12-10 Predrag] Note the cubic Biham-Wenzel potential includes the source term, as (17). Please recheck the signs!

Devaney, Nitecki, Sterling and Meiss [77, 240, 241] have shown that the Hamiltonian Hénon map has a complete Smale horseshoe for sufficiently large 'stretching parameter' values

$$a > 5.699310786700 \cdots . \tag{56}$$

In numerical [71] and analytic [95] calculations we fix (arbitrarily) the stretching parameter value to $a = 6$, in order to guarantee that all 2^n periodic points $\phi = f^n(\phi)$ of the Hénon map (51) exist.

> [2021-12-10 Predrag] Explain that ϕ^3 theory is correspond to the unimodal temporal Hénon, with the Smale horseshoe repeller cleanly split into the left (negative) and right (positive) lattice site field values. This is very much like the temporal Bernoulli, in contrast to the temporal cat which has nontrivial pruning, see table 3.

[2021-06-04 Predrag] S. Aubry [16] *Anti-integrability in dynamical and variational problems*
The equilibria and relative equilibria of Frenkel-Kontorova models [17, 203], widely studied in literature, might be closely related to temporal Hénon and ϕ^4 lattices.
D. G. Sterling [242] much (undeservedly) un-cited PhD thesis, Univ. of Colorado, *Anti-Integrable Continuation and the Destruction of Chaos* has much to teach us. He studies *coupled Hénon map lattices* in both Hamiltonian and Lagrangian formulations; his definition seems pretty much consistent with our (**??**), though he has a coupling parameter c used to make spatial couplings weak. The "anti-integrable" refers to our choice $a \geq 6$, I believe - parameter regimes in which all of the horseshoe orbits exists.
"Specifying the anti-integrable state for an orbit of a coupled map lattice requires a multidimensional symbolic object which we call a symbol tensor."
His Figures 6.7, 6.18 are reminiscent of my pruning front.
Sterling and Meiss [240] *Computing periodic orbits using the anti-integrable limit*

Politi and Torcini [220] note that a problem in reconstructing the statistical properties of an spatiotemporal Hénon attractor is ensuring that all periodic orbits used are embedded into the inertial manifold. For instance, in the single Hénon map, one of the two fixed points is isolated and it does not belong to the strange attractor.

We resolve this problem by construction, all our solutions belong to the non-wondering set.

Politi and Torcini [220] *Periodic orbits in coupled Hénon maps: Lyapunov and multifractal analysis*

They study *spatiotemporal Hénon*, a (1+1)-spacetime lattice of Hénon maps orbits which are periodic both in space and time.

Their numerical method is an extension of Biham and Wenzel [28] for the single Hénon map, with symbols m_{nt} in $\mathcal{A} = \{0, 1\}$. Any fixed point in fictitious time corresponds to a spatio-temporal cycle $[L \times T]_S$.

5. A ϕ^4 field theory

If a potential that is bounded from below is needed to make sense of the probabilistic interpretation of the configuration weight (3), or a symmetry forbids the odd-power potentials such as (55), one starts instead with a quartic potential $\sim g\phi_t^4$, leading to the 'ϕ^4 lattice field theory' (21). As ϕ^4 example adds little to understanding over what is learned from temporal Hénon, we will not discus is further in this paper.

[2021-12-10 Predrag] No! Explain that ϕ^4 theory is the bimodal extension of what we had learned for the unimodal temporal Hénon.
The Hénon map/ϕ^3 approaches should be safe for multimodal maps with complete repelling sets, and it should work for finite-grammar Smale horseshoe repellers. Smale's original horseshoe [235], his fig. 1 was unimodal, but he also explicitly gives our ϕ^4 bimodal repeller, his fig. 5.

[2021-10-13 Predrag] RECHECK, maybe applies to spatiotemporal cat: Equilibria or steady solutions of Frenkel-Kontorova lattices, the smooth function $V : \mathbb{R} \to \mathbb{R}$ is a periodic onsite potential, $V[\phi + 1] = V[\phi]$ for all $\xi \in \mathbb{R}$.
The d-dimensional Frenkel-Kontorova Hamiltonian lattice differential equation [17, 203]

$$\frac{d^2\phi_i}{dt^2} + V'[\phi_i] - \Box\,\phi_i = 0 \text{ for all } i \in \mathbb{Z}^d. \tag{57}$$

describes the motion of particles under the competing influence of an onsite periodic potential field and nearest neighbor attraction.
the goal is to find a d-dimensional "lattice configuration" (for us, lattice state) $x : \mathbb{Z}^d \to \mathbb{R}$ that satisfies

$$V'[\phi_i] - \Box\,\phi_i = 0 \quad \text{for all } i \in \mathbb{Z}^d\,. \tag{58}$$

Eq. (58) is relevant for statistical mechanics [203], because it is related to Eq. (**??**)FKeq) describes its stationary solutions.

5.1. Computing lattice states for nonlinear theories

Unlike the temporal Bernoulli (18) and the temporal cat (19), for which the lattice state fixed point condition (5) is linear and easily solved, for nonlinear lattice field theories the lattice states are roots of polynomials of arbitrarily high order. While Gallas and collaborators [92–96, 106–108] have developed a powerful theory that yields Hénon map periodic orbits in analytic form, it would be unrealistic to demand such explicit solutions for general field theories on multi-dimensional lattices. We take a pragmatic, numerical route, and search for the fixed-point solutions (5) starting with the deviation of an approximate trajectory from the 3-term recurrence (17), given by the lattice deviation vector

$$v_t = -\phi_{t+1} + (V'(\phi_t) - m_t) - \phi_{t-1}\,, \tag{59}$$

and minimizing this error term by any convenient variational or optimization method, perhaps in conjunction with a high-dimensional variant of the Newton method [64, 166].

[2021-12-10 Predrag] Form $(V'(\phi_t) - m_t)$ looks like the most convenient definition of the "m-centered" subregion $\mathcal{M}_m$ potential, applicable to both linear and nonlinear field theories?

5.2. Papers to refer to?

Simó [233] *On the Hénon-Pomeau attractor* is a very fine early paper. Cite it in Hénon remark.

Miguel, Simó and Vieir [197] *From the Hénon conservative map to the Chirikov standard map for large parameter values* (click here):

Endler and Gallas [96]. method resembles the methods earlier employed for quadratic polynomials (and their Julia sets) by Brown [38] and Stephenson [239].

Brown gives cycles up to length 6 for the logistic map, employing symmetric functions of periodic points.

Hitzl and Zele [132] study the of the Hénon map for cycle lengths up to period 6.

6. Reciprocal lattice

ChaosBook conventions:

$\omega = e^{2i\pi/n}$
$\tilde{\phi}_k = x_k + i\, y_k = |\tilde{\phi}_k| e^{i\theta_k}$
$q_k = 2\pi k/n$,
n is the Bravais cell period

No self-respecting crystallographer would be drawing longer and longer Bravais lattice states (158)-(160) - they eventually run off the sheet of paper, no matter how wide. A professional crystallographer plots all lattice states snugly together in the first Brillouin zone, where the translational orbit of a lattice state is -literally- a circle, symmetric lattice states sit on boundaries of point group's fundamental domain, and everything is maximally diagonalized in term's of space group G irreps.

Still, when we think of a temporal lattice as 'time': no dynamicist does that. Embarrassing.

It is all breathtakingly simple on the reciprocal lattice. Period-n Bravais cell maps onto a regular n-gon in the reciprocal lattice, with the usual D_n symmetry axes. Time reversal fixes the symmetric solutions to sit on the symmetry axes, the boundaries of the fundamental domain. Lattice shift r_j maps out the G-orbit by running on circles, and orbits visit the $1/2n$ wedge only once, so the points in the fundamental domain represent an orbit each.

Here is a simple way to explain what the problem is:

Think of a discrete time dynamical system (iterations of a map) as a 1-dimensional lattice with the field on each site labeled by integer time. An period-n lattice state lives on a discrete 1-torus (a ring or necklace) of period-n, and if the law is time-independent, sets of solutions are invariant under cyclic perturbations. The symmetry is C_n, and one needs to distinguish C_n orbits ("prime cycles" in ChaosBook parlance; one per each orbit). The right way to do this is by going to C_n irreps, ie, by the discrete Fourier transform, with all reciprocal lattice Brillioun zone solutions orbits in an $1/n$ sliver of a n-gon. If n is prime, this is irreducible; if it is a multiple of a prime, one should remove those solutions, as they have already been accounted for.

If, in addition, the law is time-reversal (or time-inversion) invariant, the symmetry includes time-reflection, ie, it is dihedral group D_n with $2n$ elements, so the reciprocal lattice should be a half of the above $1/n$ sliver of a n-gon, and irreps are now either 1 or 2 dimensional. Even n is different from odd n, and solutions either appear in pairs, or are self dual under reflection in 3 different ways.

The symmetry is C_n, and one needs to distinguish C_n orbits ("prime cycles" in ChaosBook; one per each orbit). The right way to do this is by going to C_n irreps, ie, by the discrete Fourier transform, with all reciprocal lattice Brillioun zone solutions orbits in an $1/n$ sliver of a n-gon. If n is prime, this is irreducible; if it is a multiple of a prime, one should remove those solutions, as they have already been accounted for.

The quantum-mechanical calculations are executed by approximating the infinite crystal by a periodic one, and going go to the *reciprocal* space by deploying C_N discrete Fourier transform. This implements the G/T quotienting by translations and reduces the calculation to a finite *Brilluoin zone*. That is the content of the *'Bloch theorem'* of solid state physics. Further work is then required to reduce the calculations to the point group irreps.

In the reciprocal lattice k takes on the values in the first Brillouin zone interval $(-\pi/a, \pi/a]$.

Consider

$$\rho_{\vec{G}}(\vec{x}) = e^{i\vec{G}\cdot\vec{r}(\vec{x})}\,,$$

where $\vec{G}$ is a reciprocal lattice vector. By definition, $\vec{G}\cdot\vec{a}$ is an integer multiple of 2π, $\rho_{\vec{G}} = 1$ for lattice vectors. For any other state, reciprocal lattice state is given by

$$e^{i\vec{G}\cdot\vec{u}(\vec{x})} \neq 1\,.$$

When a cube is a building block that tiles a $3D$ cubic lattice, it is referred to as the 'elementary' or 'Wigner-Seitz' cell, and its Fourier transform is called 'the first Brillouin zone' in 'the reciprocal space'.

For a 1-dimensional lattice with lattice spacing 1, the reciprocal lattice has spacing $2\pi/1 = 2\pi$, with the (first) Brillouin zone from $k = -\pi$ to $k = \pi$. Due to the time reversal, all $k = 2\pi/5$ irrep states are the same as the $k = 4\pi/5$ irrep states.

the time-reversal pairs to be the complex-conjugate pairs in Fourier space, as C_∞ shift moves them in opposite directions.

the reciprocal lattice is:

$$\overline{\mathcal{L}}_{\mathbf{b}} = \{n\mathbf{b}\,|\,n \in \mathbb{Z}\}\,, \tag{60}$$

where the vector $\mathbf{b}$ satisfies:

$$\mathbf{b}\cdot\mathbf{a} = 2\pi\,. \tag{61}$$

The eigenvectors of the translation operator which satisfy the periodicity of the Bravais lattice are plane waves of form:

$$f_{\mathbf{k}}(\mathbf{z}) = e^{i\mathbf{k}\cdot\mathbf{z}}\,, \quad \mathbf{k} \in \overline{\mathcal{L}}\,, \tag{62}$$

where the wave vector $\mathbf{k}$ is on the reciprocal lattice $\overline{\mathcal{L}}$.

A general plane wave does not satisfy the periodicity, unless

$$e^{ik\cdot R} = 1\,. \tag{63}$$

Since R is a vector from the Bravais lattice $\mathcal{L}$, the wave vector $\mathbf{k}$ must lie in the reciprocal lattice of $\mathcal{L}$:

$$\mathbf{k} \in \mathcal{L}^*\,, \quad \mathcal{L}^* = \{m\mathbf{b}\,|\,m \in \mathbb{Z}\}\,, \tag{64}$$

where the primitive reciprocal lattice vectors $\mathbf{b}$ satisfies:

$$\mathbf{b}\cdot\mathbf{a} = 2\pi\,. \tag{65}$$

Barvinok arXiv:/math/0504444:
Let V be a d-dimensional real vector space with the scalar product $\langle \cdot, \cdot \rangle$ and the corresponding Euclidean norm $\| \cdot \|$. Let $\mathcal{L} \subset V$ be a lattice and let $\mathcal{L}^* \subset V$ be the *dual* or the *reciprocal* lattice

$$\mathcal{L}^* = \Big\{ x \in V : \quad \langle x, y \rangle \in \mathbb{Z} \quad \text{for all} \quad y \in \mathcal{L} \Big\} .$$

6.1. Reciprocal lattice state

An infinite lattice state is periodic if the state is invariant under the action of a translation group. A translation group can be described by a Bravais lattice, the vector in which determines the direction and distance of the translation. When the dynamical system has time translation symmetry, the defining equation of the system is invariant under translations. So it is natural to use the eigenvectors of the translation operator to study the lattice states of the system.

The eigenvectors of translation operators are plane waves defined on the lattice. But to study the lattice states, we need to require that the plane wave also satisfies the periodic condition. Generally, a d-dimensional Bravais lattice can be described by:

$$\mathcal{L} = \left\{ \sum_{i=1}^{d} n_i \mathbf{b}_i | n_i \in \mathbb{Z} \right\} , \tag{66}$$

where $\mathbf{b}_i$ is the ith primitive vector of the Bravais lattice. And a plane wave on the d-dimensional lattice is:

$$f_{\mathbf{k}}(\mathbf{z}) = e^{i\mathbf{k}\cdot\mathbf{z}} , \tag{67}$$

where $\mathbf{z}$ is the position of a lattice site, and $\mathbf{k}$ is the wave vector. The periodicity given by the Bravais lattice $\mathcal{L}$ requires that:

$$f_{\mathbf{k}}(\mathbf{z} + \mathbf{R}) = f_{\mathbf{k}}(\mathbf{z}) , \quad \mathbf{R} \in \mathcal{L} . \tag{68}$$

This condition can only be satisfied if the wave vector $\mathbf{k}$ exists on the reciprocal lattice of the lattice $\mathcal{L}$:

$$\overline{\mathcal{L}} = \left\{ \sum_{j=i}^{d} n_i \mathbf{b}_i | n_i \in \mathbb{Z} \right\} , \tag{69}$$

the basis vectors of which satisfy:

$$\mathbf{b}_i \cdot \mathbf{a}_j = 2\pi\delta_{ij} . \tag{70}$$

Using these eigenvectors we can transform lattice states into reciprocal lattice states by discrete Fourier transform. Any lattice state with the periodicity given by the Bravais lattice $\mathcal{L}$ can be spanned by the plane waves with wave vectors in the reciprocal lattice $\overline{\mathcal{L}}$. And since a lattice state only has values on lattice sites, we only need a finite number of plane waves to span the lattice state. For example, if the period of a 1-dimensional lattice state is n, the lattice state can be written as an n-dimensional vector, $(\phi_0, \phi_1, \phi_2, \ldots, \phi_{n-1})$, which is spanned as:

$$(\phi_0, \phi_1, \phi_2, \ldots, \phi_{n-1}) = \tilde{\phi}_0 \tilde{e}_0 + \tilde{\phi}_1 \tilde{e}_1 + \ldots + \tilde{\phi}_{n-1} \tilde{e}_{n-1} , \tag{71}$$

where

$$\tilde{e}_k = \frac{1}{\sqrt{n}}(1, \omega^k, \omega^{2k}, \ldots, \omega^{k(n-1)})\,, \qquad k = 0, 1, \ldots, n-1\,, \omega = \mathrm{e}^{2\pi \mathrm{i}/n} \quad (72)$$

are normalized lattice states of plane waves, or Fourier modes.

6.2. Irreducible representations of the symmetry group

6.2.1. Cyclic groups When we write period-n lattice states as n-dimensional vectors, and write the shift operator r as a $[n \times n]$ matrix (32) which applies cyclic permutation to the lattice state, the matrix representation of shift operators forms a permutation representation of the cyclic translation group C_n. This permutation representation is a reducible representation, i.e., it can be block diagonalized by a similarity transformation. Each block on the diagonal is an irreducible representation (irrep).

The abelian group C_n only has 1-dimensional irreps. The permutation representation of C_n can be diagonalized by discrete Fourier transform. After the transform the representation of the shift operator becomes,

$$r^m = \begin{pmatrix} 1 & & & & \\ & \omega^m & & & \\ & & \omega^{2m} & & \\ & & & \ddots & \\ & & & & \omega^{(n-1)m} \end{pmatrix}, \quad \omega = \mathrm{e}^{2\pi \mathrm{i}/n}\,, \qquad (73)$$

with lattice states projected onto 1-dimensional subspaces in which action of the shift operators is given by corresponding irrep. As we transform the permutation representation of the shift operator into the block diagonal form, the lattice states $(\phi_0, \phi_1, \phi_2, \ldots, \phi_{n-1})$ are spanned by the Fourier modes basis, with components $(\tilde{\phi}_0, \tilde{\phi}_1, \tilde{\phi}_2, \ldots, \tilde{\phi}_{n-1})$. When the shift operator acts on the lattice state: $\Phi \to r\Phi$, the irreducible representations act on the components in the corresponding subspace: $\tilde{\phi}_k \to \omega^k \tilde{\phi}_k$.

As a concrete example, consider the temporal Bernoulli period-3 Bravais lattice. It's a linear problem and all lattice states are easily computed by hand. There is always the fixed point lattice state $(0, 0, 0)$, and for the stretching parameter value $s = 2$, there are 6 lattice states organized into 2 period-3 orbits, which we mark by a single lattice state per orbit, for example $(\frac{1}{7}, \frac{2}{7}, \frac{4}{7})$ and $(\frac{3}{7}, \frac{6}{7}, \frac{5}{7})$. The remaining lattice states are their cyclic permutations.

Discrete Fourier transform, figure 3, maps these 7 lattice states into 7 reciprocal lattice states.

[2021-09-02 Predrag] Why do you mark 1/8 in figures 3 and 4, when the units are 1/7's? I see. You have $1/\sqrt{3}$ and π's floating around, unless you redefine units...

The $k = 1$ and $k = 3 - 1$ wave-numbers reciprocal lattice states are complex conjugates of each other because the lattice states are real.

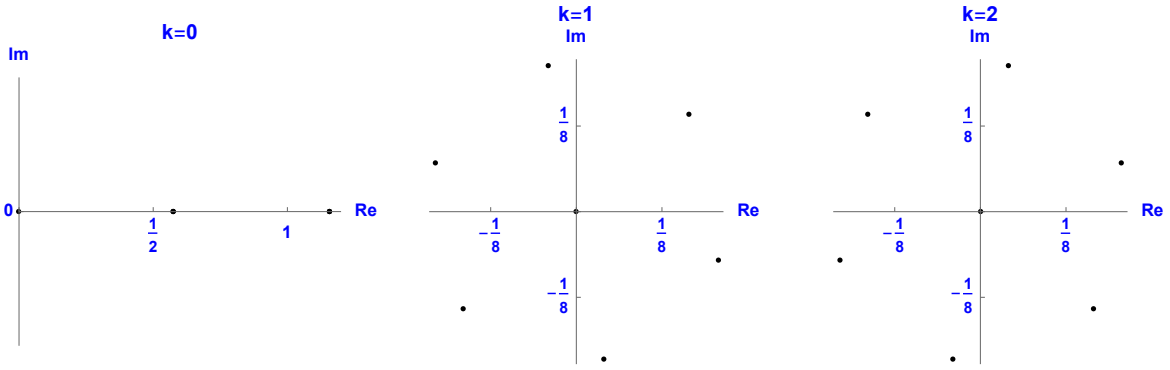

Figure 3. Period-3 lattice states of the temporal Bernoulli with $s = 2$, plotted in the C_3 permutation irreps subspaces.

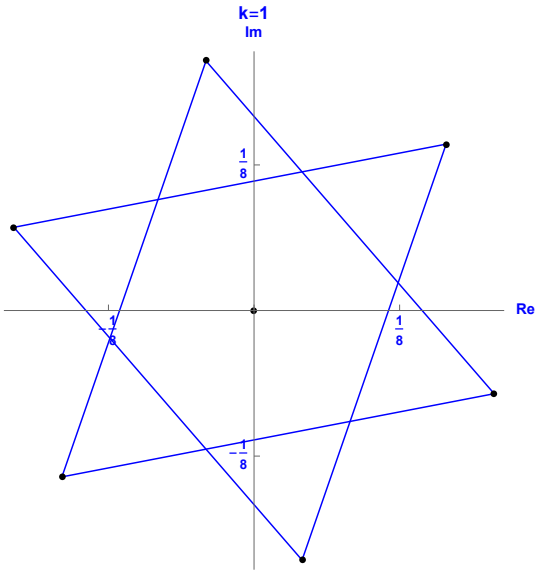

Figure 4. Period-3 lattice states of the temporal Bernoulli with $s = 2$ in the subspace of $k = 1$ irrep. Lattice states that are related by cyclic permutations are connected by blue lines. The two triangles are 2 C_3 orbits. The state in the center is the fixed point.

Consider next the action of the shift operator r on the reciprocal lattice states. In the $k = 0$ subspace, the eigenvalue of any shift is 1, so the $k = 0$ component of any reciprocal lattice state is invariant under the shift. In the $k = 1$ and $k = 2$ subspaces, the shift r acts by complex phase rotations $\exp(2\pi i/3)$ and $\exp(4\pi i/3)$, with the two subspaces rotating counter clockwise and clockwise by $2\pi/3$ in the complex plane: reciprocal lattice states that belong to the same orbit lie on a circle in the complex plane, related by complex rotations. Figure 4 illustrates this; the two orbits, built from reciprocal lattice states that are related by shifts, are connected by blue lines.

6.2.2. Dihedral group In the n-dimensional space of the period-n lattice states, the permutation representation of the Dihedral group D_n can be generated by the shift

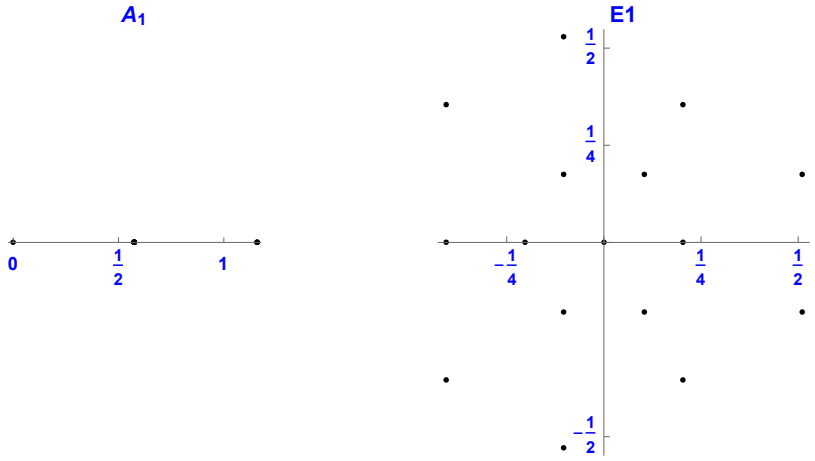

Figure 5. Period-3 lattice states of the $s = 3$ temporal cat, plotted in the D_3 permutation irreps subspaces $A_0 + E$. In contrast with the C_n complex irreps (see the C_3 example figure 3), the 2-dimensional irrep $E \in \mathbb{R}^2$ is real.

operator matrix representation (32) and the reflection operator matrix representation:

$$\sigma = \begin{pmatrix} 1 & & & & 0 \\ & & & 0 & 1 \\ & & \iddots & 1 & \\ & 0 & \iddots & & \\ 0 & 1 & & & \end{pmatrix} . \tag{74}$$

The Dihedral group D_n has: 2 1-dimensional irreps and $[(n-1)/2]$ 2-dimensional irreps if n is odd, or 4 1-dimensional irreps and $(n/2-1)$ 2-dimensional irreps if n is even. If n is odd, the permutation representation can be block diagonalized into irreps: $A_0 \oplus E_1 \oplus \ldots \oplus E_{(n-1)/2}$. If n is even, the permutation representation can be block diagonalized into irreps: $A_0 \oplus B_1 \oplus E_1 \oplus \ldots \oplus E_{n/2-1}$.

When we use the similarity transformation to diagonalize the permutation representation, the lattice states are transformed into the subspaces of the irreps. The example of period-3 lattice states of temporal cat with $s = 3$ is shown in figures 5 and 6. The permutation representation is block diagonalized by basis vectors: $e_0 = 1/\sqrt{3}(1,1,1)$, $e_1 = \sqrt{2/3}(\cos(2\pi/3), \cos(4\pi/3), 1)$ and $e_2 = \sqrt{2/3}(\sin(2\pi/3), \sin(4\pi/3), 0)$. The basis vector e_0 spans the subspace of the 1-dimensional irrep A_0. Basis vectors e_1 and e_2 span the subspace of the 2-dimensional irrep E.

Period-3 lattice states of cat map with $s = 3$ are mapped into the subspace of the irreps A_0 and E in figure 5. The irrep A_0 is the symmetric 1-dimensional irrep, so in the subspace of A_0 the components of lattice states are invariant under the action of the D_3 group. In the 2-dimensional subspace of the irrep E, the shift operator r rotates the lattice states clockwise by $2\pi/3$, while the reflection operator σ reflects the lattice states over the axis passing through the origin and pointing toward $(\cos(2\pi/3), \sin(2\pi/3))$. In

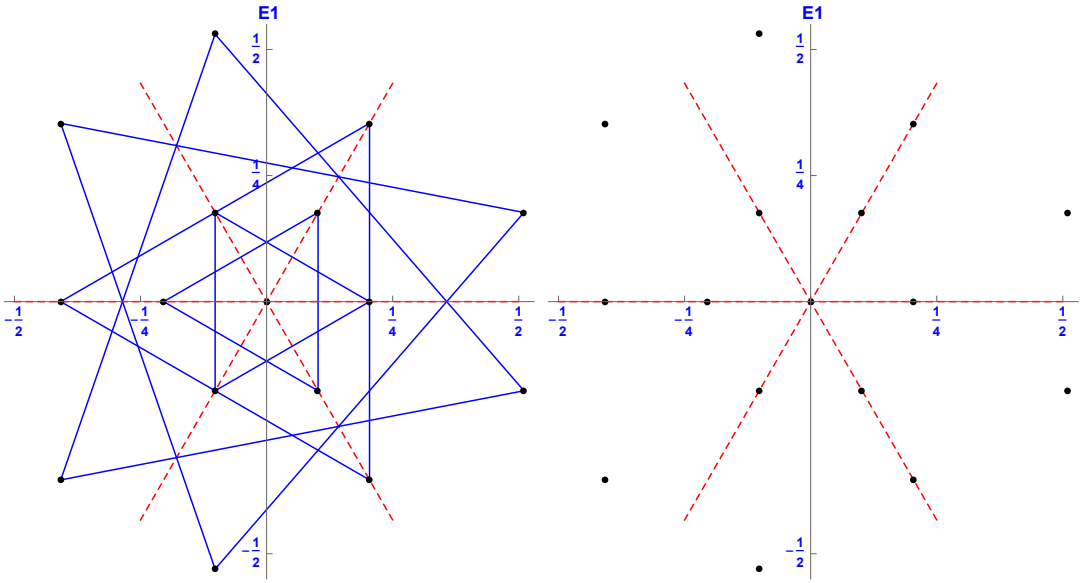

(a) (b)

Figure 6. Period-3 lattice states of the Temporal cat with $s = 3$ in the subspace of E_1 irrep. (a): Lattice states that are related by cyclic permutations are connected by blue lines. The two big triangles are a single D_3 6-lattice states orbit, what for C_3 is a pair of 3-lattice states orbits without time reversal symmetry. The remaining three smaller triangles are 3 time-reversal symmetric orbits; the pair in the middle is presumably related by the $D_1 : S\phi_i = 1 - \phi_i$ invariance specific to the temporal cat, a symmetry not yet taken into account. The state in the center is the fixed point. (b): Red dashed lines are the reflection axes of the D_3 group. There are 4 states on each reflection axis.

figure 6 lattice states that are related by shifts are connected by blue lines. The red dashed lines are reflection axis of the reflection operators. The 2 big triangles in figure 6 (a) are lattice states that belong to 2 orbits which are related by time reflection. The rest 3 triangles are lattice states from 3 orbits which are invariant under time reflection.

6.3. Fundamental domain

Given the space of the field configuration and the symmetry group acting on it, we can find a fundamental domain such that each orbit in this space visits the fundamental domain only once. Each lattice state in the fundamental domain is a representative lattice state of an orbit.

[2021-10-12 Predrag] Please read our draft [173], and either follow our definition (6) of *lattice state*, or replace it with some other definition.

One method to find the fundamental domain is based on the decomposition of the space into the subspaces of the irreps of the symmetry group. A natural way to choose the fundamental domain is to divide in the subspace of an irrep, where the irrep divides the subspace into the number of copies that is equal to the order of the symmetry group.

For example, in the space of the field configuration with C_n symmetry, the $k = 1$ subspace spanned by the eigenstate $\tilde{e}_1$, defined in (72), can be divided into n copies. One can choose the region in the complex plane of $k = 1$ subspace with argument $0 \leq \arg(\tilde{\phi}_1) < 2\pi/n$ to be the fundamental domain. Each orbit can visit the fundamental domain only once. As shown in figure 4, there are 3 points in this region, which are representative lattice states of two different period-3 orbits and the fixed point 0.

If the space of the field configuration has D_n symmetry, the subspace of the 2-dimensional irrep E_1 can be divided into $2n$ copies by the irrep. One can choose the fundamental domain to be the region with polar angle between 0 and π/n, assuming that the horizontal axis is one of the reflection axis of the irrep E_1. Each orbit only appears once in the fundamental domain, as shown in figure 6. Note that the two orbits related by the time reflection are considered one orbit of the dihedral group.

What happens when lattice states appear on the boundary of the fundamental domain? There are two possible situations. The first situation is that the lattice state belongs to an orbit with multiplicity less than the order of the symmetry group. For example, in figure 6, there are 3 points in the fundamental domain with polar angle equal to 0 or $\pi/3$. These 3 points are representative lattice states of orbits with time reflection symmetry. The multiplicities of these orbits are 3 instead of 6.

The second situation is that the multiplicity of the orbit of the lattice state is equal to the order of the symmetry group but the component in the subspace is 0. For example,

$$\Phi = \frac{1}{104}(17, 51, 49, 43, 25, 75)$$

is a period-6 lattice state of the temporal Bernoulli (18) with $s = 3$. Using the discrete Fourier transform this lattice state becomes:

$$\tilde{\phi} = \left(\frac{5}{2\sqrt{6}}, 0, \frac{-5 - 3i\sqrt{3}}{13\sqrt{6}}, -\frac{\sqrt{3}}{4\sqrt{2}}, \frac{-5 + 3i\sqrt{3}}{13\sqrt{6}}, 0 \right) .$$

This is a period-6 lattice state. It belongs to an orbit that contains 6 different lattice states. The $k = 1$ component of this lattice state is 0, which is on the boundary of the fundamental domain. To put this kind of lattice states into the fundamental domain one needs to divide other subspaces. For this lattice state the $k = 2$ and $k = 3$ components are not 0. The irreps divide the $k = 2$ subspace into 3 copies and the $k = 3$ subspace into 2 copies. One way to choose the fundamental domain in these subspaces is: the argument of the component in the $k = 1$ subspace is $0 \leq \arg(\tilde{\phi}_1) < \pi/3$; if the $k = 1$ component is 0, the arguments of the components in the $k = 2$ and $k = 3$ subspaces are $0 \leq \arg(\tilde{\phi}_2) < 2\pi/3$ and $0 \leq \arg(\tilde{\phi}_3) < \pi$. Each orbit is guaranteed to visit this fundamental domain exactly once.

7. Orbit stability

The temporal lattice reformulation gives us deep insights into how to enumerate and determine all global solutions (lattice states) of lattice field theories.

The discretized Euler–Lagrange $F[\Phi_c] = 0$ fixed point condition (5) is central to the theory of global methods for finding periodic orbits. Instead of utilizing local, forward-in-time numerical integrations, in global multi-shooting, collocation [49, 81, 119], and Lindstedt-Poincaré [254–256] searches for periodic orbits, one discretizes a periodic orbit into n segments [64, 79, 80, 166] temporal lattice configuration, and lists the field value at a point of each segment

$$\Phi^\top = (\phi_0, \phi_1, \cdots, \phi_{n-1})\,. \tag{75}$$

Starting with an initial guess for Φ, the zero of function $F[\Phi_c]$ can then be found by Newton iteration, which requires an evaluation of the $[n\times n]$ *orbit Jacobian matrix*

$$\mathcal{J}_{tt'} = \frac{\delta F[\Phi_c]_t}{\delta \phi_{t'}}\,. \tag{76}$$

7.1. Temporal Bernoulli, temporal cat

The temporal Bernoulli condition (31) and the temporal cat discretized Euler–Lagrange equation (46) can be viewed as searches for zeros of the vector of n functions

$$F[\Phi_{\mathsf{M}}] = \mathcal{J}\Phi - \mathsf{M} = 0 \tag{77}$$

$$\text{temporal Bernoulli:} \qquad \mathcal{J} = -r + s\,\mathbb{1} \tag{78}$$

$$\text{temporal cat:} \qquad \mathcal{J} = -r + s\,\mathbb{1} - r^{-1}\,, \tag{79}$$

with the entire periodic *lattice state* Φ_{M} treated as a single fixed *point* $(\phi_0, \phi_1, \cdots, \phi_{n-1})$ in the n-dimensional state space unit hyper-cube $\Phi \in [0,1)^n$, and the $[n\times n]$ orbit Jacobian matrix $\mathcal{J}$.

The $[n\times n]$ orbit Jacobian matrix $\mathcal{J}$ is a Toeplitz matrix, i.e., matrix constant along each diagonal, $\mathcal{J}_{k\ell} = j_{k-\ell}$, of circulant form, for the temporal Bernoulli,

$$\mathcal{J} = \begin{pmatrix} s & -1 & 0 & 0 & \dots & 0 & 0 \\ 0 & s & -1 & 0 & \dots & 0 & 0 \\ 0 & 0 & s & -1 & \dots & 0 & 0 \\ \vdots & \vdots & \vdots & \vdots & \ddots & \vdots & \vdots \\ 0 & 0 & 0 & 0 & \dots & s & -1 \\ -1 & 0 & 0 & 0 & \dots & 0 & s \end{pmatrix}. \tag{80}$$

and for temporal cat

$$\mathcal{J} = \begin{pmatrix} s & -1 & 0 & 0 & \dots & 0 & -1 \\ -1 & s & -1 & 0 & \dots & 0 & 0 \\ 0 & -1 & s & -1 & \dots & 0 & 0 \\ \vdots & \vdots & \vdots & \vdots & \ddots & \vdots & \vdots \\ 0 & 0 & 0 & 0 & \dots & s & -1 \\ -1 & 0 & 0 & 0 & \dots & -1 & s \end{pmatrix}. \tag{81}$$

7.2. Nonlinear field theories

The key to understanding their chaoticity are the eigenvalues of the orbit Jacobian matrix,

The temporal Bernoulli condition (31) can be thus viewed as a time-discretized, first-order ODE dynamical system

$$\dot{\Phi} \;=\; v(\Phi)\,, \tag{82}$$

where the 'velocity' vector field v is given by

$$v(\Phi) \;=\; (s-1)\,\Phi - \mathsf{M}\,,$$

with the time increment set to $\Delta t = 1$, and perturbations that grow (or decay) with rate $(s-1)$.

consider a temporal lattice with a set of d fields $\phi_t = \{\phi_{t,1}, \phi_{t,2}, \ldots, \phi_{t,d}\}$ on each lattice site t, and time evolution given by a d-dimensional map $\phi_{t+1} = \hat{f}(\phi_t)$. A period-$n$ lattice state (29) thus satisfies site-by-site the first-order difference equation

$$\phi_t - \hat{f}(\phi_{t-1}) = 0\,, \qquad t = 1, 2, \cdots, n\,. \tag{83}$$

the matrix of second variations of the action $S[\Phi]_{tt'}$,

$$\mathcal{J}[\Phi] = \begin{pmatrix} s_0 & -1 & 0 & 0 & \cdots & 0 & -1 \\ -1 & s_1 & -1 & 0 & \cdots & 0 & 0 \\ 0 & -1 & s_2 & -1 & \cdots & 0 & 0 \\ \vdots & \vdots & \vdots & \vdots & \ddots & \vdots & \vdots \\ 0 & 0 & 0 & 0 & \cdots & s_{n-2} & -1 \\ -1 & 0 & 0 & 0 & \cdots & -1 & s_{n-1} \end{pmatrix}, \tag{84}$$

evaluated on a lattice state Φ, and its Hill determinant $\mathrm{Det}\,\mathcal{J}[\Phi]$, with the 'stretching factor' $s_t = V''(\phi_t)$ at lattice site t in general a function of the site field ϕ_t for the given lattice state Φ.

[2020-06-01 Predrag] Cite Gade and Amritkar [105] as an early investigation of a lattice orbit Jacobian matrix. They did not know about 'Hill's formula.

8. Stability of an orbit vs. its time-evolution stability

His 1878-1886 study of the stability of planar motion of the Moon around the Earth led Hill to the *Hill's formula* [131]

$$|\mathrm{Det}\,\mathcal{J}_c| = |\det(\,\mathbb{1} - \mathbb{J}_c)| \tag{85}$$

which relates the characteristic polynomial of the forward-in-time evolution periodic orbit Floquet matrix (monodromy matrix) $\mathbb{J}_c$ to the determinant of the global orbit Jacobian matrix $\mathcal{J}_c$ (in Lagrangian settings, the Hessian, the second variation of the action functional). In case of Lagrangian dynamics, the discrete-time Hill's formula that we use here was derived by Mackay and Meiss [187] in 1983.

Historically, in periodic orbit theory calculations one always computes $\mathbb{J}_c$. However, as we shall argue here, it is the Hill determinant $\mathrm{Det}\,\mathcal{J}_c$ that is the computationally robust quantity that one should evaluate. In his application Hill was lucky: $\mathrm{Det}\,\mathcal{J}_c$ that he computed in a $[3\times 3]$ Fourier modes matrix approximation turned out to be a quite good approximation. But this is a remarkable formula, especially in the limit of $n \to \infty$ infinitesimal time steps, a formula that relates the ∞-dimensional *functional* Hill determinant $\mathrm{Det}\,\mathcal{J}_c$ to a determinant of the finite $[d\times d]$ matrix $\mathbb{J}_c$, and it took Poincaré [219] to prove that Hill's Fourier modes calculation is correct in the continuum limit.

While first discovered in a Lagrangian setting, Hill's formulas are much more general, with the Lagrangian formalism of [32, 164, 187, 250] getting in the way of understanding the general case. The formula applies to dissipative dynamical systems as well, from the Bernoulli map to Navier-Stokes and Kuramoto-Sivashinsky equation [120, 121]. As the formula is fundamental to the formulation of the spatiotemporal chaotic field theory, we shall rederive it here in three ways, relying on nothing more than elementary linear algebra.

The formula is so elementary that many practitioners routinely use it without ever having heard of 'Hill's formula'. Let's say that a periodic $\phi_{t+n} = \phi_t$ lattice state $\mathbf{\Phi}_c$ is known 'numerically exactly', that is to say, to a high (but not infinite) precision. One way to present the solution is to list the field value ϕ_0 at a single lattice site $t = 0$, and let the reader reconstruct the rest by stepping forward in time, $\phi_t = \hat{f}^t(\phi_0)$.

However, for a linearly unstable orbit a single field value ϕ_0 does not suffice to present the solution, because there is always a finite 'Lyapunov time' t_{Lyap} beyond which $\hat{f}^t(\phi_0)$ has lost all memory of the lattice state $\mathbf{\Phi}_c$. This problem is particularly severe in searches for 'exact coherent structures' embedded in turbulence, where even the shortest period solutions have to be computed to the (for a working fluid dynamicist excessive) machine precision [109, 110, 260], in order to complete the first return to the initial state. So, the words uttered in introductory nonlinear dynamics courses is never what is practiced.

Instead of relaying on forward-in-time numerical integration, *global methods* for finding periodic orbits [49] view them as equations for the vector fields $\dot{\phi}$ on spaces of closed curves. In numerical implementations one discretizes a periodic orbit p into

sufficiently many short segments [49, 79–81, 119], and lists one field value for each segment

$$p = (\phi_1, \phi_2, \cdots, \phi_{n_c}) \,. \tag{86}$$

For a n_c-dimensional discrete time map $\hat{f}$ obtained by cutting the flow by n_c local Poincaré sections, with the periodic orbit c of discrete period n_c, every segment can be reconstructed by short time integration, and satisfies

$$\phi_{t+1} = \hat{f}_t(\phi_t) \,, \tag{87}$$

to high accuracy, as for sufficiently short times the exponential instabilities are numerically controllable.

8.1. Hill determinant for a d-component lattice field

The orbit Jacobian matrix $\mathcal{J}_{tt'}$ (76) is a high–dimensional linear stability matrix for the extremum condition $F[\Phi_c] = 0$, evaluated on the lattice state Φ_c. How is the stability so computed related to the conventional dynamical systems' forward-in-time stability? To motivate the answer in its generality, consider a temporal lattice with a set of d fields $\phi_t = \{\phi_{t,1}, \phi_{t,2}, \ldots, \phi_{t,d}\}$ on each lattice site t, and time evolution given by a d-dimensional map $\phi_{t+1} = \hat{f}(\phi_t)$. A period-$n$ lattice state (29) thus satisfies site-by-site the first-order difference equation

$$\phi_t - \hat{f}(\phi_{t-1}) = 0 \,, \qquad t = 1, 2, \cdots, n \,. \tag{88}$$

A small deviation $\Delta\Phi$ from Φ_p then satisfies the linearized condition

$$\Delta\phi_t - r^{-1}\mathbb{J}_t\,\Delta\phi_t = 0 \,, \qquad (\mathbb{J}_t)_{ij} = \frac{\partial f(\phi_t)_i}{\partial \phi_j} \,, \tag{89}$$

where $\mathbb{J}_t$ is the 1-time step $[d\times d]$ Jacobian matrix, evaluated on lattice site t.

It suffices to work out a temporal period $n = 3$ example to understand the calculation for any period. In terms of the $[3d\times 3d]$ generalized (32) block shift matrix r, the orbit Jacobian matrix (76) has block matrix form

$$\mathcal{J}_p \;=\; \mathbb{1} - r^{-1}\mathbb{J} \,, \quad r = \begin{bmatrix} 0 & \mathbb{1}_d & 0 \\ 0 & 0 & \mathbb{1}_d \\ \mathbb{1}_d & 0 & 0 \end{bmatrix} \,, \quad \mathbb{J} = \begin{bmatrix} \mathbb{J}_1 & 0 & 0 \\ 0 & \mathbb{J}_2 & 0 \\ 0 & 0 & \mathbb{J}_3 \end{bmatrix} \,, \tag{90}$$

where $\mathbb{1}$ is the d-dimensional identity matrix. Next, consider

$$r^{-1}\mathbb{J} = \begin{bmatrix} 0 & 0 & \mathbb{J}_3 \\ \mathbb{J}_1 & 0 & 0 \\ 0 & \mathbb{J}_2 & 0 \end{bmatrix} \,, \quad (r^{-1}\mathbb{J})^2 = \begin{bmatrix} 0 & \mathbb{J}_3\mathbb{J}_2 & 0 \\ 0 & 0 & \mathbb{J}_1\mathbb{J}_3 \\ \mathbb{J}_2\mathbb{J}_1 & 0 & 0 \end{bmatrix} \,, \tag{91}$$

and note that the $n = 3$ repeat of $r^{-1}\mathbb{J}$ is block-diagonal

$$(r^{-1}\mathbb{J})^3 = \begin{bmatrix} \mathbb{J}_3\mathbb{J}_2\mathbb{J}_1 & 0 & 0 \\ 0 & \mathbb{J}_1\mathbb{J}_3\mathbb{J}_2 & 0 \\ 0 & 0 & \mathbb{J}_2\mathbb{J}_1\mathbb{J}_3 \end{bmatrix} \,, \tag{92}$$

with $[d\times d]$ blocks cyclic permutations of each other.f In general, the trace of the $[nd\times nd]$ matrix for a period n lattice state

$$\mathrm{Tr}(r^{-1}\mathbb{J})^k = \delta_{k,rn}\, n\ \mathrm{tr}\,\mathbb{J}_p^r\,, \quad \mathbb{J}_p = \mathbb{J}_n\mathbb{J}_{n-1}\cdots\mathbb{J}_2\mathbb{J}_1$$

is non-vanishing only if k is a multiple of n, where $\mathbb{J}_p$ is the forward-in-time $[d\times d]$ Floquet matrix of the periodic orbit p.

Now we can evaluate the Hill determinant $\mathrm{Det}\,\mathcal{J}_p$ by expanding

$$\begin{aligned}\ln \mathrm{Det}\,\mathcal{J}_p &= \mathrm{Tr}\ln(\,\mathbb{1} - r^{-1}\mathbb{J}) \;=\; -\sum_{k=1}^{\infty}\frac{1}{k}\,\mathrm{Tr}(r^{-1}\mathbb{J})^k \\ &= \;-\,\mathrm{tr}\sum_{r=1}^{\infty}\frac{1}{r}\mathbb{J}_p^r = \ln\det(\,\mathbb{1}_d - \mathbb{J}_p)\,. \end{aligned} \tag{93}$$

The orbit Jacobian matrix $\mathcal{J}_p$ evaluated on a lattice state Φ_p satisfying the temporal lattice first-order difference equation (88), and the dynamical, forward-in-time Jacobian matrix $\mathbb{J}_p$ are thus related by *Hill's formula*

$$\mathrm{Det}\,\mathcal{J}_p = \det(\,\mathbb{1} - \mathbb{J}_p)\,, \tag{94}$$

which relates the global orbit stability to the Floquet, forward-in-time evolution stability.

As far as the time-evolution stability is concerned, the $|\mathrm{Det}\,\mathcal{J}_\mathsf{M}| = |\det(\,\mathbb{1} - \mathbb{J}_\mathsf{M})|$ formula (94) is correct for all first-order difference equations (systems whose evolution laws are first order in time), for any $[d\times d]$ one-time-step Jacobian matrix. For the Bernoulli system that is a $[1\times 1]$ matrix $\mathbb{J} = s$, with the periodic points count (**??**) trivially verified.

The temporal Bernoulli (31) is a particularly simple, linear example. The site field ϕ_t is a scalar, the 1-time step $[1\times 1]$ time-evolution Jacobian matrix (89) at every lattice point t is simply $\mathbb{J}_t = s$, and the orbit Jacobian matrix (31) is the same for all lattice states of period n, so

$$\text{temporal Bernoulli:} \qquad N_n = |\mathrm{Det}\,\mathcal{J}| = s^n - 1\,, \tag{95}$$

in agreement with the time-evolution count (28); all itineraries are allowed, except that the periodicity of $r^n = \mathbb{1}$ accounts for $\overline{0}$ and $\overline{s-1}$ fixed points (see figure 2) being a single periodic point.

8.2. Hill determinant of a forward-in-time map

For a d-dimensional deterministic map $\phi_{t+1} = \hat{f}(\phi_t)$, the Perron-Frobenius operator

$$\mathcal{L}\,\rho(\phi_{t+1}) = \int_{\mathcal{M}} d\phi_t\,\delta(\phi_{t+1} - \hat{f}(\phi_t))\,\rho(\phi_t) \tag{96}$$

maps a density distribution $\rho(\phi_t)$ forward-in-time. Its kernel, a d-dimensional Dirac delta function

$$\mathcal{L}(\phi_{t+1},\phi_t) = \delta(\phi_{t+1} - \hat{f}(\phi_t))\,, \tag{97}$$

applied repeatedly, satisfies the group property

$$\mathcal{L}^2(\phi_{t+2},\phi_t) = \int_{\mathcal{M}} d\phi_{t+1}\, \mathcal{L}(\phi_{t+2},\phi_{t+1})\, \mathcal{L}(\phi_{t+1},\phi_t) = \delta(\phi_{t+2} - f^2(\phi_t))\,. \quad (98)$$

The time-evolution periodic orbit theory [71] relates the long time chaotic averages to the traces of the Perron-Frobenius operator

$$\mathrm{tr}\,\mathcal{L}^n = \int_{\mathcal{M}} d\phi\, \mathcal{L}^n(\phi,\phi) = \int_{\mathcal{M}} d\phi_c\, \delta(\phi_c - f^n(\phi_c)) \quad (99)$$

and its weighted, evolution operator generalizations, with support on all periodic points / lattice states $\phi_c = f^n(\phi_c)$ of period cl.

To evaluate the trace of the nth iterate of the Perron-Frobenius operator, one can either use the kernel of the operator $\mathcal{L}^n(\phi_n,\phi_0) = \delta(\phi_n - f^n(\phi_0))$,

$$\mathrm{tr}\,\mathcal{L}^n = \int_{\mathcal{M}} d\phi_0\, \delta(\phi_0 - f^n(\phi_0))\,, \quad (100)$$

or, using the group property (98) to insert integrations over intermediate lattice sites, the product of one-time-step operators $\mathcal{L}$:

$$\begin{aligned} \mathrm{tr}\,\mathcal{L}^n &= \int d\Phi \prod_{t=0}^{n-1} \delta(\phi_{t+1} - \hat{f}(\phi_t))\,, \\ \phi_n &= \phi_0\,, \quad d\Phi = \prod_{t=0}^{n-1} d\phi_t\,. \end{aligned} \quad (101)$$

The field ϕ_t on every lattice site t is a d-dimensional vector, so a period-n lattice state Φ is a nd-dimensional vector, with the Dirac function also nd-dimensional. In matrix notation this trace takes a compact form:

$$\mathrm{tr}\,\mathcal{L}^n = \int d\Phi\, \delta(r\Phi - \hat{f}(\Phi))\,, \quad (102)$$

where Φ and $\hat{f}(\Phi)$ are nd-dimensional column vectors with $(id+j)$th components $(\phi_t)_j$ and $[\hat{f}(\phi_t)]_j$, where $0 \le i < n-1$, $0 \le j < d-1$, and r is the cyclic $[nd \times nd]$ shift operator (compare with (32)):

$$r = \begin{pmatrix} 0 & \mathbb{1} & & & \\ & 0 & \mathbb{1} & & \\ & & & \ddots & \\ & & & 0 & \mathbb{1} \\ \mathbb{1} & & & & 0 \end{pmatrix}, \quad (103)$$

where $\mathbb{1}$ is the d-dimensional identity matrix. Note that the vector in the nd-dimensional Dirac delta function is the defining equation (5) of the system:

$$F[\Phi] = r\Phi - \hat{f}(\Phi)\,.$$

(5) with a global deterministic solution Φ_c satisfying this local extremal condition on every lattice site.

Restricting the integration to an infinitesimal neighborhood $\mathcal{M}_p$ around a periodic point ϕ_p, the contribution from this periodic point is:

$$\text{tr } \mathcal{L}^n|_p = \int_{\mathcal{M}_p} d\phi_0 \, \delta(\phi_0 - f^n(\phi_0)) = \frac{1}{|\det(\mathbb{1} - \mathbb{J}_p)|} \,, \tag{104}$$

where $\mathbb{J}_p$ is the $[d\times d]$ forward-in-time Floquet matrix of the periodic orbit (89) started from the periodic point ϕ_p with period n. Compute the trace using the integral on n points:

$$\begin{aligned} \text{tr}_p \, \mathcal{L}^n &= \int_{\mathcal{M}_p} d\Phi \prod_{i=0}^{n-1} \delta(\phi_{t+1} - \hat{f}(\phi_t)) = \int_{\mathcal{M}_p} d\Phi \, \delta(F[\Phi]) \\ &= \frac{1}{|\text{Det } \mathcal{J}_p|} \,, \end{aligned} \tag{105}$$

where

$$\mathcal{J}_p = \frac{\partial F[\Phi]}{\partial \Phi} \tag{106}$$

is the $[nd\times nd]$ orbit Jacobian matrix of the period-n lattice state started with ϕ_p. $\mathcal{M}_p$ is a region in the nd-dimensional state space of Φ whose first d components are the infinitesimal neighborhood around ϕ_p. Comparing the trace (104) and (105), we have proved the Hill's formula (94).

8.3. Hill determinant for a 2nd order difference equation

An n-step recurrence relation is the discrete-time analogue of an nth order differential equation. In formulating dynamical systems problems, one almost always replaces higher order derivatives (Euler-Lagrange equations) by sets of fields satisfying first order equations (Hamilton's equations), and the same is true for discrete time systems. For example, the Hamiltonian temporal cat and Hénon map are usually formulated as time-evolution over a 2-dimensional phase space (38) and (51), rather than the 3-term recurrence configuration space conditions (45) and (54).

A kth order differential equation can be discretized as a kth order difference equation. Just as a scalar field satisfying a kth order differential equation can be replaced by a set of k fields, each satisfying a first order equation, a kth order difference equation for a scalar field can be replaced by a k-dimensional vector field, satisfying k 1st order difference equations.

One can compute the orbit stability of a scalar field lattice state of such system using the forward-in-time Hill's formula for the k-dimensional vector field representation of dynamics, and the corresponding the determinant of the $[kn \times kn]$ orbit Jacobian matrix (105). However, with the recurrence relation, the orbit Jacobian matrix has a simpler form.

Consider a map with a 3-term recurrence relation, $\phi_{t+1} = f(\phi_{t-1}, \phi_t)$, where ϕ_{t-1}, ϕ_t and ϕ_{t+1} are scalars. This map can be replaced by a pair of 1st order difference equations $(\phi_t, \phi_{t+1}) = \hat{f}(\phi_{t-1}, \phi_t) = (\phi_t, f(\phi_{t-1}, \phi_t))$. The trace of the nth iterate of the

Perron-Frobenius operator can be evaluated using the Dirac delta kernel of the operator $\mathcal{L}^n$, or the product of $\mathcal{L}$ and the recurrence relation:

$$\begin{aligned}\mathrm{tr}\,\mathcal{L}^n &= \int d\phi_0 d\phi_1 \delta((\phi_0,\phi_1) - \hat{f}^n(\phi_0,\phi_1)) \\ &= \int [d\Phi] \prod_{i=0}^{n-1} \delta(\phi_{t+1} - f(\phi_{t-1},\phi_t))\,, \\ \phi_n &= \phi_0\,, \quad \phi_{-1} = \phi_{n-1}\,, \quad [d\Phi] = \prod_{i=0}^{n-1} d\phi_t\,. \end{aligned} \tag{107}$$

Using the matrix notation, the trace computed by the integral on n points along a discrete periodic orbit is:

$$\mathrm{tr}\,\mathcal{L}^n = \int [d\Phi]\delta(r\Phi - f(r^{-1}\Phi,\Phi))\,, \tag{108}$$

where Φ and $f(r^{-1}\Phi,\Phi)$ are n-dimensional column vectors with ith components ϕ_t and $f((r^{-1}\Phi)_i,\Phi_i)$, and r is the cyclic $[n\times n]$ shift operator (32). The vector in the Dirac delta function is the defining equation of the system:

$$F[\Phi] = r\Phi - f(r^{-1}\Phi,\Phi)\,. \tag{109}$$

Restricting the integration to an infinitesimal neighborhood $\mathcal{M}_p$ around a periodic point $(\phi_{p,0},\phi_{p,1})$ with period n, the contribution from this periodic point is:

$$\mathrm{tr}_p\,\mathcal{L}^n = \int_{\mathcal{M}_p} d\phi_0 d\phi_1 \delta((\phi_0,\phi_1) - \hat{f}^n(\phi_0,\phi_1)) = \frac{1}{|\det(\,\mathbb{1} - \mathbb{J}_p)|}\,, \tag{110}$$

where

$$\mathbb{J}_p = \frac{\partial \hat{f}^n(\phi_{p,0},\phi_{p,1})}{\partial(\phi_{p,0},\phi_{p,1})} \tag{111}$$

is the [2×2] forward-in-time Floquet matrix of the periodic orbit started from the periodic point $(\phi_{p,0},\phi_{p,1})$ with period n. Compute the trace using the integral on n points:

$$\begin{aligned}\mathrm{tr}_p\,\mathcal{L}^n &= \int_{\mathcal{M}_{\Phi_p}} [d\Phi]\delta(r\Phi - f(r^{-1}\Phi,\Phi)) = \int_{\mathcal{M}_{\Phi_p}} [d\Phi]\delta(F[\Phi]) \\ &= \frac{1}{|\mathrm{Det}\,\mathcal{J}_p|}\,, \end{aligned} \tag{112}$$

where

$$\mathcal{J}_p = \frac{\partial F[\Phi_p]}{\partial \Phi_p} \tag{113}$$

is the $[n\times n]$ orbit Jacobian matrix of the period-n lattice state started with $(\phi_{p,0},\phi_{p,1})$. $\mathcal{M}_{\Phi_p}$ is a region in the n-dimensional space of Φ whose first 2 components are the infinitesimal neighborhood around $(\phi_{p,0},\phi_{p,1})$. Compare the trace (110) and (112), we have proved the Hill's formula (94).

[2021-12-16 Han] The rest of this section is from the old version.

Our task is to compute the Hill determinant $|\det\mathcal{J}|$. We first show how to do that directly, by computing the volume of the fundamental parallelepiped.

8.4. Hill determinant: fundamental parallelepiped evaluation

As a concrete example consider the Bravais lattice with basis vector

The *orbit Jacobian matrix* is the $\delta/\delta\phi_k$ derivative of the temporal Hénon 3-term recurrence relation (84)

$$\mathcal{J}_p = -r + 2\,\mathbb{X}_p - r^{-1}\,, \tag{114}$$

where $\mathbb{X}_p$ is a diagonal matrix with p-lattice state ϕ_k in the kth row/column, and the '1's in the upper right and lower left corners enforce the periodic boundary conditions.

The action of the temporal Hénon orbit Jacobian matrix can be hard to visualize, as a period-2 lattice state is a 2-torus, period-3 lattice state a 3-torus, etc.. Still, the fundamental parallelepiped for the period-2 and period-3 lattice states, should suffice to convey the idea. The fundamental parallelepiped basis vectors (119) are the columns of $\mathcal{J}$. The $[2\times 2]$ orbit Jacobian matrix and its Hill determinant follow from (**??**)

$$\mathcal{J} = \begin{pmatrix} 2\,\phi_0 & -2 \\ -2 & 2\,\phi_1 \end{pmatrix}\,, \quad \det \mathcal{J} = 4\,(\phi_0\phi_1 - 1) = -4\,(a-3)\,. \tag{115}$$

The resulting fundamental parallelepiped shown in figure **??** (a). Period-3 lattice states for $s = 3$ are contained in the half-open fundamental parallelepiped of figure **??** (b), defined by the columns of $[3\times 3]$ orbit Jacobian matrix

$$\mathcal{J} = \begin{pmatrix} 2\,\phi_0 & -1 & -1 \\ -1 & 2\,\phi_1 & -1 \\ -1 & -1 & 2\,\phi_2 \end{pmatrix}\,, \qquad \det \mathcal{J} = 8\,\phi_0\phi_1\phi_2 - 2\,(\phi_0+\phi_2+\phi_3)+2\,, \tag{116}$$

8.5. Fundamental fact

The orbit Jacobian matrix $\mathcal{J}$ stretches the state space unit hyper-cube $\Phi \in [0,1)^n$ into the n-dimensional *fundamental parallelepiped*, and maps each periodic point Φ_{M} into an integer lattice $\mathbb{Z}^n$ site, which is then translated by the winding numbers M into the origin, in order to satisfy the fixed point condition (77). Hence N_n, the total number of the solutions of the fixed point condition equals the number of integer lattice points within the fundamental parallelepiped, a number given by what Baake *et al* [18] call the *'fundamental fact'*,

$$N_n = |\det \mathcal{J}|\,, \tag{117}$$

i.e., fact that the number of integer points in the fundamental parallelepiped is equal to its volume, or, what we refer to as the 'Hill determinant' below. In two dimensions this formula is known since 1899 as Pick's theorem, in higher dimensions it was given by Nielsen [37, 210] in 1920, and rederived several times since in different contexts, for example by Baake *et al* [18]. For the task at hand, Barvinok [22] lectures offer a clear and simple introduction to integer lattices, and a proof of (117).

The action of orbit Jacobian matrix $\mathcal{J}$ for the period-2 lattice states (periodic points) of the Bernoulli map of figure 2 (a), suffices to convey the idea. In this case, the

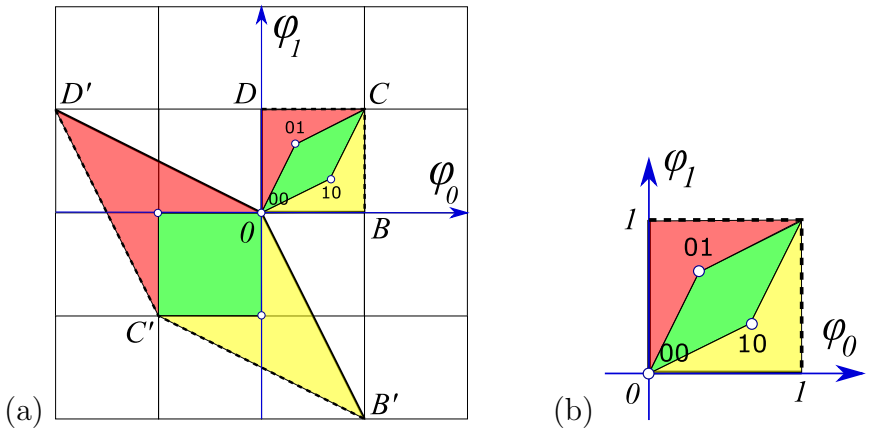

Figure 7. (Color online) (a) The Bernoulli map (22) periodic points $\Phi_{\mathsf{M}} = (\phi_0, \phi_1)$ of period 2 are the $\overline{0} = (0,0)$ fixed point, and the 2-cycle $\Phi_{01} = (1/3, 2/3)$, see figure 2 (a). They all lie within the unit square $[0BCD]$, which is mapped by the orbit Jacobian matrix $\mathcal{J}$ (118) into the fundamental parallelepiped $[0B'C'D']$. Periodic points Φ_{M} are mapped by $\mathcal{J}$ onto the integer lattice, $\mathcal{J}\Phi_{\mathsf{M}} \in \mathbb{Z}^n$, and are sent back into the origin by integer translations M, in order to satisfy the fixed point condition (77). Note that this fundamental parallelepiped is covered by 3 unit area quadrilaterals, hence $|\det \mathcal{J}| = 3$. (b) Conversely, in the flow conservation sum rule (183) sum over all lattice states M of period n, the inverse of the Hill determinant defines the 'neighborhood' of a lattices state as the corresponding fraction of the unit hypercube volume.

$[2\times 2]$ orbit Jacobian matrix (31), the unit square basis vectors, and their images are

$$\mathcal{J} = \begin{pmatrix} 2 & -1 \\ -1 & 2 \end{pmatrix}$$

$$\Phi^{(B)} = \begin{pmatrix} 1 \\ 0 \end{pmatrix} \to \Phi^{(B')} = \mathcal{J}\,\Phi^{(B)} = \begin{pmatrix} 2 \\ -1 \end{pmatrix}, \quad \cdots$$

i.e., the columns of the orbit Jacobian matrix are the edges of the fundamental parallelepiped,

$$\mathcal{J} = \left(\Phi^{(B')}\Phi^{(D')}\right), \tag{118}$$

see figure 7 (a), and $N_2 = |\det \mathcal{J}| = 3$, in agreement with the periodic orbit count (28).

In general, the unit vectors of the state space unit hyper-cube $\Phi \in [0,1)^n$ point along the n axes; orbit Jacobian matrix $\mathcal{J}$ stretches them into a fundamental parallelepiped basis vectors $\Phi^{(j)}$, each one a column of the $[n\times n]$ matrix

$$\mathcal{J} = \left(\Phi^{(1)}\Phi^{(2)}\cdots\Phi^{(n)}\right). \tag{119}$$

The Hill determinant

$$\det \mathcal{J} = \det\left(\Phi^{(1)}\Phi^{(2)}\cdots\Phi^{(n)}\right), \tag{120}$$

is then the volume of the fundamental parallelepiped whose edges are basis vectors $\Phi^{(j)}$. Note that the unit hypercubes and fundamental parallelepipeds are half-open, as indicated by dashed lines in figure 7 (a), so that their translates form a partition of

the extended state space (23). For another example of fundamental parallelepipeds, see figure 8.

Note that in the temporal lattice reformulation, the Bernoulli system involves two distinct lattices:

(i) Any lattice field theory: in the discretization (1) of the time continuum, one replaces *any* dynamical system's time-dependent field $\phi(t) \in \mathbb{R}$ at time $t \in \mathbb{R}$ by a discrete set of its values $\phi_t = \phi(a\,t)$ at time instants $t \in \mathbb{Z}$. Here the index t is a *coordinate* over which the field ϕ is defined.

(ii) Specific to the Bernoulli system: the site t field value ϕ_t (24) is confined to the unit interval $[0, 1)$, imparting integer lattice structure onto the intermediate calculational steps in the extended state space (23) on which the orbit Jacobian matrix $\mathcal{J}$ (31) acts.

[2021-10-25 Predrag] Combine the above with the temporal cat page **??** discussion into a remark that temporal Bernoulli and temporal cat aslo have a *dynamical* D_1 symmetry, not utilized in this paper, as nonlinear field theories such as temporal Hénon do not have such symmetries. Here we study only the symmetries of the floor, not the dancer.

For temporal cat the total number of lattice states is again, as for the Bernoulli system (117), given by the 'fundamental fact (117). However, while for the temporal Bernoulli every sequence of alphabet letters (26) but one is admissible, for temporal cat the condition (45) constrains admissible source blocks M.

For period-1, constant field lattice states $\phi_{t+1} = \phi_t = \phi_{t-1}$ it follows from (45) that

$$(s-2)\phi_t = m_t\,,$$

so the orbit Jacobian matrix is a $[1 \times 1]$ matrix, and there are

$$N_1 = s - 2 \tag{121}$$

period-1 lattice states. This is easy to verify by counting the admissible m_t values. Since $\phi_t \in [0, 1)$, the range of m_t is $m_t \in [0, s-2)$. So three of the (44) temporal cat letters are not admissible: $\underline{1}$ is below the range, and $s-2$ and $s-1$ are above it.

The action of the temporal cat orbit Jacobian matrix can be hard to visualize, as a period-2 lattice field is a 2-torus, period-3 lattice field a 3-torus, etc.. Still, the fundamental parallelepiped for the period-2 and period-3 lattice states, figure 8, should suffice to convey the idea. The fundamental parallelepiped basis vectors are the columns of $\mathcal{J}$. The $[2\times2]$ orbit Jacobian matrix (81) and its Hill determinant are

$$\mathcal{J} = \begin{pmatrix} s & -2 \\ -2 & s \end{pmatrix}\,, \qquad N_2 = \mathrm{Det}\,\mathcal{J} = (s-2)(s+2)\,, \tag{122}$$

(compare with the lattice states count (191)), with the resulting fundamental parallelepiped shown in figure 8 (a). Period-3 lattice states for $s = 3$ are contained

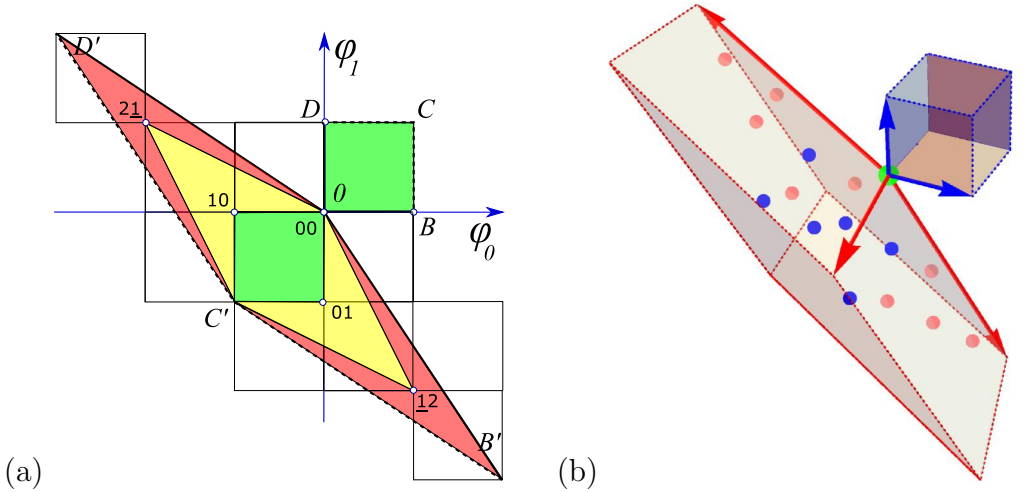

Figure 8. (Color online) (a) For $s = 3$, the temporal cat (46) has 5 period-2 lattice states $\Phi_{\mathsf{M}} = (\phi_0, \phi_1)$: Φ_{00} fixed point and 2-cycles $\{\Phi_{01}, \Phi_{10}\}$, $\{\Phi_{\underline{1}2}, \Phi_{2\underline{1}}\}$. They lie within the unit square $[0BCD]$, and are mapped by the $[2\times2]$ orbit Jacobian matrix $\mathcal{J}$ (122) into the fundamental parallelepiped $[0B'C'D']$, as in, for example, Bernoulli figure 7. The images of periodic points Φ_{M} land on the integer lattice, and are sent back into the origin by integer translations $\mathsf{M} = m_0 m_1$, in order to satisfy the fixed point condition $\mathcal{J}\Phi_{\mathsf{M}} + \mathsf{M} = 0$. (b) A 3-dimensional [blue basis vectors] unit-cube stretched by $\mathcal{J}$ (123) into the [red basis vectors] fundamental parallelepiped. For $s = 3$, the temporal cat (46) has 16 period-3 lattice states: a Φ_{000} fixed point at the vertex at the origin, [pink dots] 3 period-3 orbits on the faces of the fundamental parallelepiped, and [blue dots] 2 period-3 orbits in its interior. An n-dimensional state space unit hypercube $\Phi \in [0,1)^n$ and the corresponding fundamental parallelepiped are half-open, as indicated by dashed lines, so the integer lattice points on the far corners, edges and faces do not belong to it.

in the half-open fundamental parallelepiped of figure 8 (b), defined by the columns of $[3\times3]$ orbit Jacobian matrix

$$\mathcal{J} = \begin{pmatrix} s & -1 & -1 \\ -1 & s & -1 \\ -1 & -1 & s \end{pmatrix}, \qquad N_3 = \det \mathcal{J} = (s-2)(s+1)^2\,, \tag{123}$$

again in agreement with the periodic orbit count (191). The 16 period-3, $s = 3$ lattice states $\Phi_{\mathsf{M}} = (\phi_0, \phi_1, \phi_3)$ are the Φ_{000} fixed point at the vertex at the origin, 3 period-3 orbits on the faces of the fundamental parallelepiped, and 2 period-3 orbits in its interior.

[2021-10-29 Predrag] Dropped: , all five of form $\{\Phi_{m_0m_1m_2}, \Phi_{m_1m_2m_0}\Phi_{m_2m_0m_1}\}$.

In this example there is no need to go further with the fundamental fact Hill determinant evaluations, as the explicit formula for the numbers of periodic lattice states is well known [146, 160]. The temporal cat equation (45) is a linear 2nd-order inhomogeneous difference equation (3-term recurrence relation) with constant coefficients that can be solved by standard methods [91] that parallel the theory of linear differential equations. Inserting a solution of form $\phi_t = \Lambda^t$ into the m_t=0 homogenous

2nd-order temporal cat condition (45) yields the characteristic equation (39) with roots $\{\Lambda\,,\ \Lambda^{-1}\}$. The result is that the number of temporal lattice states of period n is

$$N_n = |\mathrm{Det}\,\mathcal{J}| = \Lambda^n + \Lambda^{-n} - 2\,, \tag{124}$$

often written as

$$N_n = 2\,T_n(s/2) - 2\,, \tag{125}$$

where $T_n(s/2)$ is the Chebyshev polynomial of the first kind.

Note that in the temporal lattice reformulation, the temporal cat happens to involve two unrelated lattices:

(i) In the latticization of a time continuum, one replaces a time-dependent field $\phi(t)$ at time $t \in \mathbb{R}$ of *any* dynamical system by a discrete set of its values $\phi_t = \phi(t\Delta T)$, $t \in \mathbb{Z}$. Here the index 't' is a *coordinate* over which the field ϕ lives.

(ii) A peculiarity of the temporal cat is that the *field* ϕ_t (43) is confined to the unit interval $[0, 1)$, imparting a $\mathbb{Z}^1$ lattice structure onto the calculationally intermediate fundamental parallelepiped $\mathcal{J}$ basis vectors (119).

8.6. Orbit Jacobian matrix on reciprocal lattice

[2021-08-28 Predrag] Define the Hill determinant somewhere, refer to it here.

we show how compute the orbit Jacobian matrix or Hill determinants $|\mathrm{Det}\,\mathcal{J}|$ using crystallographer's favorite tool, the discrete Fourier transform.

8.7. Hill determinant: Reciprocal lattice evaluation

$\omega = e^{2i\pi/n}$
$\tilde{\phi}_k = x_k + i\,y_k = |\tilde{\phi}_k| e^{i\theta_k}$
$q_k = 2\pi k/n$,
n is the Bravais cell period

The temporal Bernoulli orbit Jacobian matrix $\mathcal{J} = \partial/\partial t - (s-1)\,r^{-1}$ is a differential operator whose determinant one usually computes by a Fourier transform diagonalization (see section 8.6). The Fourier discretization approach goes all the way back to Hill's 1886 paper [131].

The first advantage of using the reciprocal lattice is that it provides a way to compute the Hill determinant. If the orbit Jacobian matrix (76) commutes with the translation operator, the plane waves are eigenvectors of the orbit Jacobian matrix. Using these eigenvectors one can find the eigenvalues and the determinant of the orbit Jacobian matrix. In the n-dimensional space of lattice states with period-n, the one-lattice spacing translation operator is a shift matrix (32), whose eigenvectors are plane waves $\tilde{e}_k$:

$$r\,\tilde{e}_k = \omega^k \tilde{e}_k\,. \tag{126}$$

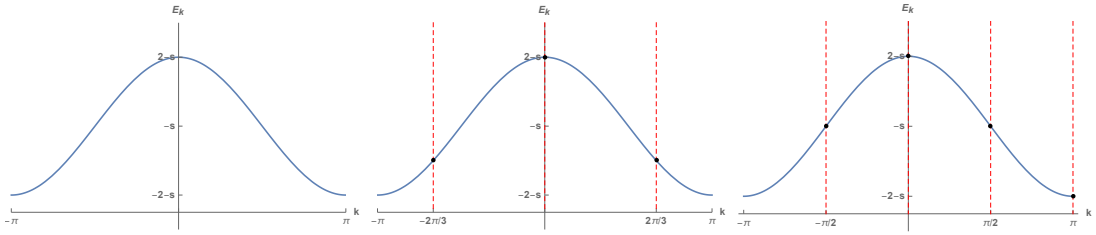

(a) (b) (c)

Figure 9. (a) The eigenvalue E_k of the orbit Jacobian matrix on the infinite lattice as a function of the wave vector k in the first Brillouin zone. The orbit Jacobian matrix has the reflection symmetry so the eigenvalue is also invariant under the reflection $k \to -k$. (b) For period 3 lattice states, the wave vectors of the eigenstates exist on the reciprocal lattice spanned by $2\pi/3$. These lattice sites are labeled by the red dashed lines. There are only 3 period 3 eigenstates, with eigenvalues $-1-s$, $2-s$ and $-1-s$. (c) For period 4 lattice states, the wave vectors of the eigenstates exist on the reciprocal lattice spanned by $\pi/2$. These lattice sites are labeled by the red dashed lines. There are only 4 period 4 eigenstates, with eigenvalues $-s$, $2-s$, $-s$ and $-2-s$. $k=\pi$ and $k=-\pi$ are different by a reciprocal lattice translation, so they are a same wave vector and should be only counted once.

For example, the eigenvalues of the temporal Bernoulli orbit Jacobian matrix (31) are

$$(s\,\mathbb{1}-r)\,\tilde{e}_k = (s-\omega^k)\,\tilde{e}_k\,, \tag{127}$$

and the Hill determinant is simply a polynomial whose roots are the nth roots of unity,

$$\mathrm{Det}\,(s\,\mathbb{1}-r) = \prod_{k=0}^{n-1}(s-\omega^k) = s^n-1\,. \tag{128}$$

see (33). The eigenvalues of the temporal cat orbit Jacobian matrix (79) are:

$$(-r+s\;\mathbb{1}-r^{-1})\,\tilde{e}_k = (s-2\cos(2\pi k/n))\,\tilde{e}_k\,, \tag{129}$$

and the Hill determinant is:

$$\begin{aligned}\text{temporal cat:}\qquad \mathrm{Det}\,(-r+s\;\mathbb{1}-r^{-1}) &= \prod_{k=0}^{n-1}[s-2\cos(2\pi k/n)] \\ &= 2T_n\,(s/2)-2\,,\end{aligned} \tag{130}$$

where T_n is the Chebyshev polynomial of the first kind.

Explain figure 9.

[2021-09-02 Predrag] I think I prefer some version of the identity (??), (??), no mention of Chebyshev polynomials. Not important, will revisit later.

8.8. Remarks

A succinct explanation of the Hill's formula:

> If you evaluate stability of the 3-term recurrence (**??**) on a periodic lattice you get the orbit Jacobian matrix $\mathcal{J}$; if you evaluate it by multiplying the 'two-configuration representation' matrix J, you get the 'time evolution' side of the Hill's formula.

The reformulation of the spatiotemporal cat 3-term recurrence (45) as the 'two-configuration' map (43) is a passage from the Lagrangian to the Hamiltonian formulation, also known as 'transfer matrix' formulation of lattice field theories [200, 204] and Ising models [154, 213]. We chose to prove it here using only elementary linear algebra, not only because the Lagrangian formalism [32] is not needed for the problem at hand, but because it actually obscures the generality of Hill's formula, which works equally well for dissipative systems, such as the Bernoulli Hill's formula (43)).

For Hamiltonian evolution (38), the $[2\times 2]$ Jacobian matrix $\mathbb{J}^n$ (the monodromy matrix of a periodic orbit) describes the growth of an initial state perturbation in n steps. For the corresponding Lagrangian system with action S, the first variation of the action $\delta S = 0$ yields the Euler–Lagrange equations (5–46), while the second variation, the $[n\times n]$ orbit Jacobian matrix (79), describes the stability of the *entire* given periodic orbit. In this, classical mechanics context, Bolotin and Treschev [32] refer to $\mathcal{J}$ as the 'Hessian operator', but, as it is clear from our Bernoulli discussion of section 7, and applications to Kuramoto-Sivashinsky and Navier-Stokes systems [121], this notion of global stability of orbits is general, and applies to all dynamical systems, not only the Hamiltonian ones.

In preparing this section we have found expositions of Lagrangian dynamics for discrete time systems by MacKay, Meiss and Percival [188, 192], and Li and Tomsovic [171] particulary helpful. Hill's formula as derived by Mackay and Meiss [187] and Allroth [2] (Allroth eq. (12)) applies to 'one-degree-of-freedom' systems, i.e., 1D lattices with only the nearest neighbor interactions. For a finite set of neighbors, Allroth [2] has partial results in the context of Frenkel-Kontorova models.

Discrete Hill's formula plays important role in the theory of Toda lattices [249], i.e., classical mechanics of one-dimensional lattices (chains) of particles with nearest neighbor interaction, discrete and infinite in space, continuous in time.

The *inverse scattering method* for periodic systems this gives a discrete Hill's equation, and in place of the scattering data, it is convenient to use the spectrum of the discrete Hill's equation.

9. Translations and reflections

2CB

Though this exposition is nominally about 'evolution in time', 'time' is such a loaded notion, a straightjacket hard to escape, that it is best to forget about 'time' for time being, and think instead like a crystallographer, about lattices and the space groups that describe their symmetries.

Of necessity, there many group-theoretic notions a crystallographer must juggle (see ChaosBook sect. 11.2), but only a few key things to understand:

(i) For a 1-dimensional lattice, there are only two kinds of qualitatively different symmetry transformations, translations (142) and

(ii) reflections (134) which reverse the direction of translation.

(iii) There are two kinds of reflections (144), across a lattice site, and across a mid-point between lattice sites, figure 10.

(iv) Even though both the lattice $\mathcal{L}$ and its space group G are infinite, *orbits* of lattice states are finite and described by finite cyclic and dihedral groups, figure 11.

Should the reader find symmetries of infinite lattices too obstruse: to understand all that one needs to know about translations and reflections, it suffices to understand the symmetries of a triangle and a square, figure 12.

9.1. Symmetries of 1-dimensional lattices, sublattices

A space group G is the set of all translations and rotations that puts a crystallographic structure $\mathcal{L}$ in coincidence with itself. To make the exposition as simple as possible, here we focus on 1-dimensional crystals, with sites labeled by integer lattice $\mathcal{L} = \mathbb{Z}$. Their space groups crystallographers [84] call *line groups*. There are only two 1-dimensional space groups G: $p1$, or the *infinite cyclic group* C_∞ of all lattice translations, and $p1m$, the *infinite dihedral group* D_∞ of all translations and reflections [162],

$$\mathrm{D}_\infty = \{\cdots, r_{-2}, \sigma_{-2}, r_{-1}, \sigma_{-1}, 1, \sigma, r_1, \sigma_1, r_2, \sigma_2, \cdots\}\,. \tag{131}$$

A half of the elements are translations ('shifts'; for finite period lattices, 'rotations'). $r_0 = 1$ denotes the identity, and the $r_1 = r$, $r_2 = r^2$, $\cdots$, $r_k = r^k$, $\cdots$, denote translations by $1, 2, \cdots, k, \cdots$ lattice points. They form the *infinite cyclic group*

$$\mathrm{C}_\infty = \{\cdots, r_{-2}, r_{-1}, 1, r_1, r_2, r_3, \cdots\}\,, \tag{132}$$

a subgroup of D_∞, in crystallography called the translation group.

The other half of elements are reflections $\sigma_k^2 = 1$ ('inversions', 'time reversals', 'flips'), defined by first translating by k steps, and then reflecting, resulting in a 'translate-reflect' operation

$$\sigma_k = \sigma r_k\,. \tag{133}$$

The defining property of translate & reflect groups ('dihedral' groups, 'flip systems' [162]) is that any reflection reverses the direction of the translation

$$\sigma_k r = r^{-1}\sigma_k\,. \tag{134}$$

The group multiplication (or 'Cayley') table for successive group actions $g_i g_j$ follows:

	r_j	σ_j
r_i	r_{i+j}	σ_{j-i}
σ_i	σ_{i+j}	r_{j-i}

. (135)

Multiplication either adds up translations, or shifts and then reverses their direction. The order in which the elements $g_i g_j$ act is right to left, i.e., a group element acts on the expression to its right.

A crystallographer organizes the *subgroups* of a space group G by means of *Bravais lattices* $\mathcal{L}_\mathbf{a}$, sublattices of the lattice $\mathbb{Z}$, each defined here by a 1-dimensional *Bravais cell* of *period* n, given by a lattice vector $\mathbf{a}$ of integer length n,

$$\mathcal{L}_\mathbf{a} = \{j\mathbf{a} \,|\, j \in \mathbb{Z}\}\,, \tag{136}$$

with the lattice generated by the infinite translation group of all discrete translations replaced by

$$r_j \to r_{j\mathbf{a}}$$

multiples of $\mathbf{a}$, resulting in

$$H_\mathbf{a} = \{\cdots, r_{-2\mathbf{a}}, r_{-\mathbf{a}}, 1, r_\mathbf{a}, r_{2\mathbf{a}}, \cdots\}\,, \tag{137}$$

infinite translation subgroup of the infinite translation group C_∞. You can visualize a lattice state invariant under subgroup $H_\mathbf{a}$ as a tiling of the lattice $\mathbb{Z}$ by a generic lattice state over tile of length n.

Another family of subgroups of D_∞ is obtained by substituting elements of D_∞ (131) by

$$r_j \to r_{j\mathbf{a}}\,, \qquad \sigma \to \sigma_k \quad 0 \le k < n\,,$$

resulting in n infinite dihedral groups

$$H_{\mathbf{a},k} = \{\cdots, r_{-2\mathbf{a}}, \sigma_k r_{-2\mathbf{a}}, r_{-\mathbf{a}}, \sigma_k r_{-\mathbf{a}}, 1, \sigma_k, r_\mathbf{a}, \sigma_k r_\mathbf{a}, r_{2\mathbf{a}}, \sigma_k r_{2\mathbf{a}}, \cdots\}\,, \tag{138}$$

each given by a Bravais cell of period n, with reflection across a symmetry point shifted k half-steps, see (147).

9.2. Classes

Definition: *A class is the set of elements left invariant by conjugation with all elements g of the group G, where an element b is* conjugate *to element a if*

$$b = g\, a\, g^{-1}\,. \tag{139}$$

By (134), a conjugation by any reflection reverses the direction of translation

$$\sigma_i r_j \sigma_{-i} = r_{-j}\,, \tag{140}$$

so every translation pairs up with the equal counter-translation to form

$$\text{identity class} \qquad \{1\}\,, \qquad j = 0 \tag{141}$$

$$\text{translation classes} \qquad \{r_j, r_{-j}\}\,, \quad j = 1, 2, 3, \cdots\,. \tag{142}$$

The $r_0 = 1$ commutes with all group elements, and is thus always a class by itself.

From the multiplication table (135) it follows that a conjugate of a reflection

$$r_i\,\sigma_j r_i^{-1} = \sigma_{j-2i}\,, \quad \sigma_i\sigma_j\sigma_i^{-1} = \sigma_{2i-j}\,. \tag{143}$$

is a reflection related to it by a $2i$ translation. Hence the even subscript reflections belong to one class, and the odd subscript reflections to the other:

$$\begin{aligned} &\text{even} \quad \{\sigma_{2m}\}\,, \qquad m \in \mathbb{Z} \\ &\text{odd} \quad \{\sigma_{2m+1}\}\,. \end{aligned} \tag{144}$$

By (143) $rH_{n,k}r^{-1} = H_{n,k-2}$, so for odd n, there are n Bravais sublattices in the class, and for even n, $H_{n,k}$ separate into 2 classes (144),

$$\begin{aligned} &\text{even} \quad \{H_{2m,2j}\}\,, \qquad 0 \le j < n/2 \\ &\text{odd} \quad \{H_{2m,2j+1}\}\,, \end{aligned} \tag{145}$$

each containing m Bravais sublattices.

9.3. Reflections

What's the difference between an 'odd' and an 'even' reflection? Every element in a class is equivalent to any other of its elements. So, to understand what everybody in a given class does, it suffices to work out what a single representative does: it suffices to analyse the $H_{n,0}$ and $H_{n,1}$ to account for all $H_{n,k}$.

So far, we have only discussed the abstract structure of the space group D_∞ and its subgroups. But the difference between an 'odd' and an 'even' is easiest to grasp by working out the action of σ_k on a lattice state.

Even class. Take $\sigma = \sigma_0$ as a representative of all even reflections σ_{2m}, and act on a lattice state (6):

$$\begin{aligned} \Phi &= \cdots\phi_{-3}\phi_{-2}\,\phi_{-1}\,\phi_0\,\phi_1\phi_2\phi_3\phi_4\cdots \\ \sigma\Phi &= \cdots\phi_5\phi_4\phi_3\phi_2\phi_1\boxed{\phi_0}\,\phi_{-1}\phi_{-2}\phi_{-3}\cdots\,, \end{aligned} \tag{146}$$

with $\boxed{\phi_0}$ indicating that the field at the lattice site 0 is unchanged by the reflection, see figure 10 (even).

Odd class. Take σ_1 as a representative of all odd reflections σ_{2m+1}. The result is:

$$\begin{aligned} \Phi &= \cdots\phi_{-3}\phi_{-2}\phi_{-1}\,\underline{\phi}_0\;\phi_1\phi_2\phi_3\phi_4\cdots \\ r\Phi &= \cdots\phi_{-3}\phi_{-2}\phi_{-1}\phi_0\,\underline{\phi}_1\;\phi_2\phi_3\phi_4\phi_5\cdots \\ \sigma_1\Phi = \sigma r\Phi &= \cdots\phi_6\phi_5\phi_4\phi_3\phi_2\,\underline{\phi}_1|\,\phi_0\phi_{-1}\phi_{-2}\phi_{-3}\cdots\,, \end{aligned} \tag{147}$$

where $\underline{\phi}_j$ indicates the field value at the lattice site 0, and $|$ indicates a reflection across midpoint between lattice sites 0 and 1, see figure 10 (odd).

More generally, one can say that the index k in the 'translate-reflection' (133) operation $\sigma_k = \sigma r_k$ advances the reflection point by $k/2$ steps, and then reflects across it.

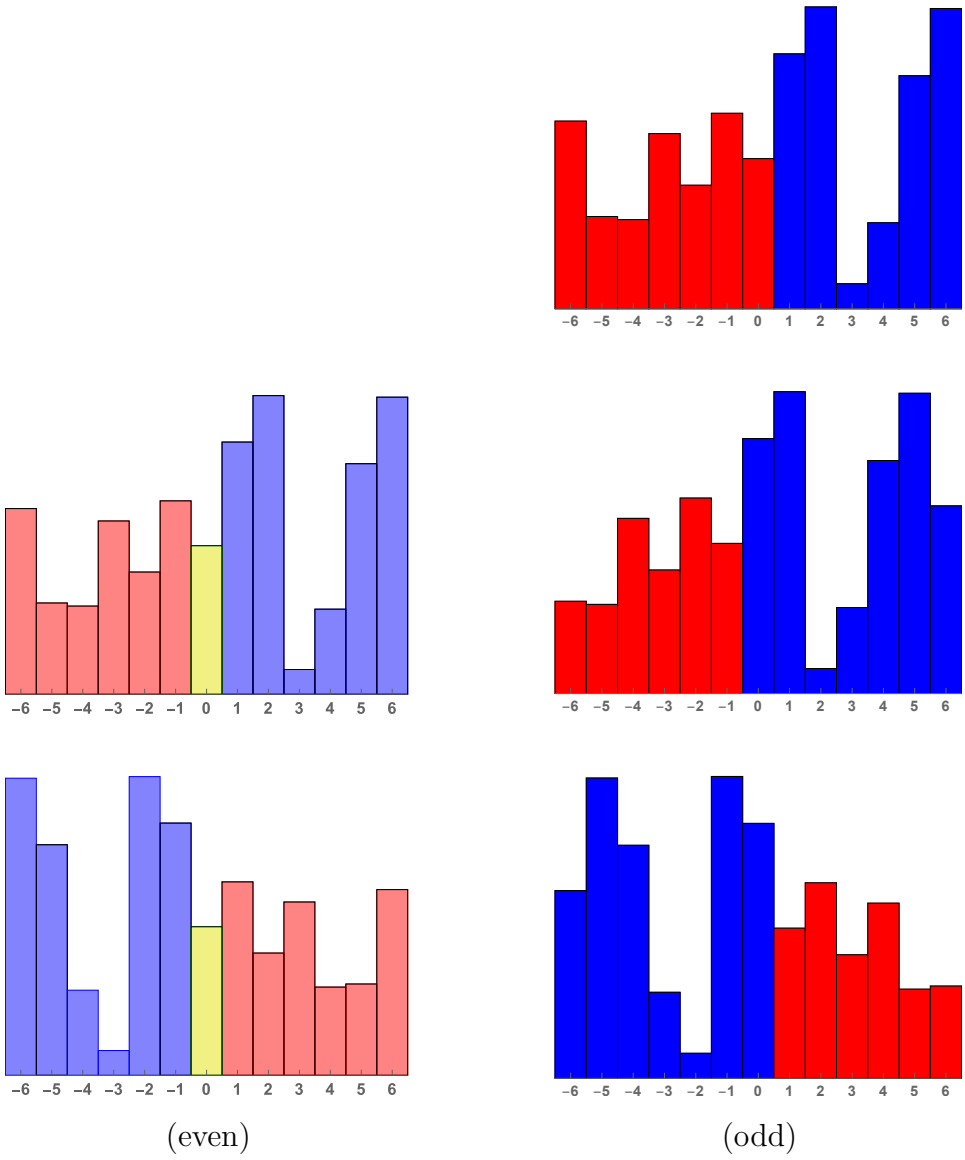

Figure 10. (Color online) There are two classes of lattice state reflections, even (146) and odd (147). (Even) reflection σ exchanges (blue ϕ_j) $\leftrightarrow$ (red ϕ_{-j}) while leaving the yellow field $\boxed{\phi_0}$ at lattice site 0 fixed. (Odd) reflection $\sigma_1 = \sigma r$ swaps the 'blues' and the 'reds' by a lattice translation $\Phi \to r\Phi$, followed by a reflection σ. The result is a reflection across the midpoint of the [01] interval, marked '—'. See figure 1 (b) for the notation.

[2021-08-17 Predrag] Before publication, fine tune figure 10 using LaTex, as in figure **??**.

If you do not find the two kinds of reflections intuitive, the distinction becomes crystal clear once you have a look at the finite periodic lattices of figure 12.

9.4. Symmetries of a system and of its solutions

What's the deal about classes? A 'class' is a refinement of our intuitive notion that "rotations are rotations, and translations are translations." Translated into a more familiar language, conjugation (139) is central to all of physics: a 'law' $f(\Phi)$ is invariant if it retains its form in all symmetry related coordinate frames,

$$f(\Phi) = g^{-1} f(g\,\Phi)\,, \tag{148}$$

where g is a representation of group element $g \in G$. If this holds, we say that G is the *symmetry* of the system.

For example, the 'temporal Bernoulli' defining equation (30) retains its form under conjugation by any C_∞ translation (132),

$$r_i(s\phi_t - \phi_{t+1})r_i^{-1} = (s\phi_{t+i} - \phi_{t+i+1})r_i^{-1} = s\phi_t - \phi_{t+1}\,, \tag{149}$$

while the Euler–Lagrange second-order difference equations (17), 'temporal cat', 'temporal Hénon', and 'temporal ϕ^4 theory' defining equations (19), (20) and (21) retain their form also under any D_∞ reflection,

[2021-08-22 Predrag] This is not quite right, one does not 'conjugate' a vector ϕ_j. Not sure how to elegantly deal with ϕ^k_{-t} term. Could have defined actions, but that does not work for the Bernoulli (149).

$$\sigma_i(-\phi_{t+1} + g\,V'(\phi_t) - \phi_{t-1})\sigma_i^{-1} = -\phi_{-t+1} + g\,V'(\phi_{-t}) - \phi_{-t-1}\,. \tag{150}$$

Given that G is the symmetry of the system does not mean that G is also the symmetry of its solutions, or what we here call *lattice state*s. They can satisfy all of system's symmetries, a subgroup of them, or have no symmetry at all. For example, a generic lattice state (6) sketched in figure 10 has no symmetry beyond the identity, so its symmetry group is the trivial subgroup $\{e\}$; any translation r_j or reflection σ_k maps it into a different, distinct lattice state, as shown in figure 11. At the other extreme, the constant lattice state $\phi_j = \phi$ is invariant under any translation or reflections - its symmetry group is the full G, the symmetry of the system. In between, there are lattice states whose symmetry is any subgroup of G.

9.5. What are 'lattice states'? Orbits?

Remember, for evolution-in-time, every period-n periodic point is a fixed point of the nth iterate of the 1 time-step map. In the lattice formulation, the totality of finite-period lattice states is the *set of fixed points* of all $H_{\mathbf{a}}$ and $H_{\mathbf{a},k}$ subgroups of D_∞.

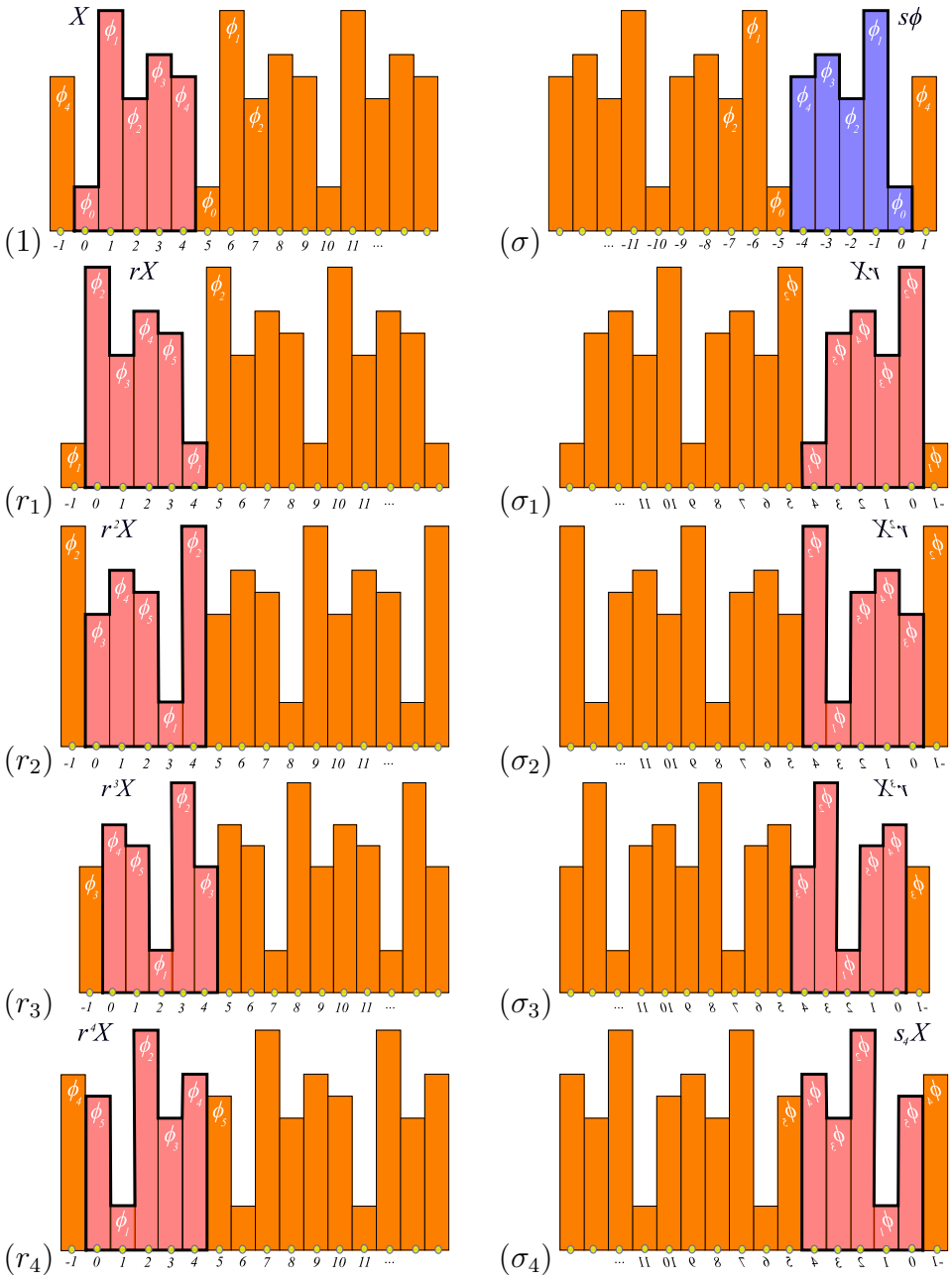

Figure 11. (Color online) (1) A Bravais cell **a** with lattice state $\Phi = \overline{\phi_0\phi_1\phi_2\phi_3\phi_4}$ with no reflection symmetry, outlined in bold, invariant under the translation group H_5. Its C_∞ orbit are the $n = 5$ distinct lattice states (1) to (r_4), obtained by all of the C_5 translations. Its D_∞-orbit are $2n = 10$ distinct lattice states, 5 translations (1) to (r_4) and 5 translate-reflections (σ) to (σ_4), obtained by all of the D_5 actions. See figure 1 (b) for the notation. Continued in figure 13.

You can visualize a lattice state invariant under ("fixed by') subgroup $H_{\mathbf{a},k}$ as a tiling of the lattice $\mathbb{Z}$ by a lattice state tile of length n, symmetric under reflection σ_k, see figure 13 (b-c).

Definition: Orbit *or* G-orbit *of a lattice state* Φ *is the set of all lattice states*

$$\mathcal{M}_\Phi = \{g\,\Phi \mid g \in G\} \tag{151}$$

into which Φ *is mapped under the action of group* G*. We label the orbit* $\mathcal{M}_\Phi$ *by any lattice state* Φ *belonging to it.*

As an example, the D_∞ orbit of the period-5 lattice state is shown in figure 11.

[2021-09-05 Predrag] This "maximal subgroup" does not seem to me to be defined here. Clean up!

Definition: Symmetry of a solution. *We shall refer to the maximal subgroup* $G_\Phi \subseteq G$ *of actions on lattice states within the orbit* $\mathcal{M}_\Phi$*, which leave the orbit invariant, as the* symmetry G_Φ *of the orbit* $\mathcal{M}_\Phi$*,*

$$G_\Phi = \{g \in G_\Phi \mid g\Phi \in \mathcal{M}_\Phi\}\,. \tag{152}$$

An orbit $\mathcal{M}_\Phi$ is G_Φ*-symmetric* (*symmetric*, *set-wise symmetric*, *self-dual*) if the action of elements of G_Φ on the set of lattice states $\mathcal{M}_\Phi$ reproduces the orbit.

Definition: Multiplicity *of orbit* $\mathcal{M}_\Phi$ *is given by*

$$m_\Phi = |G|/|G_\Phi|\,. \tag{153}$$

(See ChaosBook p. 166.)

And now, a pleasant surprise, obvious upon an inspection of figures 11 and 13: what happens in the Bravais cell, stays in the Bravais cell. Even though the lattices $\mathcal{L}$, $\mathcal{L}_\mathbf{a}$ are infinite, and their symmetries D_∞, $H_\mathbf{a}$, $H_{\mathbf{a},k}$ are *infinite* groups, the Bravais lattice states' *orbits* are *finite*, described by the finite group permutations of the infinite lattice curled up in a Bravais cell periodic n-site ring.

Indeed, to grasp everything one needs to know about translations r_j (for regular polygons, 'rotations'), and reflections σ_k, it suffices to understand the symmetries of an equilateral triangle (dihedral group D_3) and a square (dihedral group D_4), depicted in figure 12. It is clear by inspection that an n-sided regular polygon has n-fold translational symmetry and n reflection symmetry axes. The group of such symmetries is the finite dihedral group

$$D_n = \{1, \sigma, r, \sigma_1, r_2, \sigma_2, \ \cdots, r_{n-1}, \sigma_{n-1}\} \tag{154}$$

of order $2n$. A half of its elements are the n cyclic group C_n translations r_j. The other half are the n reflections σ_k, one for the reflection across each symmetry axis. The group multiplication table is the same as the D_∞ (135), but with all subscripts mod n. As in (140), conjugation by any reflection reverses the direction of translation

$$\sigma_i r_j \sigma_{-i} = r_{n-j}\,, \qquad 0 < j < n\,, \tag{155}$$

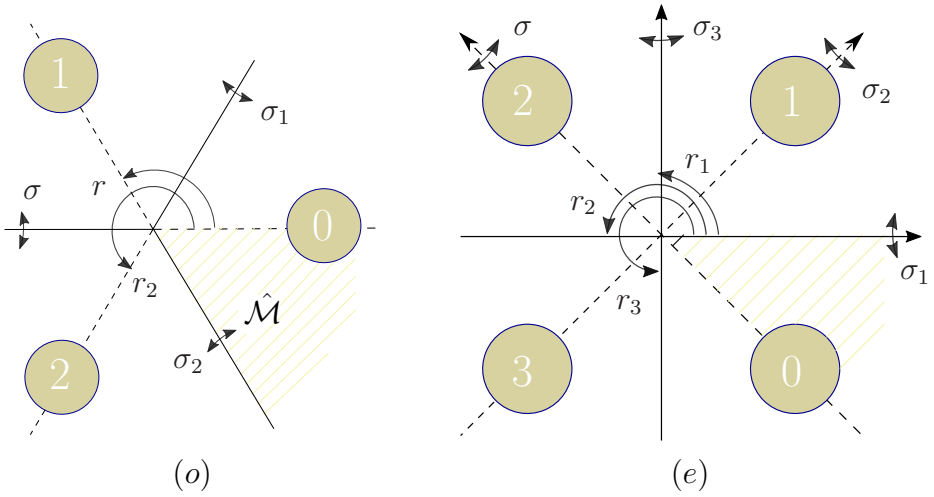

Figure 12. Translational and rotational symmetries of (o) an equilateral triangle, $n = 3$ lattice sites; (e) a square, $n = 4$ lattice sites. The n rotations r_j and the n translate-reflect σ_k (elements of dihedral group D_n (154), even reflection axes dashed, odd reflections full line) overly an n-sided regular polygon onto itself. They also tile it with the $2n$ copies $\hat{\mathcal{M}}_\ell$ of the fundamental domain, indicated by the shaded wedge.

now mod n, so every translation pairs up with the equal counter-translation to form a 2-element class (142).

The distinction between the classes of even and odd reflections (144) is visually self-evident by inspection of figure 12: the symmetry axes either connect opposite lattice sites, or bisect the edges, or both, if n is odd (a triangle, for example). One can say that the index k in the 'translate-reflection' (133) operation σ_k advances the reflection point by k 1/2 steps, and then reflects across it.

For a polygon with an *odd* number of lattice sites (a triangle, for example), we see by contemplating the triangle of figure 12, as well as by taking mod n of the conjugation relation (143), that all reflections are in the same conjugacy class $\{\sigma_j\}$: there is no splitting into odd and even cases, in contrast to the infinite lattice case (144).

For a polygon with an *even* number of lattice sites (a square, for example), one must distinguish the 'long' axes that connect lattice sites (we label them by even numbers $0, 2, \cdots$) from the 'short' symmetry axes that bisect opposite edges (labelled by odd numbers $1, 3, \cdots$). The corresponding reflections belong to different D_n (subclasses of (144),

$$\begin{aligned} &\text{even reflections} \quad \{\sigma, \sigma_2, \sigma_4, \cdots, \sigma_{n/2}\} \\ &\text{odd reflections} \quad \{\sigma_1, \sigma_3, \cdots, \sigma_{n/2+1}\}\,. \end{aligned} \tag{156}$$

9.6. Symmetries of lattice states

A Bravais lattice state Φ has one of the four symmetries:

no reflection symmetry

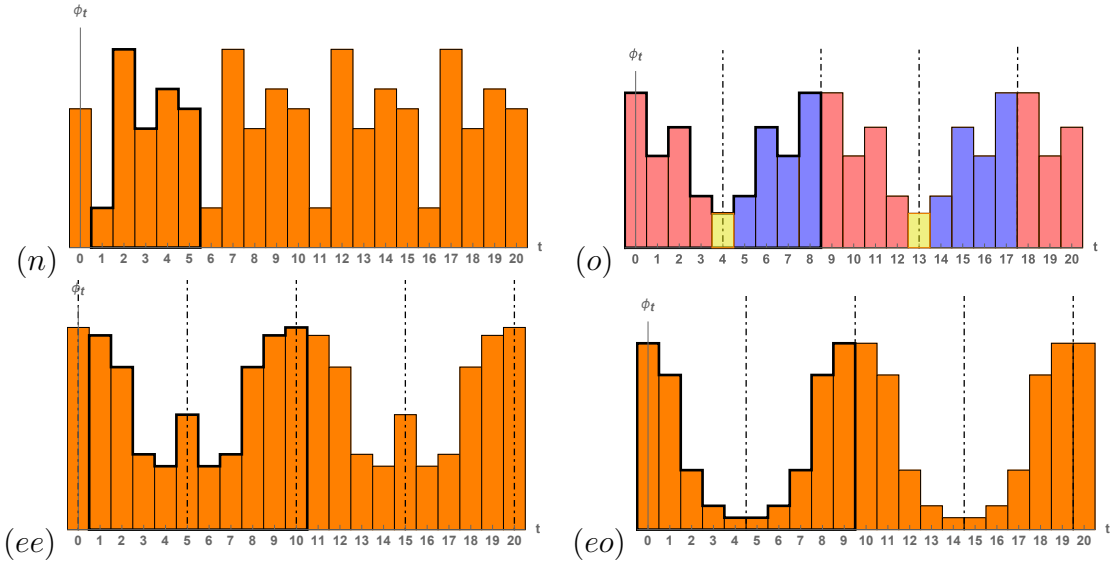

Figure 13. (Color online) A Bravais lattice state Φ has one of the 4 possible symmetries, illustrated by: (n) *No reflection symmetry:* an H_5 invariant period-5 lattice state (157). For its G-orbit, see figure 11. (o) *Odd period, reflection-symmetric:* an $H_{9,8}$ invariant period-9 lattice state (158), reflection symmetric over the lattice sites interval [8-9] midpoint and over the lattice site 4. (ee) *Even period, even reflection-symmetric:* an $H_{10,0}$ invariant period-10 lattice state (159), reflection symmetric over lattice sites 0 and 5. (eo) *Even period, odd reflection-symmetric:* an $H_{10,9}$ invariant period-10 lattice state (160), reflection symmetric over the [4-5] and [9-10] interval midpoints. Horizontal: lattice sites labelled by $t \in \mathbb{Z}$. Vertical: value of field ϕ_t, plotted as a bar centred at lattice site t. Even reflection axes dashed, odd reflections full line.

$$(n) \quad \overline{\phi_0\phi_1\phi_2\phi_3\cdots\phi_{n-1}} \qquad (157)$$
$$\text{multiplicity } m_\Phi = 2n$$

lattice state invariant under the translation group H_n. Its G-orbit, generated by all actions of D_∞, results in $2n$ distinct, D_n related lattice states. This is illustrated by the H_5-invariant lattice state Φ of figure 11. Its D_5 orbit are $2n = 10$ lattice states, 5 translations and 5 translate-reflections.

[2021-08-20 Predrag] Merge figure 13 (n) with *1dLatStatC_5_0x3.svg*.

Next, the reflection-symmetric lattice states. As illustrated in figures 10 and 12, there are two classes (144) of lattice state reflections: even, across a lattice site, and odd, across the mid-point between a pair of adjacent lattice sites. However, as is evident by inspection of figure 12, curling up the lattice $\mathcal{L}$ into a Bravais cell periodic n-site ring implies that an axis cuts the ring twice, and constrains the possible reflection points to three configurations:

$$\text{odd period } n = 2m+1$$
$$(o) \quad \overline{\boxed{\phi_0}\phi_1\phi_2\cdots\phi_m|\phi_m\cdots\phi_2\phi_1} \qquad (158)$$

multiplicity $m_{\Phi} = n$

lattice state invariant under the dihedral group $H_{n,k}$, illustrated by the $H_{9,8}$ invariant lattice state Φ of figure 13 (*o*).

[2021-08-17 Predrag] See (**??**). We also MUST explain the relation to literature, as in the post including (**??**).

$$(ee) \quad \begin{array}{l} \text{even period } n = 2m+2\,,\ \text{even reflection } k \\ \overline{\boxed{\phi_0}\phi_1\phi_2\cdots\phi_m\boxed{\phi_{m+1}}\phi_m\cdots\phi_2\phi_1} \\ \text{multiplicity } m_{\Phi} = n/2 \end{array} \tag{159}$$

lattice state invariant under the dihedral group $H_{n,k}$, k even, illustrated by the $H_{10,0}$ invariant lattice state Φ of figure 13 (*ee*).

$$(eo) \quad \begin{array}{l} \text{even period } n = 2m\,,\ \text{odd reflection } k \\ \overline{\phi_1\phi_2\phi_3\cdots\phi_m|\phi_m\cdots\phi_2\phi_1|} \\ \text{multiplicity } m_{\Phi} = n/2 \end{array} \tag{160}$$

lattice state invariant under the dihedral group $H_{n,k}$, k odd, illustrated by the $H_{10,9}$ invariant lattice state Φ of figure 13 (*eo*).

For long periods n, almost all orbits are of no-symmetry type (157). So why do we care about the symmetric orbits so much? The reason is that the periodic orbit expansions are dominated by the short orbits, and many, if not the most of those are reflection-symmetric.

The lattice state symmetry G_{Φ} (152) of the above (*o*)–(*eo*) reflection-symmetric lattice states Φ is the reflection group $\mathrm{D}_1 = \{1, \sigma_k\}$, but we will spare the reader the group-theorist's cosets and group quotients. For us, this symmetry means two things:

(1) The D_∞ orbits of reflection-symmetric lattice states contain only translations, as any reflection amounts to a cyclic group C_n translation. (Try reflecting a lattice state in figure 13 (b-d) over any lattice site or mid-interval.)

(2) lattice state is a 'half' of it, the length m orbit,

$$\tilde{\Phi} = \phi_1\phi_2\phi_3\cdots\phi_m\,. \tag{161}$$

Reflection breaks the translational invariance, and how one reconstructs the period-n orbit from this length-m block is a bit tricky. To develop intuition about that, it is helpful to have a look at a matrix representation of D_n.

10. Permutation representation

A lattice state Φ over a Bravais cell $\mathbf{a}$ can be assembled into an n-dimensional vector whose components are lattice site fields

$$\Phi^{\top} = (\phi_0, \phi_1, \phi_2, \phi_3, \cdots, \phi_{n-1})\,, \tag{162}$$

with the first field in such vector placed at the lattice site 0, the second at the lattice site 1, and so on. Matrices that reshuffle the components of such vectors form the *permutation representation* of a finite group G, which gives us a different and helpful perspective on the three kinds of symmetric solutions of the preceding section.

The permutation representation of 1-step lattice translation r acts on a Bravais lattice state by the off-diagonal $[n\times n]$ matrix (32). This is a cyclic C_n permutation that translates the lattice state Φ "forward-in-time" by one site,

$$(r\Phi)^\top = (\phi_1, \phi_2, \cdots, \phi_{n-1}, \phi_0)\,.$$

A permutation representation of a D_n translate-reflect should morally be an anti-diagonal matrix that reverses the order of site fields,

$$(\sigma_k\Phi)^\top = (\phi_{n-1}, \cdots, \phi_2, \phi_1, \phi_0)\,.$$

Symmetries of triangles and squares help us make this precise.

Odd period: In odd dimensions, the n translate-reflect matrices of D_n are related by translations (143).

A period-3 example: For $n = 3$ lattice state with out symmetry $\Phi^\top = (\phi_0, \phi_1, \phi_2)$, they are

$$\sigma = \begin{pmatrix} 1 & 0 & 0 \\ 0 & 0 & 1 \\ 0 & 1 & 0 \end{pmatrix}, \quad \sigma_1 = \begin{pmatrix} 0 & 1 & 0 \\ 1 & 0 & 0 \\ 0 & 0 & 1 \end{pmatrix}, \quad \sigma_2 = \begin{pmatrix} 0 & 0 & 1 \\ 0 & 1 & 0 \\ 1 & 0 & 0 \end{pmatrix}.$$

In agreement with (158), figure 12 (o) and figure 13 (o), reflections keep one lattice site fixed (for each permutation matrix σ_k there is only one '1' on the diagonal), swap the rest.

A period-5 example: reflection symmetric lattice states tiles the infinite lattice $\mathcal{L}$ with a reflection-fixed $\boxed{\phi_0}$, and a length-2 block (ϕ_1, ϕ_2),

$$\Phi = \cdots \phi_2\phi_1\boxed{\phi_0}\phi_1\phi_2|\phi_2\phi_1\boxed{\phi_0}\phi_1\phi_2|\cdots\,. \tag{163}$$

D_5 permutation representation of reflections of a pentagon, illustrates that fixpoints Φ of σ_k are cyclicly related:

$$\begin{aligned} \sigma\Phi &= \begin{pmatrix} 1 & 0 & 0 & 0 & 0 \\ 0 & 0 & 0 & 0 & 1 \\ 0 & 0 & 0 & 1 & 0 \\ 0 & 0 & 1 & 0 & 0 \\ 0 & 1 & 0 & 0 & 0 \end{pmatrix} \begin{pmatrix} \boxed{\phi_0} \\ \phi_1 \\ \phi_2 \\ \phi_2 \\ \phi_1 \end{pmatrix} = \begin{pmatrix} \boxed{\phi_0} \\ \phi_1 \\ \phi_2 \\ \phi_2 \\ \phi_1 \end{pmatrix} \\ \sigma_4(r_{-2}\Phi) &= \begin{pmatrix} 0 & 0 & 0 & 0 & 1 \\ 0 & 0 & 0 & 1 & 0 \\ 0 & 0 & 1 & 0 & 0 \\ 0 & 1 & 0 & 0 & 0 \\ 1 & 0 & 0 & 0 & 0 \end{pmatrix} \begin{pmatrix} \phi_2 \\ \phi_1 \\ \boxed{\phi_0} \\ \phi_1 \\ \phi_2 \end{pmatrix} = \begin{pmatrix} \phi_2 \\ \phi_1 \\ \boxed{\phi_0} \\ \phi_1 \\ \phi_2 \end{pmatrix}. \end{aligned} \tag{164}$$

The symmetry conditions are the Bravais lattice site 5-periodicity mod 5, and the even reflection across $\boxed{\phi_0}$:

$$\phi_i = \phi_{i+5}\,, \quad \phi_{-i} = \phi_i\,. \tag{165}$$

A lattice state satisfies the defining equation (17)

$$-\phi_{t-1} + V'(\phi_t) - \phi_{t+1} = m_t\,, \tag{166}$$

on the period-5 Bravais cell,

$$\begin{aligned}
V'(\phi_0) - 2\phi_1 \qquad &= m_0 \\
-\phi_0 + V'(\phi_1) - \phi_2 &= m_1 \\
-\phi_1 + V'(\phi_2) - \phi_2 &= m_2 \\
-\phi_1 + V'(\phi_2) - \phi_2 &= m_2 \\
-\phi_0 + V'(\phi_1) - \phi_2 &= m_1
\end{aligned} \tag{167}$$

where we have used (165). The result is a length-3 block lattice state condition for $\boxed{\phi_0}$, followed by the 2-block (ϕ_1, ϕ_2),

$$\begin{aligned}
V'(\phi_0) - 2\phi_1 \qquad &= m_0 \\
-\phi_0 + V'(\phi_1) - \phi_2 &= m_1 \\
-\phi_1 + V'(\phi_2) - \phi_2 &= m_2
\end{aligned} \tag{168}$$

with a 3-dimensional orbit Jacobian matrix (84)

$$\mathcal{J}_+ = \begin{pmatrix} s_0 & -2 & 0 \\ -1 & s_1 & -1 \\ 0 & -1 & s_2 - 1 \end{pmatrix}\,, \tag{169}$$

While the translational symmetry is broken, the even $\boxed{\phi_0}$ and odd | reflection bc's only affect the top and the bottom rows.

The orbit Jacobian matrix (84), 3 symmetry cases:

Odd period Bravais cell (158), is $[(m+1)\times(m+1)]$-dimensional (compare with (**??**)):

[2021-09-01 Predrag] The bottom, odd, looks like Neumann boundary condition, see Pozrikidis [223] (click here) eq. (1.5.4). The top, time-direction symmetry breaking b.c. I do not recognize.

$$\mathcal{J}[\Phi] = \begin{pmatrix} s_0 & -2 & 0 & 0 & \cdots & 0 & 0 & 0 \\ -1 & s_1 & -1 & 0 & \cdots & 0 & 0 & 0 \\ 0 & -1 & s_2 & -1 & \cdots & 0 & 0 & 0 \\ \vdots & \vdots & \vdots & \vdots & \ddots & \vdots & \vdots & \vdots \\ 0 & 0 & 0 & 0 & \cdots & -1 & s_{m-1} & -1 \\ 0 & 0 & 0 & 0 & \cdots & 0 & -1 & s_m - 1 \end{pmatrix}\,. \tag{170}$$

Even period $n = 2m + 2$, *even reflection* k (159) (compare with (**??**)):

$$\mathcal{J}[\Phi] = \begin{pmatrix} s_0 & -2 & 0 & 0 & \cdots & 0 & 0 & 0 \\ -1 & s_1 & -1 & 0 & \cdots & 0 & 0 & 0 \\ 0 & -1 & s_2 & -1 & \cdots & 0 & 0 & 0 \\ \vdots & \vdots & \vdots & \vdots & \ddots & \vdots & \vdots & \vdots \\ 0 & 0 & 0 & 0 & \cdots & -1 & s_m & -1 \\ 0 & 0 & 0 & 0 & \cdots & 0 & -2 & s_{m+1} \end{pmatrix} . \tag{171}$$

Even period $n = 2m$, *odd reflection* k (160) (compare with (**??**)):

$$\mathcal{J}[\Phi] = \begin{pmatrix} s_1 -1 & -1 & 0 & \cdots & 0 & 0 & 0 \\ -1 & s_2 & -1 & \cdots & 0 & 0 & 0 \\ \vdots & \vdots & \vdots & \ddots & \vdots & \vdots & \vdots \\ 0 & 0 & 0 & \cdots & -1 & s_{m-1} & -1 \\ 0 & 0 & 0 & \cdots & 0 & -1 & s_m -1 \end{pmatrix} . \tag{172}$$

orbit Jacobian matrix $\mathcal{J}$ evaluated on the lattice state commutes with σ,

$$\mathcal{J}\sigma = \begin{pmatrix} s_0 & -1 & 0 & 0 & -1 \\ -1 & s_1 & -1 & 0 & 0 \\ 0 & -1 & s_2 & -1 & 0 \\ 0 & 0 & -1 & s_2 & -1 \\ -1 & 0 & 0 & -1 & s_1 \end{pmatrix} \begin{pmatrix} 1 & 0 & 0 & 0 & 0 \\ 0 & 0 & 0 & 0 & 1 \\ 0 & 0 & 0 & 1 & 0 \\ 0 & 0 & 1 & 0 & 0 \\ 0 & 1 & 0 & 0 & 0 \end{pmatrix} = \sigma\mathcal{J} . \tag{173}$$

Even period examples: For even dimensions, there are two classes of reflections, the even ones, figure 13 (*ee*), that leave two 'yellow' site fields fixed, swap the rest, and the odd ones, figure 13 (*eo*), that swap the 'reds' and 'blues'. This is illustrated by the D_4 permutation representation of the even σ, odd σ_3 reflection symmetries of a square, figure 12 (*e*):

$$\sigma = \begin{pmatrix} 1 & 0 & 0 & 0 \\ 0 & 0 & 0 & 1 \\ 0 & 0 & 1 & 0 \\ 0 & 1 & 0 & 0 \end{pmatrix} , \quad \sigma_3 = \begin{pmatrix} 0 & 0 & 0 & 1 \\ 0 & 0 & 1 & 0 \\ 0 & 1 & 0 & 0 \\ 1 & 0 & 0 & 0 \end{pmatrix} . \tag{174}$$

The even reflection keeps two site fields fixed,

$$(\sigma\Phi)^\top = (\boxed{\phi_0}, \phi_3, \boxed{\phi_2}, \phi_1) ,$$

in agreement with (159). while the odd reflection reverses the order of site fields

$$(\sigma_3\Phi)^\top = (\phi_3, \phi_2 | \phi_1, \phi_0) ,$$

in agreement with (160),

(**??**) is invariant under the 1/2 lattice spacing reflection:

$$\sigma = \begin{pmatrix} 0&0&0&0&0&0&0&1\\ 0&0&0&0&0&0&1&0\\ 0&0&0&0&0&1&0&0\\ 0&0&0&0&1&0&0&0\\ 0&0&0&1&0&0&0&0\\ 0&0&1&0&0&0&0&0\\ 0&1&0&0&0&0&0&0\\ 1&0&0&0&0&0&0&0 \end{pmatrix} . \tag{175}$$

(**??**) the corresponding reflection operator leaves sites 1 and 4 invariant:

$$\sigma_1 = \begin{pmatrix} 1&0&0&0&0&0&0&0\\ 0&0&0&0&0&0&0&1\\ 0&0&0&0&0&0&1&0\\ 0&0&0&0&0&1&0&0\\ 0&0&0&0&1&0&0&0\\ 0&0&0&1&0&0&0&0\\ 0&0&1&0&0&0&0&0\\ 0&1&0&0&0&0&0&0 \end{pmatrix} . \tag{176}$$

Combination $r + r^{-1}$ commutes with σ_k, and σ_k conjugacy reverses $\mathbb{S}$

$$\begin{aligned} \sigma_k \mathcal{J} \sigma_k &= -r + \sigma_k \mathbb{S} \sigma_k - r^{-1} \\ &= \begin{pmatrix} s_{n-1} & -1 & 0 & 0 & \dots & 0 & -1\\ -1 & s_{n-2} & -1 & 0 & \dots & 0 & 0\\ 0 & -1 & s_2 & -1 & \dots & 0 & 0\\ \vdots & \vdots & \vdots & \vdots & \ddots & \vdots & \vdots\\ 0 & 0 & \dots & \dots & \dots & s_2 & -1\\ -1 & 0 & \dots & \dots & \dots & -1 & s_1 \end{pmatrix} \end{aligned} \tag{177}$$

where $\mathbb{S}$ is a diagonal matrix with the lattice site k 'stretching' factor s_k in the kth row/column.

If a period-9 orbit is invariant under the reflection operator (see (**??**))

$$\sigma = \begin{pmatrix} 0&0&0&0&0&0&0&0&1\\ 0&0&0&0&0&0&0&1&0\\ 0&0&0&0&0&0&1&0&0\\ 0&0&0&0&0&1&0&0&0\\ 0&0&0&0&1&0&0&0&0\\ 0&0&0&1&0&0&0&0&0\\ 0&0&1&0&0&0&0&0&0\\ 0&1&0&0&0&0&0&0&0\\ 1&0&0&0&0&0&0&0&0 \end{pmatrix} . \tag{178}$$

If a period-8 orbit is of form (see (159))

$$\overline{\boxed{\phi_0}\phi_1\phi_2\phi_3\boxed{\phi_4}\phi_3\phi_2\phi_1} \,, \tag{179}$$

Table 1. The temporal Hénon period-5 and -6 symmetric lattice states of type figure 13 (b), with symmetry indicated in the σ-reflection format (164). For odd $n = 2m+1$, symmetric orbits reduce to blocks of length $m+1$. For even $n = 2m$, their lengths are either $m+1$ or m. The period-5 lattice states are plotted in figure **??** (to supersede figure **??** (left)). There is no asymmetric period-5, the first C_n asymmetric pair is period-6. Indicated: the binary code m_j of the field ϕ_j at the lattice site $j = 0, 1, 2, 3, 4$.

C_5	$\phi_{-2}\phi_{-1}\boxed{\phi_0}\,\phi_1\phi_2\vert$	D_5
11110	11 $\boxed{0}$ 11 $\vert$	$\boxed{0}$ 11 $\vert$
00011	10 $\boxed{0}$ 01 $\vert$	$\boxed{0}$ 01 $\vert$
00101	01 $\boxed{0}$ 10 $\vert$	$\boxed{0}$ 10 $\vert$
00001	00 $\boxed{1}$ 00 $\vert$	$\boxed{1}$ 00 $\vert$
11010	10 $\boxed{1}$ 01 $\vert$	$\boxed{1}$ 01 $\vert$
11100	01 $\boxed{1}$ 10 $\vert$	$\boxed{1}$ 10 $\vert$

C_6	$\phi_0\phi_1\phi_2\phi_3\phi_4\phi_5$	D_6
001011	001011	001011
110100	110100	
	$\boxed{\phi_0}\phi_1\phi_2\boxed{\phi_3}\phi_2\phi_1$	
010001	$\boxed{0}$ 10 $\boxed{0}$ 01	$\boxed{0}$ 10 $\boxed{0}$
011111	$\boxed{0}$ 11 $\boxed{1}$ 11	$\boxed{0}$ 11 $\boxed{1}$
001110	$\boxed{0}$ 01 $\boxed{1}$ 10	$\boxed{0}$ 01 $\boxed{1}$
100000	$\boxed{1}$ 00 $\boxed{0}$ 00	$\boxed{1}$ 00 $\boxed{0}$
101110	$\boxed{1}$ 01 $\boxed{1}$ 10	$\boxed{1}$ 01 $\boxed{1}$
	$\phi_0\phi_1\phi_2\vert\phi_2\phi_1\phi_0\vert$	
001100	001$\vert$100$\vert$	$\vert$001$\vert$
011110	011$\vert$110$\vert$	$\vert$011$\vert$

the corresponding reflection operator leaves sites 0 and 4 invariant (see (**??**)):

$$\sigma = \begin{pmatrix} 1 & 0 & 0 & 0 & 0 & 0 & 0 & 0 \\ 0 & 0 & 0 & 0 & 0 & 0 & 0 & 1 \\ 0 & 0 & 0 & 0 & 0 & 0 & 1 & 0 \\ 0 & 0 & 0 & 0 & 0 & 1 & 0 & 0 \\ 0 & 0 & 0 & 0 & 1 & 0 & 0 & 0 \\ 0 & 0 & 0 & 1 & 0 & 0 & 0 & 0 \\ 0 & 0 & 1 & 0 & 0 & 0 & 0 & 0 \\ 0 & 1 & 0 & 0 & 0 & 0 & 0 & 0 \end{pmatrix} . \tag{180}$$

n	1	2	3	4	5	6	7	8	9	10	11
N_n	2	4	8	16	32	64	128	256	512	1024	.
M_n	2	1	2	3	6	9	18	30	56	99	186

Table 2. Lattice states and orbit counts for the $a = 6$ Hénon map.

11. Periodic orbit theory

Recurrent phenomena, the simplest of which is periodic motion, are particularly interesting and practical objects of study. Scientists have long been captivated by the near periodic motions of the planets. Among them, Poincaré was the first to truly recognize the importance of periodic solutions in understanding more complex dynamical behavior.

The problem of counting periodic orbits and how they partition the state space partitions is among the first problems that one needs to address [11, 30, 36, 39, 43, 45, 62, 183, 184, 265]. For the quadratic map it was addressed in 1950's by Myrberg, in perhaps the first application of computers to dynamics [205–209].

The problem of counting orbits for the Hénon map was also addressed very early, in a pioneering work by Simó [233] using an approach centered in the strange attractor creation/destruction.

MacKay [186] 1982 PhD thesis, published as *Renormalisation in Area-preserving Maps* has a chapter on reversible maps. Do cite in our paper(s). MacKay had these numbers already listed in Table 1.2.3.5.1 of his 1982 PhD thesis [186].

This is the 'periodic orbit theory'. And if you don't know, now you know.

11.1. Periodic orbit theory

How come that a 'Det ' in (117) counts lattice states?

For a general, nonlinear fixed point condition $F[\Phi] = 0$, expansion (93) in terms of traces is a cycle expansion [12, 58, 71], with support on *periodic orbits*. Ozorio de Almeida and Hannay [3] were the first to relate the number of periodic points to a Jacobian matrix generated volume; in 1984 they used such relation as an illustration of their 'principle of uniformity': "periodic points of an ergodic system, counted with their natural weighting, are uniformly dense in phase space." In periodic orbit theory [58, 63] this principle is stated as a flow conservation sum rule, where the sum is over all lattice states M of period n,

$$\sum_{|\mathsf{M}|=n} \frac{1}{|\det(\mathbb{1} - \mathbb{J}_{\mathsf{M}})|} = 1\,, \tag{181}$$

or, by Hill's formula (94),

$$\sum_{|\mathsf{M}|=n} \frac{1}{|\mathrm{Det}\,\mathcal{J}_{\mathsf{M}}|} = 1\,. \tag{182}$$

For the Bernoulli system the 'natural weighting' takes a particularly simple form, as the Hill determinant of the orbit Jacobian matrix is the same for all periodic points of period n, $\mathrm{Det}\,\mathcal{J}_{\mathsf{M}} = \mathrm{Det}\,\mathcal{J}$, whose number is thus given by (95). For example, the sum over the $n = 2$ lattice states is,

$$\frac{1}{|\mathrm{Det}\,\mathcal{J}_{00}|} + \frac{1}{|\mathrm{Det}\,\mathcal{J}_{01}|} + \frac{1}{|\mathrm{Det}\,\mathcal{J}_{10}|} = 1\,, \tag{183}$$

see figure 7 (b). Furthermore, for any piece-wise linear system all curvature corrections [62] for orbits of periods $k > n$ vanish, leading to explicit lattice state-counting formulas of kind reported in this paper.

In the case of temporal Bernoulli or temporal cat, the hyperbolicity is the same everywhere and does not depend on a particular solution Φ_p, counting periodic orbits is all that is needed to solve a cat-map dynamical system completely; once periodic orbits are counted, all cycle averaging formulas [61] follow.

A zeta function relates the totality of admissible states to the orbits generated by all symmetries of a given theory.

11.2. Topological zeta function

Now that we have the numbers of lattice states N_n for any period n, we can combine them all into a single generating function by substituting N_n into the *topological* or *Artin-Mazur* zeta function [11, 62],

[2020-02-16 Predrag] Do I need to derive this, rather than refer to ChaosBook?

$$1/\zeta_{\rm top}(z) = \exp\left(-\sum_{n=1}^{\infty}\frac{z^n}{n}N_n\right)\,, \tag{184}$$

which, when expanded as a Taylor series in z, is built from *primitive* (or *prime*), i.e., non-repeating lattice states [58]. Conversely, given the topological zeta function, the number of periodic points of period n is given by the logarithmic derivative of the topological zeta function (see ChaosBook [62])

$$\sum_{n=1} N_n z^n \;=\; -\,\frac{1}{1/\zeta_{\rm top}}\,z\frac{d}{dz}(1/\zeta_{\rm top})\,. \tag{185}$$

For a Bernoulli system (**??**),

$$\begin{aligned} 1/\zeta_{\rm top}(z) \;&=\; \exp\left(-\sum_{n=1}^{\infty}\frac{z^n}{n}(s^n-1)\right) \;=\; \exp\left[\ln(1-sz)-\ln(1-z)\right] \\ &= \frac{1-sz}{1-z}\,. \end{aligned} \tag{186}$$

The numerator $(1-sz)$ says that a Bernoulli system is a full shift [62]: there are s fundamental lattice states, in this case fixed points $\{\phi_0, \phi_1, \cdots, \phi_{s-1}\}$, and every other lattice state is built from their concatenations and repeats. The denominator $(1-z)$ compensates for the single overcounted lattice state, the fixed point $\phi_{s-1} = \phi_0 \pmod 1$ of figure 2 and its repeats.

For non-integer values of the stretching factor $s = \beta$, the map (24) is called the 'β-transformation'. For its topological zeta function see [101].

11.3. Counting temporal Bernoulli prime periodic orbits

Substituting the Bernoulli map topological zeta function (186) into (185) we obtain

$$\sum_{n=1} N_n z^n = z + 3z^2 + 7z^3 + 15z^4 + 31z^5 + 63z^6 + 127z^7 + 255z^8 + 511z^9 + 1023z^{10} + 2047z^{11} \cdots , \tag{187}$$

in agreement with the lattice states count (95). The number of *prime* cycles of period n is given recursively by subtracting repeats of shorter prime cycles [62],

$$M_n = \frac{1}{n}\left(N_n - \sum_{d|n}^{d<n} d M_d \right) , \tag{188}$$

where d's are all divisors of n, hence

$$\sum_{n=1} M_n z^n = z + z^2 + 2z^3 + 3z^4 + 6z^5 + 9z^6 + 18z^7 + 30z^8 + 56z^9 + 99z^{10} + 186z^{11} \cdots , \tag{189}$$

in agreement with the usual numbers of binary symbolic dynamics prime cycles [62].

11.4. Topological zeta function

Substituting the numbers of lattice states N_n (124) into the *topological zeta function* (184), Isola [146] obtains

$$\begin{aligned} 1/\zeta_{\rm top}(z) &= \exp\left(-\sum_{n=1}^{\infty} \frac{z^n}{n} N_n \right) = \exp\left(-\sum_{n=1}^{\infty} \frac{z^n}{n} (\Lambda^n + \Lambda^{-n} - 2) \right) \\ &= \exp\left[\ln(1 - z\Lambda) + \ln(1 - z\Lambda^{-1}) - 2\ln(1 - z) \right] \\ &= \frac{(1 - z\Lambda)(1 - z\Lambda^{-1})}{(1 - z)^2} = \frac{1 - sz + z^2}{(1 - z)^2} . \end{aligned} \tag{190}$$

Topological zeta functions count *prime orbits*, i.e., time invariant *sets* of equivalent lattice states related by translations (cyclic permutations), and other symmetries [62].

Conversely, given the topological zeta function, the generating function for the number of temporal lattice states of period n is given by the logarithmic derivative of the topological zeta function (185),

$$\begin{aligned} \sum_{n=0}^{\infty} N_n z^n &= \frac{2 - sz}{1 - sz + z^2} - \frac{2}{1 - z} \\ &= (s - 2)\left[z + (s + 2)z^2 + (s + 1)^2 z^3 \right. \\ &\qquad \left. + (s + 2)\, s^2 z^4 + (s^2 + s - 1)^2 z^5 + \cdots \right] , \end{aligned} \tag{191}$$

which is indeed the generating function for $T_n(s/2)$, the *Chebyshev polynomial of the first kind* (125).

n	1	2	3	4	5	6	7	8	9	10	11
N_n	1	5	16	45	121	320	841	2205	5776	15125	39601
M_n	1	2	5	10	24	50	120	270	640	1500	3600

Table 3. Lattice states and prime orbit counts for the $s = 3$ cat map (Bird and Vivaldi [29]).

Why Chebyshev? Essentially because $T_k(x)$ are also defined by a 3-term recurrence:

$$T_0(x) = 1\,, \quad T_1(x) = x$$
$$T_k(x) = 2xT_{k-1}(x) - T_{k-2}(x) \quad \text{for } k \geq 2\,, \tag{192}$$

The numbers of periodic points and *prime* cycles M_n (given by (188)) are tabulated in table 3.

12. Topological D_∞-zeta function

We use the temporal 1D lattice for systems with time-reversal symmetry to explain how such zeta functions are constructed.

A topological zeta function is the generating function of all distinct orbits (151) for a given system.

We shall refer to G-orbit (151) counting generating function for a symmetry group G as the topological G-zeta function, or the Lind zeta function [179]. The classic example is (184), the *Artin-Mazur* zeta function [11, 62] for the *infinite cyclic group* C_∞ of all integer time translations. Here we focus on the *infinite dihedral group* topological D_∞-zeta function (Kim-Lee-Park [162] or flip-zeta function).

The *infinite dihedral group* D_∞ (**??**)

the *trace formula for maps*:

[Predrag] box this relation

$$\sum_p n_p \sum_{r=1}^{\infty} \frac{z^{n_p r}}{\left|\det\left(\mathbf{1}-M_p^r\right)\right|}\,. \tag{193}$$

the trace formula (193) can be recovered from the spectral determinant by taking a derivative

$$-z\frac{d}{dz}\ln\det(1-z\mathcal{L})\,. \tag{194}$$

For every integer temporal period n, we first determine N_n, the number of all periodic *lattice state* $\mathsf{\Phi}_\mathsf{M}$ solutions on a tile of length n.

Due to the time invariance of the defining equations, there are n_p physically equivalent copies of a given solution in the orbit of every $\mathsf{\Phi}_p$. So all we really have to do is to enumerate M_n *orbits* of the time-invariance equivalent periodic orbit solutions, whose generating function is the topological zeta function.

That Hill determinant factors as $\mathrm{Det}\,\mathcal{J} = \mathrm{Det}\,\mathcal{J}_-\,\mathrm{Det}\,\mathcal{J}_+$ for all symmetric states must propagate into the factorization of the dynamical zeta function, mirroring the Kim *et al* [162] topological (counting) Lind eta function (**??**).

multiplicity $m_\mathsf{\Phi}$ of orbit $\mathcal{M}_\mathsf{\Phi}$ (153)

Let G be a group, $\mathcal{M}$ a set and $f : G\times\mathcal{M}\to\mathcal{M}$ a G-action on $\mathcal{M}$. The Lind zeta function [179] is defined by

$$\zeta_{Lind}(t) = \exp\left(\sum_H \frac{N_H}{|G/H|}t^{|G/H|}\right)\,, \tag{195}$$

where the sum is over all finite-index subgroups H of G, such that $|G/H|<\infty$, and N_H is defined by (see (201)):

$$N_H = |\{\phi\in\mathcal{M}:\ \text{all } h\in H\quad f(h,\phi)=\phi\}|. \tag{196}$$

A flip system $(\mathcal{M}, f, \sigma)$ is a dynamical system, where $\mathcal{M}$ is a topological space and $f : \mathcal{M} \to \mathcal{M}$ is a homeomorphism. $\sigma : \mathcal{M} \to \mathcal{M}$ is flip for $(\mathcal{M}, f)$ that satisfy:

$$\sigma \circ f \circ \sigma = f^{-1} \quad \text{and} \quad \sigma^2 = \mathbf{1}\,. \tag{197}$$

Kim *et al* [162] showed that the zeta function ζ_σ of a flip system $(\mathcal{M}, f, \sigma)$ can be defined as a Lind zeta function ζ_{Lind} of the D_∞-action $f : \mathrm{D}_\infty \times \mathcal{M} \to \mathcal{M}$ that is given by:

$$f(r, x) = f(x) \quad \text{and} \quad f(\sigma, x) = \sigma(x)\,. \tag{198}$$

Every finite index subgroup of the infinite dihedral group D_∞ is either

$$H_n = \langle r^n \rangle \qquad \text{or} \qquad H_{n,k} = \langle r^n, r^k\sigma \rangle\,, \tag{199}$$

with indices

$$|\mathrm{D}_\infty / H_n| = 2|n| \qquad \text{or} \qquad |\mathrm{D}_\infty / H_{n,k}| = |n|\,. \tag{200}$$

If n is a positive integer and k is an integer, then $N_{n,k}$ will denote the number of points in $\mathcal{M}$ fixed by f^n and $f^k \circ \sigma$:

$$N_{n,k} = |\{\phi \in \mathcal{M} : f^n(\phi) = f^k \circ \sigma(\phi) = \phi\}|\,. \tag{201}$$

They obtain

[2021-07-04, 2021-08-25 Predrag] our notation, replaced subscript $_{f,\sigma}$ by noting.

$$\zeta_\sigma(t) = \exp\Big(\sum_{n=1}^{\infty} \frac{N_n}{2n} t^{2n} + \sum_{n=1}^{\infty} \sum_{k=0}^{n-1} \frac{N_{n,k}}{n} t^n \Big)\,. \tag{202}$$

The first sum factors as an Artin-Mazur zeta function (**??**):

$$\exp\left(\sum_{n=1}^{\infty} \frac{t^{2n}}{2n} N_n \right) = \sqrt{\zeta_{top}(t^2)} \tag{203}$$

The class count (145), (156) tells us that

$$N_{n,k} = \Big\{ \quad N_{n,0} \qquad \text{if } n \text{ is odd, } N_{n,0} \qquad \text{if } n \text{ and } k \text{ are even, } N_{n,1} \qquad \text{if } n \text{ is even and } k \text{ i}$$

Hence

$$\sum_{k=0}^{n-1} \frac{N_{n,k}}{n} = \Big\{ \quad N_{n,0} \qquad\qquad \text{if } n \text{ is odd}\,, \ \frac{N_{n,0} + N_{n,1}}{2} \qquad \text{if } n \text{ is even}\,. \tag{205}$$

so the Lind zeta function of the flip triple system $(\mathcal{M}, f, \sigma)$ is

$$\zeta_\sigma(t) = \sqrt{\zeta_{top}(t^2)}\; e^{h(t)}, \tag{206}$$

where ζ_{top} is the Artin-Mazur zeta function ArtMaz5, and the counts of symmetric orbits

$$h(t) = \sum_{m=1}^{\infty} \left\{ N_{2m-1,0}\, t^{2m-1} + (N_{2m,0} + N_{2m,1})\, \frac{t^{2m}}{2} \right\}\,. \tag{207}$$

The $\exp(h(t))$ in (206) can be factored into terms that presumably correspond –in the particular, Hénon case– to the $D_n N_n$ factors in (**??**), but this is now totally general,

in the spirit of table **??**, for any time-reversal discrete time dynamical system. Should be generalizable also to systems with continuous time.

The zeta function ζ_σ can be written as a product over orbits. Let O_1 be the collection of finite orbits with time reversal (flip) symmetry, and O_2 be the collection of the pairs of orbits without time reversal symmetry, each an orbit and the flipped orbit. A finite orbit p is a periodic points set

$$p = \{\phi, f(\phi), \ldots, f^{n_p-1}(\phi)\}$$

if $p \in O_1$, and

$$p = \{\phi, f(\phi), \ldots, f^{k-1}(\phi)\} \cup \{\sigma(\phi), f \circ \sigma(\phi), \ldots, f^{k-1} \circ \sigma(\phi)\}$$

if $p \in O_2$, where $k = n_p/2$.

If $p \in O_1$,

$$\zeta_p(t) = \sqrt{\frac{1}{1-t^{2n_p}}} \exp\left(\frac{t^{n_p}}{1-t^{n_p}}\right) , \tag{208}$$

and if $p \in O_2$,

$$\zeta_p(t) = \frac{1}{1-t^{n_p}} . \tag{209}$$

The product form of the zeta function is:

$$1/\zeta_\sigma(t) = \sqrt{\prod_{p_1 \in O_1} (1-t^{2n_{p_1}})} \exp\left(-\frac{t^{n_{p_1}}}{1-t^{n_{p_1}}}\right) \prod_{p_2 \in O_2} (1-t^{n_{p_2}}) . \tag{210}$$

12.1. Counting temporal cat lattice states

(**??**), (**??**) introduce μ. See also (**??**), (**??**), (**??**), (**??**), (**??**),

For $s > 2$ the stability multipliers $(\Lambda^+, \Lambda^-) = (\Lambda\,,\ \Lambda^{-1})$ are real,

$$\Lambda^{\pm} = \frac{1}{2}(s \pm \sqrt{D})\,, \qquad \Lambda = e^{\lambda}\,, \tag{211}$$

where

$$\begin{aligned} s \qquad\qquad & = \Lambda + \Lambda^{-1} = 2\cosh(\lambda) \\ s-2 \qquad\qquad & = \mu^2 \\ \sqrt{D} \qquad\qquad & = \Lambda - \Lambda^{-1} = 2\sinh(\lambda) \\ \text{discriminant } D & = s^2 - 4 = \mu^2(\mu^2+4) \end{aligned} \tag{212}$$

The sine, sinh, cos, cosh are related by the identities (**??**) and (**??**). For D_n irreps, I think we should use the (**??**) form of eigenvalues, and Klein-Gordon mass μ

$$\begin{aligned} \lambda_m &= \mu^2 + 4\sin^2(\alpha_m/2) \\ &= \left(\mu - i\,2\sin\left(\frac{\alpha_m}{2}\right)\right)\left(\mu + i\,2\sin\left(\frac{\alpha_m}{2}\right)\right) \\ \alpha_m &= 2\pi m/n\,, \end{aligned} \tag{213}$$

rather than (**??**) and stretching s, which is appropriate to C_n irreps. Identities like (**??**), (**??**), (**??**) and Gradshteyn and Ryzhik [117] Eq. 1.317.1 (click here)

$$2\sin^2(\theta/2) = 1 - \cos(\theta) \tag{214}$$

are also suggestive in this context.

How to count the number of lattice states for temporal cat?

No symmetry lattice states Hill determinant:

$$N_n = \prod_{j=0}^{n-1}\left(s - 2\cos\frac{2\pi j}{n}\right)\,.$$

The products of eigenvalues for the C_n discrete Fourier case follows from (**??**):

$$\prod_{j=0}^{n-1}\left(s - 2\cos\frac{2\pi j}{n}\right) = (\Lambda^{n/2} - \Lambda^{-n/2})^2\,, \tag{215}$$

It's a square, because of the D_n symmetry. Consider even, odd casses, use $\cos 0 = 1$, $\cos\pi = -1$, $\cos(-\theta) = \cos\theta$. The product over non-trivial eigenvalues is:

$$n = 2mM_{n,0} = \prod_{j=1}^{m-1}\left(s - 2\cos\frac{\pi j}{m}\right) = \frac{|\Lambda^{n/2} - \Lambda^{-n/2}|}{\mu\sqrt{\mu^2+4}}\,, \tag{216}$$

$$n = 2m-1M_{n,1} = \prod_{j=1}^{m-1}\left(s - 2\cos\frac{2j\pi}{2m-1}\right) = \frac{|\Lambda^{n/2} - \Lambda^{-n/2}|}{\mu}\,, \tag{217}$$

Next, look at the *symmetric* lattice states Hill determinants:

For odd $n = 2m-1$,

$$N_{n,1} = \prod_{j=0}^{m-1} \left(s - 2\cos\frac{2\pi j}{n} \right) = \mu M_{n,1} \,. \tag{218}$$

For $n = 2m$,

$$\begin{aligned} N_{n,1} &= \prod_{j=0}^{m-1} \left(s - 2\cos\frac{2\pi j}{n} \right) \\ N_{n,0} &= (s+2)\, N_{n,1} \,, \end{aligned} \tag{219}$$

and

$$\frac{1}{2}\left(N_{n,0} + N_{n,1}\right) = \frac{\mu^2+5}{2} \prod_{j=0}^{m-1} \left(s - 2\cos\frac{2\pi j}{n} \right) = \frac{\mu^2+5}{2\mu} \sqrt{\frac{(\Lambda^n + \Lambda^{-n} - 2)}{\mu^2+4}} \tag{220}$$

The number of lattice states can be written as polynomials: For $n = 2m-1$:

$$\begin{aligned} N_{n,0} &= \mu \left(\Lambda^{n/2} - \Lambda^{-n/2} \right) \\ &= \mu^2 \Lambda^{-1/2} \left(\Lambda^m - \Lambda^{-m+1} \right) \,. \end{aligned} \tag{221}$$

For $n = 2m$:

$$\begin{aligned} \frac{1}{2}\left(N_{n,0} + N_{n,1}\right) &= \frac{s+3}{2(\Lambda - \Lambda^{-1})} \left(\Lambda^{n/2} - \Lambda^{-n/2} \right) \\ &= \frac{\mu^2+5}{2\mu\sqrt{\mu^2+4}} \left| \Lambda^m - \Lambda^{-m} \right| \,. \end{aligned} \tag{222}$$

Now we can compute the $h(t)$ from (207)

$$\begin{aligned} h(t) &= \sum_{m=1}^{\infty} \left[N_{2m-1,0}\, t^{2m-1} + \left(N_{2m,0} + N_{2m,1}\right) \frac{t^{2m}}{2} \right] \\ &= \mu \frac{\Lambda^{1/2} t}{1 - \Lambda t^2} - \mu \frac{\Lambda^{-1/2} t}{1 - \Lambda^{-1} t^2} \\ &\quad + \frac{\mu^2+5}{2(\Lambda - \Lambda^{-1})} \frac{\Lambda t^2}{1 - \Lambda t^2} - \frac{\mu^2+5}{2(\Lambda - \Lambda^{-1})} \frac{\Lambda^{-1} t^2}{1 - \Lambda^{-1} t^2} \,. \end{aligned} \tag{223}$$

Using (206) we have the "flip" part of the zeta function. Testing this zeta function using (233), we have:

$$\begin{aligned} -t\frac{\partial}{\partial t}(\ln e^{-h(t)}) &= t + 6t^2 + 12t^3 + 36t^4 + 55t^5 + 144t^6 \\ &\quad + 203t^7 + 504t^8 + 684t^9 + 1650t^{10} + \dots \,, \end{aligned} \tag{224}$$

which is in agreement with (233) and table **??**.

12.2. Counting lattice states

Given the topological zeta function (202) we can count the number of lattice states from the generating function:

[2021-08-25 Predrag] We have the counts of the Bravais lattice states N_n, $N_{n,k}$ already, from (204), so why don't we reverse the logic, start here, and get the zeta function (206) by integration? Mention that this is an example of Lind zeta function [179] (195) without ever writing it down, so we do not have to explain it? It's a side issue for us, really.

$$\frac{-t\frac{d}{dt}(1/\zeta_\sigma(t))}{1/\zeta_\sigma(t)} = \sum_{n=1}^{\infty} N_n t^{2n} + \sum_{n=1}^{\infty}\sum_{k=0}^{n-1} N_{n,k} t^n = \sum_{m=1}^{\infty} a_m t^m \,, \tag{225}$$

where the coefficients are:

$$a_m = \begin{cases} \sum_{k=0}^{m-1} N^\sigma_{m,k} = m N^\sigma_{m,0} \,, & m \text{ is odd} \,, \\ N_{m/2} + \sum_{k=0}^{m-1} N^\sigma_{m,k} = N_{m/2} + \frac{m}{2}\left(N^\sigma_{m,0} + N^\sigma_{m,1}\right) \,, & m \text{ is even} \,. \end{cases} \tag{226}$$

Using the product formula of topological zeta function (210) and the numbers of orbits with length up to 5 from the table **??**, we can write the topological zeta function:

$$\begin{aligned} 1/\zeta_\sigma(t) = \sqrt{1-t^2}\exp\left(-\frac{t}{1-t}\right)(1-t^4)\exp\left(-\frac{2t^2}{1-t^2}\right)\left(\sqrt{1-t^6}\right)^3 \\ \exp\left(-\frac{3t^3}{1-t^3}\right)(1-t^6)(1-t^8)^3\exp\left(-\frac{6t^4}{1-t^4}\right) \\ (1-t^8)^2(1-t^{10})^5\exp\left(-\frac{10t^5}{1-t^5}\right)(1-t^{10})^6\ldots \,. \end{aligned} \tag{227}$$

The generating function is:

$$\frac{-t\frac{d}{dt}(1/\zeta_\sigma)}{1/\zeta_\sigma} = t + 7t^2 + 12t^3 + 41t^4 + 55t^5 + \ldots \,, \tag{228}$$

which is in agreement with (226), where the N_n and N^σ_n are the C_n and SF_n in the table **??**.

We are not able to retrieve the numbers of fixed points by their symmetry groups using this topological zeta function (202), unless we rewrite the topological zeta function with two variables:

$$\zeta_\sigma(t,u) = \exp\left(\sum_{n=1}^{\infty}\frac{N_n}{2n}t^{2n} + \sum_{n=1}^{\infty}\sum_{k=0}^{n-1}\frac{N_{n,k}}{n}u^n\right) . \tag{229}$$

Using this topological zeta function $\zeta_\sigma(t,u)$ we can write two generating functions:

$$\frac{-t\frac{\partial}{\partial t}(1/\zeta_\sigma(t,u))}{1/\zeta_\sigma(t,u)} = \sum_{n=1}^{\infty} N_n t^{2n} \,, \tag{230}$$

and

$$\frac{-u\frac{\partial}{\partial u}(1/\zeta_\sigma(t,u))}{1/\zeta_\sigma(t,u)} = \sum_{n=1}^{\infty}\sum_{k=0}^{n-1} N_{n,k} u^n \,. \tag{231}$$

Using the product formula of this topological zeta function and the numbers of orbits with length up to 5 from the table **??**, the topological zeta function is:

$$1/\zeta_\sigma(t,u) = \sqrt{1-t^2}\exp\left(-\frac{u}{1-u}\right)(1-t^4)\exp\left(-\frac{2u^2}{1-u^2}\right)\left(\sqrt{1-t^6}\right)^3$$
$$\exp\left(-\frac{3u^3}{1-u^3}\right)(1-t^6)(1-t^8)^3\exp\left(-\frac{6u^4}{1-u^4}\right)$$
$$(1-t^8)^2(1-t^{10})^5\exp\left(-\frac{10u^5}{1-u^5}\right)(1-t^{10})^6\ldots . \tag{232}$$

And the generating function from this topological zeta function is:

$$\frac{-u\frac{\partial}{\partial u}(1/\zeta_\sigma(t,u))}{1/\zeta_\sigma(t,u)} = u + 6u^2 + 12u^3 + 36u^4 + 55u^5 + \ldots , \tag{233}$$

which is in agreement with (231), where the N_n^σ is the SF_n in the table **??**.

13. Summary

How to think about matters spatiotemporal? While dynamics of a turbulent system might appear so complex to defy any precise description, the laws of motion drive a spatially extended system (clouds, say) through a repertoire of unstable patterns, each defined over a finite spatiotemporal region [120, 121]. The local dynamics, observed through such finite spatiotemporal windows, can be thought of as a visitation sequence of a finite repertoire of finite patterns. To make predictions about such system, one needs to know how often a given pattern occurs, and that is a purview of periodic orbit theory [60].

However, the initial rapid progress in description of turbulence in terms of such 'exact coherent structures' [110, 159] has slowed down to a crawl due to our inability to extend the theory and the computations to spatially large or infinite computational domains [40].

But in dynamics, we have no fear of the infinite extent in time. That is periodic orbit theory's [72] raison d'être; the dynamics itself describes the infinite time strange sets by a hierarchical succession of periodic orbits, of longer and longer, but always finite periods (with no artificial external periodicity imposed along the time axis). And, since 1996 we know how to deal with both spatially and temporally infinite regions by tiling them with finite spatiotemporally periodic tiles [50, 110]. More precisely: a time periodic orbit is computed in a finite time, with period T, but its repeats "tile" the time axis for all times. Similarly, a spatiotemporally periodic "tile" or "periodic orbit" is computed on a finite spatial region L, for a finite period T, but its repeats in both time and space directions tile the infinite spacetime.

Taken together, these open a path to determining exact solutions on *spatially infinite* regions. This is important, as many turbulent flows of physical interest come equipped with D continuous spatial symmetries. For example, in a pipe flow at transitional Reynolds number, the azimuthal and radial directions (measured in viscosity length units) are compact, while the pipe length is infinite. If the theory is recast as a d-dimensional space-time theory, $d = D + 1$, spatiotemporally translational invariant recurrent solutions are invariant d-tori (and *not* the 1-dimensional periodic orbits of the traditional periodic orbit theory), and the symbolic dynamics is likewise d-dimensional (rather than what is today taken for given, a single 1-dimensional temporal string of symbols).

This changes everything. Instead of studying time evolution of a chaotic system, one now studies the repertoire of spatiotemporal patterns allowed by a given PDE, or, in the discretized spacetime, partial difference equations. To put it more provocatively: junk your old equations and look for guidance in clouds' repeating patterns. There is no more *time* in this vision of nonlinear *dynamics*! Instead, there is the space of all spatiotemporal patterns, and the likelihood that a given finite spatiotemporally pattern can appear, like the mischievous grin of Cheshire cat, anywhere in the turbulent evolution of a flow. A bold vision, but how does it work?

and thus a d-dimensional spatiotemporal pattern is mapped one-to-one onto a d-dimensional discrete lattice state, symbolic dynamics labelled configuration - a configuration very much like that of an Ising model of statistical mechanics.

In this paper we have analyzed

in particular, a spatiotemporal lattice formulation of time reversal.

corresponding dynamical zeta functions should be sums over d-dimensional Bravais cells, rather than 1-dimensional time-periodic orbits.

While the setting is classical, such deterministic field-theory advances offer new semi-classical approaches to quantum field theory and many-body problems.

Acknowledgments

Work of P. C. and H. L. was in part supported by the family of late G. Robinson, Jr.. No actual cats, graduate or undergraduate were harmed during this research. This paper sets up the necessary underpinnings for the quantum field theory of spatiotemporal cat, the details of which we leave to our friends Jon Keating and Marcos Saraceno.

References

[1] V. V. Albert, L. I. Glazman, and L. Jiang, "Topological properties of linear circuit lattices", Phys. Rev. Lett. **114**, 173902 (2015).

[2] E. Allroth, "Ground state of one-dimensional systems and fixed points of 2n-dimensional map", J. Phys. A **16**, L497 (1983).

[3] A. M. Ozorio de Almeida and J. H. Hannay, "Periodic orbits and a correlation function for the semiclassical density of states", J. Phys. A **17**, 3429 (1984).

[4] R. E. Amritkar, P. M. Gade, A. D. Gangal, and V. M. Nandkumaran, "Stability of periodic orbits of coupled-map lattices", Phys. Rev. A **44**, R3407–R3410 (1991).

[5] S. Anastassiou, "Complicated behavior in cubic Hénon maps", Theoret. Math. Phys. **207**, 572–578 (2021).

[6] S. Anastassiou, A. Bountis, and A. Bäcker, "Homoclinic points of 2D and 4D maps via the parametrization method", Nonlinearity **30**, 3799–3820 (2017).

[7] S. Anastassiou, A. Bountis, and A. Bäcker, "Recent results on the dynamics of higher-dimensional Hénon maps", Regul. Chaotic Dyn. **23**, 161–177 (2018).

[8] W. N. Anderson and T. D. Morley, "Eigenvalues of the Laplacian of a graph", Lin. Multilin. Algebra **18**, 141–145 (1985).

[9] V. I. Arnol'd and A. Avez, *Ergodic Problems of Classical Mechanics* (Addison-Wesley, Redwood City, 1989).

[10] F. Arrigo, P. Grindrod, D. J. Higham, and V. Noferini, "On the exponential generating function for non-backtracking walks", Linear Algebra Appl. **556**, 381–399 (2018).

[11] M. Artin and B. Mazur, "On periodic points", Ann. Math. **81**, 82–99 (1965).

[12] R. Artuso, E. Aurell, and P. Cvitanović, "Recycling of strange sets: I. Cycle expansions", Nonlinearity **3**, 325–359 (1990).

[13] R. Artuso, E. Aurell, and P. Cvitanović, "Recycling of strange sets: II. Applications", Nonlinearity **3**, 361–386 (1990).

[14] J. H. Asad, "Differential equation approach for one- and two-dimensional lattice green's function", Mod. Phys. Lett. B **21**, 139–154 (2007).

[15] D. Atkinson and F. J. van Steenwijk, "Infinite resistive lattices", Am. J. Phys **67**, 486–492 (1999).

[16] S. Aubry, "Anti-integrability in dynamical and variational problems", Physica D **86**, 284–296 (1995).

[17] S. Aubry and G. Abramovici, "Chaotic trajectories in the standard map. The concept of anti-integrability", Physica D **43**, 199–219 (1990).

[18] M. Baake, J. Hermisson, and A. B. Pleasants, "The torus parametrization of quasiperiodic LI-classes", J. Phys. A **30**, 3029–3056 (1997).

[19] J.-C. Ban, W.-G. Hu, S.-S. Lin, and Y.-H. Lin, *Zeta Functions for Two-dimensional Shifts of Finite Type*, Vol. 221, Memoirs Amer. Math. Soc. (Amer. Math. Soc., Providence RI, 2013).

[20] R. Band, J. M. Harrison, and C. H. Joyner, "Finite pseudo orbit expansions for spectral quantities of quantum graphs", J. Phys. A **45**, 325204 (2012).

[21] A. Barvinok, *A Course in Convexity* (Amer. Math. Soc., New York, 2002).

[22] A. Barvinok, Lattice Points, Polyhedra, and Complexity, tech. rep. (Univ. of Michigen, Ann Arbor MI, 2004).

[23] A. Barvinok, *Integer Points in Polyhedra* (European Math. Soc. Pub., Berlin, 2008).

[24] H. Bass, "The Ihara-Selberg zeta function of a tree lattice", Int. J. Math. **3**, 717–797 (1992).

[25] R. J. Baxter, "The bulk, surface and corner free energies of the square lattice Ising model", J. Phys. A **50**, 014001 (2016).

[26] M. Beck and S. Robins, *Computing the Continuous Discretely* (Springer, New York, 2007).

[27] H. S. Bhat and B. Osting, "Diffraction on the two-dimensional square lattice", SIAM J. Appl. Math. **70**, 1389–1406 (2010).

[28] O. Biham and W. Wenzel, "Characterization of unstable periodic orbits in chaotic attractors and repellers", Phys. Rev. Lett. **63**, 819 (1989).

[29] N. Bird and F. Vivaldi, "Periodic orbits of the sawtooth maps", Physica D **30**, 164–176 (1988).

[30] R. L. Bivins, J. D. Louck, N. Metropolis, and M. L. Stein, "Classification of all cycles of the parabolic map", Physica D **51**, 3–27 (1991).

[31] P. Blanchard and D. Volchenkov, *Random Walks and Diffusions on Graphs and Databases* (Springer, Berlin, 2011).

[32] S. V. Bolotin and D. V. Treschev, "Hill's formula", Russ. Math. Surv. **65**, 191 (2010).

[33] R. Bowen and O. Lanford, Zeta functions of restrictions of the shift transformation, in Global Analysis (Proc. Sympos. Pure Math., Berkeley, CA, 1968), Vol. 1, edited by S.-S. Chern and S. Smale (1970), pp. 43–50.

[34] A. Boyarsky and P. Góra, *Laws of Chaos: Invariant Measures and Dynamical Systems in One Dimension* (Birkhäuser, Boston, 1997).

[35] L. Boyle and P. J. Steinhardt, Self-similar one-dimensional quasilattices, 2016.

[36] A. Bridy and R. A. Pérez, "A count of maximal small copies in Multibrot sets", Nonlinearity **18**, 1945–1953 (2005).

[37] R. B. S. Brooks, R. F. Brown, J. Pak, and D. H. Taylor, "Nielsen numbers of maps of tori", Proc. Amer. Math. Soc. **52**, 398–398 (1975).

[38] A. Brown, "Equations for periodic solutions of a logistic difference equation", J. Austral. Math. Soc. Ser. B **23**, 78–94 (1981).

[39] K. M. Brucks, "MSS sequences, colorings of necklaces, and periodic points of $f(z) = z^2$-2", Adv. Appl. Math. **8**, 434–445 (1987).

[40] N. B. Budanur, K. Y. Short, M. Farazmand, A. P. Willis, and P. Cvitanović, "Relative periodic orbits form the backbone of turbulent pipe flow", J. Fluid Mech. **833**, 274–301 (2017).

[41] B. L. Buzbee, G. H. Golub, and C. W. Nielson, "On direct methods for solving Poisson's equations", SIAM J. Numer. Anal. **7**, 627–656 (1970).

[42] J. L. Cardy, "Operator content of two-dimensional conformally invariant theories", Nucl. Phys. B **270**, 186–204 (1986).

[43] O. Chavoya-Aceves, F. Angulo-Brown, and E. Piña, "Symbolic dynamics of the cubic map", Physica D **14**, 374–386 (1985).

[44] M. Chen, "On the solution of circulant linear systems", SIAM J. Numer. Anal. **24**, 668–683 (1987).

[45] W. Y. C. Chen and J. D. Louck, "Necklaces, MSS sequences, and DNA sequences", Adv. Appl. Math. **18**, 18–32 (1997).

[46] G. Chinta, J. Jorgenson, and A. Karlsson, "Zeta functions, heat kernels, and spectral asymptotics on degenerating families of discrete tori", Nagoya Math. J. **198**, 121–172 (2010).

[47] G. Chinta, J. Jorgenson, and A. Karlsson, "Heat kernels on regular graphs and generalized Ihara zeta function formulas", Monatsh. Math. **178**, 171–190 (2014).

[48] B. V. Chirikov, "A universal instability of many-dimensional oscillator system", Phys. Rep. **52**, 263–379 (1979).

[49] W. G. Choe and J. Guckenheimer, "Computing periodic orbits with high accuracy", Computer Meth. Appl. Mech. and Engin. **170**, 331–341 (1999).

[50] F. Christiansen, P. Cvitanović, and V. Putkaradze, "Spatiotemporal chaos in terms of unstable recurrent patterns", Nonlinearity **10**, 55–70 (1997).

[51] F. Chung and S.-T. Yau, "Discrete Green's functions", J. Combin. Theory A **91**, 19–214 (2000).

[52] D. Cimasoni, "The critical Ising model via Kac-Ward matrices", Commun. Math. Phys. **316**, 99–126 (2012).

[53] B. Clair, "The Ihara zeta function of the infinite grid", Electron. J. Combin. **21**, P2–16 (2014).

[54] B. Clair and S. Mokhtari-Sharghi, "Zeta functions of discrete groups acting on trees", J. Algebra **237**, 591–620 (2001).

[55] B. Clair and S. Mokhtari-Sharghi, "Convergence of zeta functions of graphs", Proc. Amer. Math. Soc. **130**, 1881–1887 (2002).

[56] J. Cserti, "Application of the lattice Green's function for calculating the resistance of an infinite network of resistors", Amer. J. Physics **68**, 896–906 (2000).

[57] J. Cserti, G. Széchenyi, and G. Dávid, "Uniform tiling with electrical resistors", J. Phys. A **44**, 215201 (2011).

[58] P. Cvitanović, "Invariant measurement of strange sets in terms of cycles", Phys. Rev. Lett. **61**, 2729–2732 (1988).

[59] P. Cvitanović, "Chaotic Field Theory: A sketch", Physica A **288**, 61–80 (2000).

[60] P. Cvitanović, "Recurrent flows: The clockwork behind turbulence", J. Fluid Mech. Focus Fluids **726**, 1–4 (2013).

[61] P. Cvitanović, "Trace formulas", in *Chaos: classical and quantum*, edited by P. Cvitanović, R. Artuso, R. Mainieri, G. Tanner, and G. Vattay (Niels Bohr Inst., Copenhagen, 2017).

[62] P. Cvitanović, "Counting", in *Chaos: Classical and Quantum* (Niels Bohr Inst., Copenhagen, 2020).

[63] P. Cvitanović, "Why cycle?", in *Chaos: Classical and Quantum*, edited by P. Cvitanović, R. Artuso, R. Mainieri, G. Tanner, and G. Vattay (Niels Bohr Inst., Copenhagen, 2020).

[64] P. Cvitanović and Y. Lan, Turbulent fields and their recurrences, in Correlations and Fluctuations in QCD : Proceedings of 10. International Workshop on Multiparticle Production, edited by N. Antoniou (2003), pp. 313–325.

[65] P. Cvitanović and H. Liang, Spatiotemporal cat: A chaotic field theory, In preparation, 2021.

[66] P. Cvitanović and D. Lippolis, Knowing when to stop: How noise frees us from determinism, in Let's Face Chaos through Nonlinear Dynamics, edited by M. Robnik and V. G. Romanovski (2012), pp. 82–126.

[67] P. Cvitanović, C. P. Dettmann, R. Mainieri, and G. Vattay, "Trace formulas for stochastic evolution operators: Weak noise perturbation theory", J. Stat. Phys. **93**, 981–999 (1998).

[68] P. Cvitanović, N. Søndergaard, G. Palla, G. Vattay, and C. P. Dettmann, "Spectrum of stochastic evolution operators: Local matrix representation approach", Phys. Rev. E **60**, 3936–3941 (1999).

[69] P. Cvitanović, C. P. Dettmann, R. Mainieri, and G. Vattay, "Trace formulae for stochastic evolution operators: Smooth conjugation method", Nonlinearity **12**, 939 (1999).

[70] P. Cvitanović, R. Artuso, L. Rondoni, and E. A. Spiegel, "Transporting densities", in *Chaos: Classical and Quantum*, edited by P. Cvitanović, R. Artuso, R. Mainieri, G. Tanner, and G. Vattay (Niels Bohr Inst., Copenhagen, 2017).

[71] P. Cvitanović, R. Artuso, R. Mainieri, G. Tanner, and G. Vattay, *Chaos: Classical and Quantum* (Niels Bohr Inst., Copenhagen, 2020).

[72] P. Cvitanović, R. Artuso, R. Mainieri, G. Tanner, and G. Vattay, *Chaos: Classical and Quantum* (Niels Bohr Inst., Copenhagen, 2020).

[73] F. Dannan, S. Elaydi, and P. Liu, "Periodic solutions of difference equations", J. Difference Equations and Applications **6**, 203–232 (2000).

[74] J. A. De Loera, R. Hemmecke, J. Tauzer, and R. Yoshida, "Effective lattice point counting in rational convex polytopes", J. Symbolic Comp. **38**, 1273–1302 (2004).

[75] A. Deitmar, "Ihara zeta functions of infinite weighted graphs", SIAM J. Discrete Math. **29**, 2100–2116 (2015).

[76] R. L. Devaney, *An Introduction to Chaotic Dynamical systems*, 2nd ed. (Westview Press, Cambridge, Mass, 2008).

[77] R. L. Devaney and Z. Nitecki, "Shift automorphisms in the Hénon mapping", Commun. Math. Phys. **67**, 137–146 (1979).

[78] A. Dienstfrey, F. Hang, and J. Huang, "Lattice sums and the two-dimensional, periodic Green's function for the Helmholtz equation", Proc. Roy. Soc. Ser A **457**, 67–85 (2001).

[79] X. Ding and P. Cvitanović, "Periodic eigendecomposition and its application in Kuramoto-Sivashinsky system", SIAM J. Appl. Dyn. Syst. **15**, 1434–1454 (2016).

[80] X. Ding, H. Chaté, P. Cvitanović, E. Siminos, and K. A. Takeuchi, "Estimating the dimension of the inertial manifold from unstable periodic orbits", Phys. Rev. Lett. **117**, 024101 (2016).

[81] E. J. Doedel, A. R. Champneys, T. F. Fairgrieve, Y. A. Kuznetsov, B. Sandstede, and X. Wang, *AUTO: Continuation and Bifurcation Software for Ordinary Differential Equations* (2007).

[82] F. W. Dorr, "The direct solution of the discrete Poisson equation on a rectangle", SIAM Rev. **12**, 248–263 (1970).

[83] P. G. Doyle and J. L. Snell, "Random walks and electric networks", in *Intelligent Systems, Control and Automation: Science and Engineering* (Springer, 2012), pp. 259–265.

[84] M. S. Dresselhaus, G. Dresselhaus, and A. Jorio, *Group Theory: Application to the Physics of Condensed Matter* (Springer, New York, 2007).

[85] D. J. Driebe, *Fully Chaotic Maps and Broken Time Symmetry* (Springer, New York, 1999).

[86] J. Dubout, Zeta functions of graphs, their symmetries and extended Catalan numbers.

[87] D. Dudgeon and R. M. Mersereau, *Multidimensional Digital Signal Processing* (Prentice-Hall, Englewood Cliffs, NJ, 1984).

[88] H. R. Dullin and J. D. Meiss, "Stability of minimal periodic orbits", Phys. Lett. A **247**, 227–234 (1998).

[89] H. R. Dullin and J. D. Meiss, "Generalized Hénon maps: the cubic diffeomorphisms of the plane", Physica D **143**, 262–289 (2000).

[90] E. N. Economou, *Green's Functions in Quantum Physics* (Springer, Berlin, 2006).

[91] S. Elaydi, *An Introduction to Difference Equations*, 3rd ed. (Springer, Berlin, 2005).

[92] A. Endler and J. A. C. Gallas, "Period four stability and multistability domains for the Hénon map", Physica A **295**, 285–290 (2001).

[93] A. Endler and J. A. C. Gallas, "Arithmetical signatures of the dynamics of the Hénon map", Phys. Rev. E **65**, 036231 (2002).

[94] A. Endler and J. A. C. Gallas, "Conjugacy classes and chiral doublets in the Hénon Hamiltonian repeller", Phys. Lett. A **356**, 1–7 (2006).

[95] A. Endler and J. A. C. Gallas, "Reductions and simplifications of orbital sums in a Hamiltonian repeller", Phys. Lett. A **352**, 124–128 (2006).

[96] A. Endler and J. A. C. Gallas, "Reductions and simplifications of orbital sums in a Hamiltonian repeller", Phys. Lett. A **352**, 124–128 (2006).

[97] M. J. Feigenbaum and B. Hasslacher, "Irrational decimations and path-integrals for external noise", Phys. Rev. Lett. **49**, 605–609 (1982).

[98] A. L. Fetter and J. D. Walecka, *Theoretical Mechanics of Particles and Continua* (Dover, New York, 2003).

[99] M. Fiedler, "Algebraic connectivity of graphs", Czech. Math. J **23**, 298–305 (1973).

[100] D. Fischer, G. Golub, O. Hald, C. Leiva, and O. Widlund, "On Fourier-Toeplitz methods for separable elliptic problems", Math. Comput. **28**, 349–349 (1974).

[101] L. Flatto, J. C. Lagarias, and B. Poonen, "The zeta function of the beta transformation", Ergodic Theory Dynam. Systems **14**, 237–266 (1994).

[102] F. Flicker, "Time quasilattices in dissipative dynamical systems", SciPost Phys. **5**, 001 (2018).

[103] E. Fradkin, *Field Theories of Condensed Matter Physics* (Cambridge Univ. Press, Cambridge UK, 2013).

[104] S. Friedland and J. Milnor, "Dynamical properties of plane polynomial automorphisms", Ergodic Theory Dynam. Systems **9**, 67–99 (1989).

[105] P. M. Gade and R. E. Amritkar, "Spatially periodic orbits in coupled-map lattices", Phys. Rev. E **47**, 143–154 (1993).

[106] J. A. C. Gallas, "Equivalence among orbital equations of polynomial maps", Int. J. Modern Phys. C **29**, 1850082 (2018).

[107] J. A. C. Gallas, "Orbital carriers and inheritance in discrete-time quadratic dynamics", Int. J. Modern Phys. C **31**, 2050100 (2020).

[108] J. A. C. Gallas, "Preperiodicity and systematic extraction of periodic orbits of the quadratic map", Int. J. Modern Phys. C **31**, 2050174 (2020).

[109] J. F. Gibson, Channelflow: A spectral Navier-Stokes simulator in C++, tech. rep., `Channelflow.org` (U. New Hampshire, 2019).

[110] J. F. Gibson, J. Halcrow, and P. Cvitanović, "Visualizing the geometry of state-space in plane Couette flow", J. Fluid Mech. **611**, 107–130 (2008).

[111] R. Giles and C. B. Thorn, "Lattice approach to string theory", Phys. Rev. D **16**, 366–386 (1977).

[112] J. I. Glaser, "Numerical solution of waveguide scattering problems by finite-difference Green's functions", IEEE Trans. Microwave Theory Tech. **18**, 436–443 (1970).

[113] S. Gnutzmann, T. Guhr, H. Schomerus, and K. Życzkowski, "Special issue in honour of the life and work of Fritz Haake", J. Phys. A **54**, 130301 (2021).

[114] C. Godsil and G. F. Royle, *Algebraic Graph Theory* (Springer, New York, 2013).

[115] J. W. von Goethe, *Faust I, Studierzimmer 2.* M. Greenberg, transl. (Yale Univ. Press, 1806).

[116] G. H. Golub and C. F. Van Loan, *Matrix Computations*, 4th ed. (J. Hopkins Univ. Press, Baltimore, MD, 2013).

[117] I. S. Gradshteyn and I. M. Ryzhik, *Tables of Integrals, Series and Products*, 8th ed. (Elsevier LTD, Oxford, New York, 2014).

[118] G. Grimmett, *Probability on Graphs: : Random Processes on Graphs and Lattices* (Cambridge Univ. Press, 2009).

[119] J. Guckenheimer and B. Meloon, "Computing periodic orbits and their bifurcations with automatic differentiation", SIAM J. Sci. Comput. **22**, 951–985 (2000).

[120] M. N. Gudorf, Spatiotemporal Tiling of the Kuramoto-Sivashinsky Equation, PhD thesis (School of Physics, Georgia Inst. of Technology, Atlanta, 2020).

[121] M. N. Gudorf, N. B. Budanur, and P. Cvitanović, Spatiotemporal tiling of the Kuramoto-Sivashinsky flow, In preparation, 2021.

[122] D. Guido, T. Isola, and M. L. Lapidus, "A trace on fractal graphs and the Ihara zeta function", Trans. Amer. Math. Soc. **361**, 3041–3041 (2009).

[123] B. Gutkin and V. Osipov, "Classical foundations of many-particle quantum chaos", Nonlinearity **29**, 325–356 (2016).

[124] B. Gutkin, L. Han, R. Jafari, A. K. Saremi, and P. Cvitanović, "Linear encoding of the spatiotemporal cat map", Nonlinearity **34**, 2800–2836 (2021).

[125] A. J. Guttmann, "Lattice Green's functions in all dimensions", J. Phys. A **43**, 305205 (2010).

[126] M. C. Gutzwiller, *Chaos in Classical and Quantum Mechanics* (Springer, New York, 1990).

[127] P. G. Harper, "Single band motion of conduction electrons in a uniform magnetic field", Proc. Phys. Soc. London, Sect. A **68**, 874–878 (1955).

[128] K. Hashimoto, "Zeta functions of finite graphs and representations of p-adic groups", Adv. Stud. Pure Math. **15**, 211–280 (1989).

[129] J. F. Heagy, "A physical interpretation of the Hénon map", Physica D **57**, 436–446 (1992).

[130] M. Hénon, "A two-dimensional mapping with a strange attractor", Commun. Math. Phys. **50**, 94–102 (1976).

[131] G. W. Hill, "On the part of the motion of the lunar perigee which is a function of the mean motions of the sun and moon", Acta Math. **8**, 1–36 (1886).

[132] D. L. Hitzl and F. Zele, "An exploration of the Hénon quadratic map", Physica D **14**, 305–326 (1985).

[133] H. Hobrecht and F. Hucht, "Anisotropic scaling of the two-dimensional Ising model I: the torus", SciPost Phys. **7**, 026 (2019).

[134] H. Hobrecht and F. Hucht, "Anisotropic scaling of the two-dimensional Ising model II: surfaces and boundary fields", SciPost Physics **8**, 032 (2020).

[135] F. Hofbauer and G. Keller, "Zeta-functions and transfer-operators for piecewise linear transformations", J. Reine Angew. Math. (Crelle) **1984**, 100–113 (1984).

[136] D. R. Hofstadter, "Energy levels and wave functions of Bloch electrons in rational and irrational magnetic fields", Phys. Rev. B **14**, 2239–2249 (1976).

[137] T. Horiguchi, "Lattice Green's function for the simple cubic lattice", J. Phys. Soc. Jpn. **30**, 1261–1272 (1971).

[138] T. Horiguchi and T. Morita, "Note on the lattice Green's function for the simple cubic lattice", J. Phys. C **8**, L232 (1975).

[139] M. D. Horton, "Ihara zeta functions of digraphs", Linear Algebra Appl. **425**, 130–142 (2007).

[140] G. Y. Hu and R. F. O'Connell, "Analytical inversion of symmetric tridiagonal matrices", J. Phys. A **29**, 1511 (1996).

[141] G. Y. Hu, J. Y. Ryu, and R. F. O'Connell, "Analytical solution of the generalized discrete Poisson equation", J. Phys. A **31**, 9279 (1998).

[142] A. Hucht, "The square lattice Ising model on the rectangle I: finite systems", J. Phys. A **50**, 065201 (2017).

[143] B. D. Hughes, *Random Walks and Random Environments: Vol. I, Random Walks* (Clarendon Press, Oxford, 1995).

[144] C. A. Hurst and H. S. Green, "New solution of the Ising problem for a rectangular lattice", J. Chem. Phys. **33**, 1059–1062 (1960).

[145] Y. Ihara, "On discrete subgroups of the two by two projective linear group over p-adic fields", J. Math. Soc. Japan **18**, 219–235 (1966).

[146] S. Isola, "ζ-functions and distribution of periodic orbits of toral automorphisms", Europhys. Lett. **11**, 517–522 (1990).

[147] E. V. Ivashkevich, N. S. Izmailian, and C.-K. Hu, "Kronecker's double series and exact asymptotic expansions for free models of statistical mechanics on torus", J. Phys. A **35**, 5543–5561 (2002).

[148] N. S. Izmailian, "Finite-size effects for anisotropic 2D Ising model with various boundary conditions", J. Phys. A **45**, 494009 (2012).

[149] N. S. Izmailian and C.-K. Hu, "Finite-size effects for the Ising model on helical tori", Phys. Rev. E **76**, 041118 (2007).

[150] K. Jansen, "Lattice field theory", Int. J. Mod. Phys. E **16**, 2638–2679 (2007).

[151] J. Jorgenson and S. Lang, "The ubiquitous heat kernel", in *Mathematics Unlimited - 2001 and Beyond* (Springer, Berlin, 2001), pp. 655–683.

[152] L. P. Kadanoff, *Statistical Physics: Statics, Dynamics and Renormalization* (World Scientific, Singapore, 2000).

[153] A. Karlsson and M. Neuhauser, "Heat kernels, theta identities, and zeta functions on cyclic groups", Contemp. Math. **394**, 177–190 (2006).

[154] B. Kastening, "Simplified transfer matrix approach in the two-dimensional Ising model with various boundary conditions", Phys. Rev. E **66**, 057103 (2002).

[155] S. Katsura and S. Inawashiro, "Lattice Green's functions for the rectangular and the square lattices at arbitrary points", J. Math. Phys. **12**, 1622–1630 (1971).

[156] S. Katsura, S. Inawashiro, and Y. Abe, "Lattice Green's function for the simple cubic lattice in terms of a Mellin-Barnes type integral", J. Math. Phys. **12**, 895–899 (1971).

[157] S. Katsura, T. Morita, S. Inawashiro, T. Horiguchi, and Y. Abe, "Lattice Green's function. Introduction", J. Math. Phys. **12**, 892–895 (1971).

[158] B. Kaufman, "Crystal statistics. II. Partition function evaluated by spinor analysis", Phys. Rev. **76**, 1232–1243 (1949).

[159] G. Kawahara and S. Kida, "Periodic motion embedded in plane Couette turbulence: Regeneration cycle and burst", J. Fluid Mech. **449**, 291 (2001).

[160] J. P. Keating, "The cat maps: quantum mechanics and classical motion", Nonlinearity **4**, 309–341 (1991).

[161] V. Khoromskaia and B. N. Khoromskij, "Block circulant and Toeplitz structures in the linearized Hartree-Fock equation on finite lattices: Tensor approach", Comput. Methods Appl. Math. **17**, 43–455 (2017).

[162] Y.-O. Kim, J. Lee, and K. K. Park, "A zeta function for flip systems", Pacific J. Math. **209**, 289–301 (2003).

[163] G. Kirchhoff, "Üeber die Auflösung der Gleichungen, auf welche man bei der Untersuchung der linearen Vertheilung galvanischer Ströme geführt wird", Ann. Phys. Chem. **148**, 497–508 (1847).

[164] H.-T. Kook and J. D. Meiss, "Application of Newton's method to Lagrangian mappings", Physica D **36**, 317–326 (1989).

[165] M. Kotani and T. Sunada, "Zeta functions of finite graphs", J. Math. Sci. Univ. Tokyo **7**, 7–25 (2000).

[166] Y. Lan and P. Cvitanović, "Variational method for finding periodic orbits in a general flow", Phys. Rev. E **69**, 016217 (2004).

[167] C. H. Lee, S. Imhof, C. Berger, F. Bayer, J. Brehm, L. W. Molenkamp, T. Kiessling, and R. Thomale, "Topolectrical circuits", Commun. Phys. **1**, 39 (2018).

[168] D. Lenz, F. Pogorzelski, and M. Schmidt, "The Ihara zeta function for infinite graphs", Trans. Amer. Math. Soc. **371**, 5687–5729 (2018).

[169] S. Levit and U. Smilansky, "A new approach to Gaussian path integrals and the evaluation of the semiclassical propagator", Ann. Phys. **103**, 198–207 (1977).

[170] S. Levit and U. Smilansky, "A theorem on infinite products of eigenvalues of Sturm-Liouville type operators", Proc. Amer. Math. Soc. **65**, 299–299 (1977).

[171] J. Li and S. Tomsovic, "Exact relations between homoclinic and periodic orbit actions in chaotic systems", Phys. Rev. E **97**, 022216 (2017).

[172] M.-C. Li and M. Malkin, "Bounded nonwandering sets for polynomial mappings", J. Dynam. Control Systems **10**, 377–389 (2004).

[173] H. Liang and P. Cvitanović, Time reversal for discrete time dynamical systems, In preparation, 2021.

[174] T. M. Liaw, M. C. Huang, Y. L. Chou, S. C. Lin, and F. Y. Li, "Partition functions and finite-size scalings of Ising model on helical tori", Phys. Rev. E **73**, 041118 (2006).

[175] A. J. Lichtenberg and M. A. Lieberman, *Regular and Chaotic Dynamics*, 2nd ed. (Springer, New York, 2013).

[176] W. J. Lick, *Difference Equations from Differential Equations* (Springer, Berlin, 1989).

[177] J. S. Lim, *Two-dimensional Signal and Image Processing* (Prentice Hall, Englewood Cliffs, N.J, 1990).

[178] D. Lind and K. Schmidt, "Symbolic and algebraic dynamical systems", in *Handbook of Dynamical Systems*, Vol. 1, edited by B. Hasselblatt and A. Katok (Elsevier, New York, 2002), pp. 765–812.

[179] D. A. Lind, "A zeta function for Z^d-actions", in *Ergodic Theory of Z^d Actions*, edited by M. Pollicott and K. Schmidt (Cambridge Univ. Press, 1996), pp. 433–450.

[180] D. A. Lind and B. Marcus, *An Introduction to Symbolic Dynamics and Coding* (Cambridge Univ. Press, Cambridge, 1995).

[181] D. Lippolis and P. Cvitanović, "How well can one resolve the state space of a chaotic map?", Phys. Rev. Lett. **104**, 014101 (2010).

[182] R. de la Llave, Variational methods for quasiperiodic solutions of partial differential equations, in Hamiltonian Systems and Celestial Mechanics (HAMSYS–98), edited by J. Delgado, E. A. Lacomba, E. Pérez-Chavela, and J. Llibre (2000).

[183] M. Lutzky, "Counting stable cycles in unimodal iterations", Phys. Lett. A **131**, 248–250 (1988).

[184] M. Lutzky, "Counting hyperbolic components of the Mandelbrot set", Phys. Lett. A **177**, 338–340 (1993).

[185] I. Lyberg, "Free energy of the anisotropic Ising lattice with Brascamp-Kunz boundary conditions", Phys. Rev. E **87**, 062141 (2013).

[186] R. S. MacKay, *Renormalisation in Area-preserving Maps* (World Scientific, Singapore, 1993).

[187] R. S. MacKay and J. D. Meiss, "Linear stability of periodic orbits in Lagrangian systems", Phys. Lett. A **98**, 92–94 (1983).

[188] R. S. MacKay, J. D. Meiss, and I. C. Percival, "Transport in Hamiltonian systems", Physica D **13**, 55–81 (1984).

[189] E. C. Marino, *Quantum Field Theory Approach to Condensed Matter Physics* (Cambridge Univ. Press, Cambridge UK, 2017).

[190] P. A. Martin, "Discrete scattering theory: Green's function for a square lattice", Wave Motion **43**, 619–629 (2006).

[191] B. M. McCoy and T. T. Wu, *The Two-Dimensional Ising Model*, 2nd ed. (Dover, 1973).

[192] J. D. Meiss, "Symplectic maps, variational principles, and transport", Rev. Mod. Phys. **64**, 795–848 (1992).

[193] B. D. Mestel and I. Percival, "Newton method for highly unstable orbits", Physica D **24**, 172 (1987).

[194] H. B. Meyer, "Lattice QCD: A brief introduction", in *Lattice QCD for Nuclear Physics*, edited by H.-W. Lin and H. B. Meyer (Springer, York New, 2015), pp. 1–34.

[195] D. Micciancio and S. Goldwasser, *Complexity of Lattice Problems - A Cryptographic Perspective* (Springer, New York, 2002).

[196] M. Michałek and B. Sturmfels, *Invitation to Nonlinear Algebra* (MPI Leipzig, 2020).

[197] N. Miguel, C. Simó, and A. Vieiro, "From the Hénon conservative map to the Chirikov standard map for large parameter values", Regul. Chaotic Dyn. **18**, 469–489 (2013).

[198] R. Miles, "A dynamical zeta function for group actions", Monatsh. Math. **182**, 683–708 (2016).

[199] J. W. Mintmire, B. I. Dunlap, and C. T. White, "Are Fullerene tubules metallic?", Phys. Rev. Lett. **68**, 631–634 (1992).

[200] I. Montvay and G. Münster, *Quantum Fields on a Lattice* (Cambridge Univ. Press, Cambridge, 1994).

[201] T. Morita, "Useful procedure for computing the lattice Green's function - square, tetragonal, and bcc lattices", J. Math. Phys. **12**, 1744–1747 (1971).

[202] T. Morita and T. Horiguchi, "Calculation of the lattice Green's function for the bcc, fcc, and rectangular lattices", J. Math. Phys. **12**, 986–992 (1971).

[203] B. Mramor and B. Rink, "Ghost circles in lattice Aubry-Mather theory", J. Diff. Equ. **252**, 3163–3208 (2012).

[204] G. Münster and M. Walzl, Lattice gauge theory - A short primer, 2000.

[205] P. J. Myrberg, "Iteration der reellen Polynome zweiten Grades I", Ann. Acad. Sc. Fenn. A **256**, 1–10 (1958).

[206] P. J. Myrberg, "Iteration von quadratwurzeloperationen", Ann. Acad. Sc. Fenn. A **259**, 1–10 (1958).

[207] P. J. Myrberg, "Iteration der reellen Polynome zweiten Grades II", Ann. Acad. Sc. Fenn. A **268**, 1–13 (1959).

[208] P. J. Myrberg, "Sur l'itération des polynomes réels quadratiques", J. Math. Pures Appl. **41**, 339–351 (1962).

[209] P. J. Myrberg, "Iteration der reellen Polynome zweiten Grades III", Ann. Acad. Sc. Fenn. A **336**, 1–13 (1963).

[210] J. Nielsen, "Über die Minimalzahl der Fixpunkte bei den Abbildungstypen der Ringflächen", Math. Ann. **82**, 83–93 (1920).

[211] J. Ningyuan, C. Owens, A. Sommer, D. Schuster, and J. Simon, "Time- and site-resolved dynamics in a topological circuit", Phys. Rev. X **5**, 021031 (2015).

[212] Y. Okabe, K. Kaneda, M. Kikuchi, and C.-K. Hu, "Universal finite-size scaling functions for critical systems with tilted boundary conditions", Phys. Rev. E **59**, 1585–1588 (1999).

[213] L. Onsager, "Crystal statistics. I. A Two-dimensional model with an order-disorder transition", Phys. Rev. **65**, 117–149 (1944).

[214] G. Papathanasiou and C. B. Thorn, "Worldsheet propagator on the lightcone worldsheet lattice", Phys. Rev. D **87**, 066005 (2013).

[215] W. Parry, "On the β-expansions of real numbers", Acta Math. Acad. Sci. Hung. **11**, 401–416 (1960).

[216] R. Peierls, "Zur Theorie des Diamagnetismus von Leitungselektronen", Z. Phys. **80**, 763–791 (1933).

[217] I. Percival and F. Vivaldi, "A linear code for the sawtooth and cat maps", Physica D **27**, 373–386 (1987).

[218] A. Poghosyan, N. Izmailian, and R. Kenna, "Exact solution of the critical Ising model with special toroidal boundary conditions", Phys. Rev. E **96**, 062127 (2017).

[219] H. Poincaré, "Sur les déterminants d'ordre infini", Bull. Soc. Math. France **14**, 77—90 (1886).

[220] A. Politi and A. Torcini, "Periodic orbits in coupled Hénon maps: Lyapunov and multifractal analysis", Chaos **2**, 293–300 (1992).

[221] A. Politi, A. Torcini, and S. Lepri, "Lyapunov exponents from node-counting arguments", J. Phys. IV **8**, 263 (1998).

[222] M. Pollicott, Dynamical zeta functions, in Smooth Ergodic Theory and Its Applications, Vol. 69, edited by A. Katok, R. de la Llave, Y. Pesin, and H. Weiss (2001), pp. 409–428.

[223] C. Pozrikidis, *An Introduction to Grids, Graphs, and Networks* (Oxford Univ. Press, Oxford , UK, 2014).

[224] L. Qi, H. Chen, and Y. Chen, *Tensor Eigenvalues and Their Applications* (Springer, Singapore, 2018).

[225] P. Ren, T. Aleksić, D. Emms, R. C. Wilson, and E. R. Hancock, "Quantum walks, Ihara zeta functions and cospectrality in regular graphs", Quantum Inf. Process. **10**, 405–417 (2010).

[226] A. Rényi, "Representations for real numbers and their ergodic properties", Acta Math. Acad. Sci. Hung. **8**, 477–493 (1957).

[227] M. Rezghi and L. Eldén, "Diagonalization of tensors with circulant structure", Linear Algebra Appl. **435**, 422–447 (2011).

[228] O. E. Rössler, "An equation for continuous chaos", Phys. Lett. A **57**, 397–398 (1976).

[229] H. J. Rothe, *Lattice Gauge Theories - An Introduction* (World Scientific, Singapore, 2005).

[230] I. Sato, "Bartholdi zeta functions of group coverings of digraphs", Far East J. Math. Sci. **18**, 321–339 (2005).

[231] J.-P. Serre, *Trees* (Springer, Berlin, 1980).

[232] R. Shankar, *Quantum Field Theory and Condensed Matter* (Cambridge Univ. Press, Cambridge UK, 2017).

[233] C. Simó, "On the Hénon-Pomeau attractor", J. Stat. Phys. **21**, 465–494 (1979).

[234] B. Simon, "Almost periodic schródinger operators: A review", Adv. Appl. Math. **3**, 463–490 (1982).

[235] S. Smale, "Differentiable dynamical systems", Bull. Amer. Math. Soc. **73**, 747–817 (1967).

[236] J. Smit, *Introduction to Quantum Fields on a Lattice* (Cambridge Univ. Press, Cambridge, 2002).

[237] R. Sommer, Introduction to Lattice Gauge Theories, tech. rep. (Humboldt Univ., 2015).

[238] H. M. Stark and A. A. Terras, "Zeta functions of finite graphs and coverings", Adv. Math. **121**, 124–165 (1996).

[239] J. Stephenson and D. T. Ridgway, "Formulae for cycles in the Mandelbrot set II", Physica A **190**, 104–116 (1992).

[240] D. Sterling and J. D. Meiss, "Computing periodic orbits using the anti-integrable limit", Phys. Lett. A **241**, 46–52 (1998).

[241] D. G. Sterling, H. R. Dullin, and J. D. Meiss, "Homoclinic bifurcations for the Hénon map", Physica D **134**, 153–184 (1999).

[242] G. Sterling D., Anti-integrable Continuation and the Destruction of Chaos, PhD thesis (Univ. Colorado, Boulder, CO, 1999).

[243] I. Stewart and D. Gökaydin, "Symmetries of quotient networks for doubly periodic patterns on the square lattice", Int. J. Bifur. Chaos **29**, 1930026 (2019).

[244] R. Sturman, J. M. Ottino, and S. Wiggins, *The Mathematical Foundations of Mixing* (Cambridge Univ. Press, 2006).

[245] R. Suarez, "Difference equations and a principle of double induction", Math. Mag. **62**, 334–339 (1989).

[246] T. Sunada, *Topological Crystallography* (Springer, Tokyo, 2013).

[247] A. Tarfulea and R. Perlis, "An Ihara formula for partially directed graphs", Linear Algebra Appl. **431**, 73–85 (2009).

[248] A. Terras, *Zeta Functions of Graphs: A Stroll through the Garden* (Cambridge Univ. Press, 2010).

[249] M. Toda, *Theory of Nonlinear Lattices* (Springer, Berlin, 1989).

[250] D. Treschev and O. Zubelevich, "Hill's formula", in *Introduction to the Perturbation Theory of Hamiltonian Systems* (Springer, Berlin, 2009), pp. 143–162.

[251] J. H. Van Vleck, "The correspondence principle in the statistical interpretation of quantum mechanics", Proc. Natl. Acad. Sci. **14**, 178–188 (1928).

[252] G. Venezian, "On the resistance between two points on a grid", Am. J. Phys **62**, 1000–1004 (1994).

[253] Y. Colin de Verdière, "Spectrum of the Laplace operator and periodic geodesics: thirty years after", Ann. Inst. Fourier **57**, 2429–2463 (2007).

[254] D. Viswanath, "The Lindstedt-Poincaré technique as an algorithm for finding periodic orbits", SIAM Rev. **43**, 478–496 (2001).

[255] D. Viswanath, "Symbolic dynamics and periodic orbits of the Lorenz attractor", Nonlinearity **16**, 1035–1056 (2003).

[256] D. Viswanath, "The fractal property of the Lorenz attractor", Physica D **190**, 115–128 (2004).

[257] U.-J. Wiese, An Introduction to Lattice Field Theory, tech. rep. (Univ. Bern, 2009).

[258] I. Wigman, "Counting singular matrices with primitive row vectors", Monatsh. Math. **144**, 71–84 (2005).

[259] H. S. Wilf, *Generatingfunctionology* (Academic Press, New York, 1994).

[260] A. P. Willis, Openpipeflow: Pipe flow code for incompressible flow, tech. rep., `Openpipeflow.org` (U. Sheffield, 2014).

[261] W. L. Wood, "Periodicity effects on the iterative solution of elliptic difference equations", SIAM J. Numer. Anal. **8**, 439–464 (1971).

[262] J. Woods, *Multidimensional Signal, Image, and Video Processing and Coding* (Academic Press, Amsterdam, 2012).

[263] F. Y. Wu, "Theory of resistor networks: the two-point resistance", J. Phys. A **37**, 6653–6673 (2004).

[264] M.-C. Wu and C.-K. Hu, "Exact partition functions of the Ising model on M x N planar lattices with periodic-aperiodic boundary conditions", J. Phys. A **35**, 5189–5206 (2002).

[265] F.-G. Xie and B. L. Hao, "Counting the number of periods in one-dimensional maps with multiple critical points", Physica A **202**, 237–263 (1994).

[266] Z.-J. Xie, X.-Q. Jin, and Y.-M. Wei, "A fast algorithm for solving circulant tensor systems", Lin. Multilin. Algebra **65**, 1894–1904 (2016).

[267] Y. Yamasaki, "An explicit prime geodesic theorem for discrete tori and the hypergeometric functions", Math. Z. **289**, 361–376 (2017).

[268] Q. Zhilin, A. Gangal, M. Benkun, and T. Gang, "Spatiotemporally periodic patterns in symmetrically coupled map lattices", Phys. Rev. E **50**, 163–170 (1994).

[269] D. Zhou, Y. Xiao, and Y.-H. He, "Seiberg duality, quiver gauge theories, and Ihara's zeta function", Int. J. Mod. Phys. A **30**, 1550118 (2015).

[270] R. M. Ziff, C. D. Lorenz, and P. Kleban, "Shape-dependent universality in percolation", Physica A **266**, 17–26 (1999).

14. Integer lattices literature

There are many reasons why one needs to compute an "orbit Jacobian matrix" Hill determinant $|\mathrm{Det}\,\mathcal{J}|$, in fields ranging from number theory to engineering, and many methods to accomplish that:

discretizations of Helmholtz [78, 98, 176] and screened Poisson or Klein–Gordon or Yukawa [82, 116, 140, 141] equations

Green's functions on integer lattices [8, 14, 27, 41, 44, 51, 99, 112, 137, 138, 155–157, 182, 190, 193, 201, 202, 217, 243, 261]

linearized Hartree-Fock equation on finite lattices [161]

random walks, resistor networks, electrical circuits [1, 15, 31, 56, 57, 83, 118, 125, 143, 163, 167, 211, 223, 246, 252, 263]

Gaussian model [103, 152, 189, 232]

tight-binding Hamiltonians [56, 57, 90]

discrete Schrödinger equation [216], Harper or Hofstadter model [127, 136] or almost Mathieu operator [234]

quasilattices [35, 102]

circulant tensor systems [41, 44, 196, 224, 227, 266]

Ising model [25, 133, 134, 142, 144, 147–149, 158, 174, 185, 191, 212, 218, 264],

Ising model transfer matrices [213, 264]

lattice field theory [150, 194, 200, 204, 229, 236, 237, 257]

modular transformations [42, 270]

lattice string theory [111, 214]

spatiotemporal stability in coupled map lattices [4, 105, 268]

Van Vleck determinant, Laplace operator spectrum, semiclassical Gaussian path integrals [169, 170, 251, 253]

Jacobi operator

time reversal

Hill determinant [32, 187, 253]; discrete Hill's formula and the Hill discriminant, Toda lattice [249]

Lindstedt-Poincaré technique [254–256]

heat kernel [46, 86, 91, 151, 153, 193, 217, 267]

chronotopic models [221]

lattice points enumeration [21, 23, 26, 74]

cryptography [195]

primitive parallelogram [18, 37, 210, 258]

difference equations [73, 100, 245]

Bernoulli map [34, 85, 135], beta transformation [101, 215, 226]

digital signal processing [87, 177, 262]

generating functions, Z-transforms [91, 259]

integer-point transform [26]

graph Laplacians [52, 114, 180, 222]

graph zeta functions [10, 20, 24, 33, 53–55, 75, 86, 122, 128, 139, 145, 165, 168, 222, 225, 230, 231, 238, 247, 248, 269]
zeta functions for multi-dimensional shifts [19, 178, 179, 198]
zeta functions on discrete tori [46, 47, 267]

15. Kittens' LC21blog

Internal discussions of [173] edits: Move good text not used in [173] to this file, for possible reuse later.

Tentative title: "Is there anything cats cannot do?"

2016-11-18 Predrag A theory of turbulence that has done away with *dynamics*? We rest our case.
As a gentle introduction for a reader too busy [60] to study the book [71], we disguise a brief course on chaos theory as something everyone understands, a Bernoulli coin toss, section 2.
one determines the total number of lattice states by computing the Hill determinant (**??**) of the *orbit Jacobian matrix*
The observation that a Bernoulli system can be viewed as a discretization of a first-order in time ODE, eq. (35), with solutions whose temporal global linear stability is described by the orbit Jacobian matrix $\mathcal{J}_{tt'} = \delta F[\Phi]_t/\delta\phi_{t'}$, has profound implications for dissipative spatiotemporal systems such as Navier-Stokes and Kuramoto-Sivashinsky [121].
As we shall here have to traverse territory unfamiliar to many, we follow Mephistopheles pedagogical dictum "You have to say it three times" [115], and sing our song thrice.
The deep insight here is that the two formulations of mechanics, the forward-in-time Hamiltonian evolution, and the global, Lagrangian, temporal cat formulation are related by the *Hill's formula*.
The deep insight here is the realization that the *Hill determinant*, i.e., the volume of the *orbit Jacobian matrix* (figure 7 and 8) partitions system's state space.
Next, we address two questions: (i) how is the high-dimensional orbit orbit Jacobian matrix $\mathcal{J}$ related to the temporal $[d\times d]$ Jacobian matrix $\mathbb{J}$? (section 8), and (ii) how does one evaluate the orbit Jacobian matrix $\mathcal{J}$? (sections 8.6 and 8.6).
The theory is compactly summarized by its topological zeta function (190) that counts Bravais lattices.

2021-07-07 Predrag Experimenting with (234) by:
a flip across the kth axis, $k = 0, 1, 2, \cdots, n-1$,

$$\text{dihedral } \mathrm{D}_n: \quad H_{n,k} = \langle r, \sigma_k = r^k\sigma \mid \sigma_k r \sigma_k = r^{-1},\ r^n = \sigma_k^2 = 1 \rangle \tag{234}$$

that Han had replaced with (**??**) and n with $|n|$ in (**??**).

2021-07-07 Predrag A presentation of the *infinite dihedral group* [162] is

$$\mathrm{D}_\infty = \langle r_i, \sigma_j \mid r_i\sigma_j = \sigma_j r_{-i};\ \sigma_j^2 = 1;\ i,j \in \mathbb{Z} \rangle\ . \tag{235}$$

2021-08-10 Predrag dropped:

Applying the projection operator $P_{0-} = \frac{1}{2}(\mathbf{1} - \sigma_0)/2$ we obtain a lattice state

$$\cdots \underline{y_4}\,\underline{y_3}\,\underline{y_2}\,\underline{y_1}\,\boxed{0}y_1y_2y_3y_4\cdots\ , \tag{236}$$

antisymmetric under reflection, where the field $\boxed{0} = (\phi_0 - \phi_0)/2 = 0$ at the reflection lattice site 0 vanishes by antisymmetry, while the rest, $y_j = (\phi_j - \phi_{-j})/2$, are pairwise antisymmetric under the reflection σ. The underline indicates the negative of, i.e., $\underline{y_j} = -y_j$.

Applying the antisymmetric projection operator $P_{1-} = \frac{1}{2}(\mathbf{1} - \sigma r)/2$ we obtain a lattice state

$$\cdots \underline{y_4}\,\underline{y_3}\,\underline{y_2}\,\underline{y_1}\,|y_1y_2y_3y_4\cdots\ , \tag{237}$$

antisymmetric under reflection, where $y_j = (\phi_j - \phi_{1-j})/2$, are pairwise antisymmetric under the reflection σ_1.

2021-08-21 Predrag The old definition of Bernoulli m_t in (21) conflicted with the definition (25). I changed (25) to current form.

2021-10-29 Predrag Dropped: Cat maps are beloved by ergodicists and statistical mechanicians because, even though the field (q_t, p_t) is 2-dimensional, for integer values of the stretching parameter s, a cat map has a finite alphabet linear code, just like the Bernoulli map, and its unit torus can be tiled by two rectangles,

[2020-12-17 Predrag] Link to the ChaosBook.

in analogy with the forward-in-time Bernoulli map subinterval partitioning of figure 2. From this it follows that all admissible symbol blocks can be generated as shifts of finite type, and all periodic points determined and counted.

As all that is well known, and a side issue for this paper, we relegate the details of the Hamiltonian cat map dynamics and periodic orbit counting to ??.

[2020-12-17 Predrag] Link to the ChaosBook.

Here we focus on reformulating the cat dynamics as a temporal lattice (or discrete Lagrangian) problem, as we have done for the Bernoulli system in section 2.2.

2021-10-29 Predrag Dropped: The Lagrangian formulation requires only temporal lattice states and their actions, replacing the phase space 'cat map' (38) by a 'temporal cat' lattice (49). The temporal cat has no generating partition analogue of the Adler-Weiss partition for a Hamiltonian cat map (see

[2020-12-17 Predrag] Link to the ChaosBook.

). As we have shown here, no funky Hamiltonian state space partitioning magic (such as

[2020-12-17 Predrag] Link to the ChaosBook.

) is needed to count the lattice states of a temporal cat. Not only are no such partitions needed to solve the system, but the Lagrangian,

2021-08-12 Predrag Sidney will chuckle at this comment: The usual $a\phi_t^2$ form (**??**) might be preferable, as the 'a' is a stretching parameter, just like in (19). See section **??** Temporal Hénon.

2020-12-17 Predrag Link to the ChaosBook? or drop?

In section 3.1 we review the traditional cat map in its Hamiltonian formulation. (but relegate to the explicit Adler-Weiss generating partition of the cat map state space).

We evaluate and cross-check Hill determinants by two methods, either the 'fundamental fact' evaluation, or by the discrete Fourier transform diagonalization, section 8.6.

2021-10-13 Predrag Is there a - sign specific to Sidney's definition of the Hénon orbit Jacobian matrix Han and Predrag have to redefine both temporal cat and temporal Hénon orbit Jacobian matrix throughout, so we do not pick up an extraneous '-' sign for odd period lattice states. See also (**??**), and Pozrikidis [223] (click here) eq. (1.8.2). The main thing is to have a Laplacian with positive eigenvalues, right? Maybe not, the main thing is to have hyperbolic eigenvalues for $s > 2$. Rethink. determinants in periodic orbit formulas.

$Z[\mathsf{M}]$ notation extracted from *lattFTnotat.tex*, called *by lattFT.tex*.

, in field theorist's parlance, m_z are 'sources', and

The orbit Jacobian matrix $\mathcal{J}[\Phi]$ is best understood by starting with the period-n Bravais cell stability.

As in section 8.5, the fundamental parallelepiped given the stretching of the n-dimensional state space unit hyper-cube $\Phi \in [0,1)^n$ by the orbit Jacobian matrix counts lattice states, with the admissible lattice states of period T constrained to field values within $0 \le \phi_t < 1$. The fundamental parallelepiped contains images of all lattice states Φ_{M}, which are then translated by integer winding numbers M into the origin, in order to satisfy the fixed point condition (77).

2021-10-21 Predrag Han, RECHECK all m_t, as well as formulas starting with (88)!!! Bernoulli m_t in (21) conflicted with the old definition (25), so I changed (25).

When the force is proportional to displacement, that is, when Hooke's law is obeyed, the spring is said to be linear, the potential is quadratic.

A matrix $\mathbb{J}$ with no eigenvalue on the unit circle is called hyperbolic.

Ignoring (mod 1) for a moment, we can use (36) to eliminate p_t from (37) and rewrite the kicked rotor equation as the

For the problem at hand, it pays to go from the Hamiltonian (configuration, momentum) phase space formulation to the discrete Lagrangian (ϕ_{t-1}, ϕ_t) formulation.

temporal lattice condition

'Temporal' again refers to the discretized time $1d$ lattice

In atomic physics applications, the values of the angle q differing by integers are identified, but the momentum p is unbounded. In dynamical systems theory one compactifies the momentum as well, by adding (mod 1) to (37), as for the Bernoulli map (24). This reduces the phase space to a square $[0,1)\times[0,1)$ of unit area, with the opposite edges identified, i.e., 2-torus.

Thom-Anosov diffeomorphism

Cat maps with the same s are equivalent up to a similarity transformation, so it suffices to work out a single convenient realization, as we shall do here for the Percival-Vivaldi [217] 'two-configuration representation' (43).

2021-11-29 Predrag Might need to introduce the inverse temperature $\beta = 1/T$ and the free energy F, as in (**??**), multiplied by 'volume' N the number of lattice sites;

$$Z[\mathsf{M}] = e^{W[\mathsf{M}]}\,, \qquad W[\mathsf{M}] = \beta N F[\Phi]$$

So, $W[\mathsf{M}]$ is not the 'free energy'.

Hill's formula here is the discrete Hill's formula [32, 187] (**??**).

The temporal Bernoulli orbit Jacobian matrix $\mathcal{J} = \partial/\partial t - (s-1)\,r^{-1}$ is a differential operator whose determinant one usually computes by a Fourier transform diagonalization (see section 8.6). The Fourier discretization approach goes all the way back to Hill's 1886 paper [131];

2021-11-29 Predrag !!!WARNING!!! Following Han (**??**), we are changing the sign of the action $S[\Phi]$ and the orbit Jacobian matrix, as in (17), THROUGHOUT! (Totally Predrag's fault). This makes spatiotemporal cat and ϕ^4 theory action strictly positive for $s > 2$, as needed for the probability interpretation (3). Han, Sidney and Predrag have to redefine temporal cat, spatiotemporal cat and temporal Hénon orbit Jacobian matrices throughout, to avoid the extraneous '-' sign for odd period lattice states. See also (**??**), and Pozrikidis [223] (click here) eq. (1.8.2).

2016-11-08 Predrag Say: THE BIG DEAL is

for d-dimensional field theory, symbolic dynamics is not one temporal sequence with a huge alphabet, but d-dimensional spatiotemporal tiling by a finite alphabet

2021-12-27 Predrag removed:

Hill determinant: time-evolution evaluation

However, in classical and statistical mechanics, one often computes the Hill determinant using a Hamiltonian, or 'transfer matrix' formulation.

Define

$$\hat{\boldsymbol{\phi}}_t = \begin{bmatrix} \phi_{t-1} \\ \phi_t \end{bmatrix}, \quad \hat{\mathsf{m}}_t = \begin{bmatrix} 0 \\ m_t \end{bmatrix},$$

where the hat $\hat{}$ indicates a 2-dimensional 'two-configuration' [217] lattice site t state.

The 1-dimensional field theory 3-term recurrence (17) written in the Percival-Vivaldi [217] 'two-configuration representation' (43).

$\mathcal{J}_1$ is the spatial $[L\times L]$ orbit Jacobian matrix of $d=1$ temporal cat form (79),

This proves that $\det \hat{\mathcal{J}}$ of the 'Hamiltonian' or 'two-configuration' $[2Ln \times 2Ln]$ 'phase space' orbit Jacobian matrix $\hat{\mathcal{J}}$ defined by (**??**) equals the 'Lagrangian' Hill determinant of the $[Ln \times Ln]$ orbit Jacobian matrix $\mathcal{J}$.

2021-12-26 Han I think (36–37) should be written as:

$$q_{t+1} = q_t + p_{t+1} \qquad (\text{mod } 1), \tag{238}$$

$$p_{t+1} = p_t + P(q_t)\,. \tag{239}$$

Otherwise the angle of the rotor q is not constrained to $[0, 1)$.

Predrag: you are right, corrected.

Note to Predrag - send this paper to Vladimir Rosenhaus ¡vladr@kitp.ucsb.edu¿, Xiangyu Cao ¡xiangyu.cao08@gmail.com¿, George Savvidy, "Demokritos", Athens, and David Berenstein ¡dberens@physics.ucsb.edu¿